

**DEVELOPMENT OF SMALL FLOATING PLATFORM WITH TUNED
LIQUID COLUMN DAMPER**

CHOI KEAN BOON

**A project report submitted in partial fulfilment of the
requirements for the award of Bachelor of Engineering
(Hons.) Mechanical Engineering**

**Lee Kong Chian Faculty of Engineering and Science
Universiti Tunku Abdul Rahman**

May 2015

DECLARATION

I hereby declare that this project report is based on my original work except for citations and quotations which have been duly acknowledged. I also declare that it has not been previously and concurrently submitted for any other degree or award at UTAR or other institutions.

Signature : _____

Name : CHOI KEAN BOON

ID No. : 10UEB04226

Date : _____

APPROVAL FOR SUBMISSION

I certify that this project report entitled **“DEVELOPMENT OF SMALL FLOATING PLATFORM WITH TUNED LIQUID DAMPER”** was prepared by **CHOI KEAN BOON** has met the required standard for submission in partial fulfilment of the requirements for the award of Bachelor of Engineering (Hons.) Mechanical Engineering at Universiti Tunku Abdul Rahman.

Approved by,

Signature : _____

Supervisor : Mr King Yeong Jin

Date : _____

The copyright of this report belongs to the author under the terms of the copyright Act 1987 as qualified by Intellectual Property Policy of Universiti Tunku Abdul Rahman. Due acknowledgement shall always be made of the use of any material contained in, or derived from, this report.

© 2015, CHOI KEAN BOON. All right reserved.

Specially dedicated to
my beloved grandmother, mother and father

ACKNOWLEDGEMENTS

First of all, I would like to express my deepest gratitude as well as appreciation to my research supervisor, Mr King Yeong Jin for his precious advice, guidance and his enormous patience throughout the course of my Final Year Project. Besides this, advice given by Mr Wong Hong Mun has been a great help in my project. Without the relentless help and support from Mr King and Mr Wong, it would impossible to see to the success of this project

In addition, I would also like to express my gratitude to my loving family member and friends; Zack Thiem, Steve Lim, Francis Ong, and Tan Cher Ching who had helped out in my project and given me invaluable encouragement during the development of my project.

Last but not least, a special thanks to Uncle Ho and Mr Hwang from the mechanical and civil workshop which has provide me with priceless advice on manufacturing my prototype.

Finally, I would like to utilise this opportunity to express my utmost gratitude to everyone who may possibly has contributed to the success of this project.

DEVELOPMENT OF SMALL FLOATING PLATFORM WITH TUNED LIQUID COLUMN DAMPER

ABSTRACT

Nowadays, offshore engineering has been growing rapidly, indirectly results in the advancement of the floating platform design. However, the fundamental concept still remains the same which is the buoyant force required by the floating platform is determined by using the Archimedes' Principle while the stability can be quantified by computing the metacentric height and the critical tilting angle. In order to suppress the vibration of the platform, TLCD is implemented onto the platform. The parameter affecting the performance of TLCD against seismic loading on mainland has been investigated extensively by the researcher around the world, but no the wave loading. Hence, it is important to validate the effect of the parameter of TLCD when it is reacted toward wave loading as a badly tuned TLCD may ended up in a disastrous way by causing the structure to vibrate more vigorously. The main parameter that will be investigated by this paper will be the head loss coefficient, tuning ratio and mass ratio. It is shown that there is an optimum value of head loss coefficient depending on the mass ratio of the floating platform. On the other hand, the effect of mass ratio on the TLCD is the higher the better. However, the mass ratio is usually restricted by the practicability as a TLCD of high mass ratio is too costly to manufacture. Thus, the mass ratio is restricted below 5% for cost saving as the improvement in performance of the TLCD is not significant anymore when it increase beyond the 5%. The tuning ratio acts in a similar way of the head loss coefficient. There is an optimum value to which the TLCD will function the best. Theoretically, the optimum tuning ratio is 1, however in reality, the optimum tuning ratio is slightly less than 1 due to the fact that the installation of TLCD onto the platform has induce an addition degree of freedom onto the platform.

TABLE OF CONTENTS

DECLARATION	ii
APPROVAL FOR SUBMISSION	iii
ACKNOWLEDGEMENTS	vi
ABSTRACT	vii
TABLE OF CONTENTS	viii
LIST OF TABLES	x
LIST OF FIGURES	xi
LIST OF SYMBOLS / ABBREVIATIONS	xiv
LIST OF APPENDICES	xvi

CHAPTER

1	INTRODUCTION	17
	1.1 Background	17
	1.2 Types of Floating Platform	18
	1.3 Tuned Liquid Column Damper (TLCD)	19
	1.4 Problem Statement	20
	1.5 Aims and Objectives	22
2	LITERATURE REVIEW	23
	2.1 Floating Platform	23
	2.2 Archimedes' Principle	26
	2.3 Head Loss Coefficient, of TLCD	27
	2.4 Length Ratio, α of TLCD	31
	2.5 Tuning Ratio, β of TLCD	32

2.6	Mass Ratio, μ of TLCD	34
3	METHODOLOGY	36
3.1	Platform Design Stage	36
3.2	TLCD Design Stage	38
3.2.1	Head Loss Coefficient Study	39
3.2.2	Tuning Ratio and Mass Ratio Study	39
3.3	Manufacturing and Material Selection Approach	40
3.3.1	Platform Manufacturing	41
3.3.2	Bone Frame Reinforcement Manufacturing	44
3.3.3	TLCD Manufacturing	45
3.4	Experimental Setup	47
4	RESULTS, CALCULATION AND DISCUSSION	51
4.1	Theoretical Buoyancy Calculation and Comparison to Experimental Result	51
4.2	Metacentric Height Calculation and Evaluation	53
4.2.1	Metacentric Height and Righting Arm at Different Tilting Angle	56
4.3	Effect of Head Loss Coefficient	60
4.4	Composite Effect of Mass Ratio and Tuning Ratio	68
4.5	Hydrostatic Force Simulation Result and Specification of Platform	71
4.5.1	Technical Drawing of Platform and TLCD	72
4.5.2	Simulation Result	73
5	CONCLUSION AND RECOMMENDATIONS	74
5.1	Problem Encountered and Future Recommendations	74
5.2	Conclusion	75
	REFERENCES	77
	APPENDICES	79

LIST OF TABLES

TABLE	TITLE	PAGE
2.1	Head Loss Coefficient of TLCD With Varied Blocking Ratio. (Wu, et al., 2005)	28
2.2	Optimum Parameter of TLCD for Various Mass Ratio(μ in this table) and Liquid Length Ratio(α in this table). (Shum, 2005)	30
3.1	Example of The Simulation Done on The Platform	37
4.1	Metacentric Height and Righting Arm Distribution on Different Tilting Angle	57
4.2	Blocking Ratio and Head Loss Coefficient for Different Diameter Orifice Plate	61
4.2	Maximum Absolute Displacement Amplitude of Channel 1 and Channel 2 for Each Orifice Plate Diameter	65
4.4	Table of Reciprocal of Amplitude of Power Spectrum for each Orifice Plate	67
4.2	Mass Ratio and Tuning Ratio for Different Water Level	69

LIST OF FIGURES

FIGURE	TITLE	PAGE
1.1	Types of Offshore Structure (Subrata, 2005)	18
1.2	Illustration of TLCD (Lee, Wong and Lee, 2005)	19
1.3	Family of TLCD. (Venkateswara, 2013)	19
1.4	Illustration of Metacentre. (Donald, et al., 2013)	20
2.1	Illustration of TLP (Subrata, 2005)	23
2.2	Mechanics of Tendon (Subrata, 2005)	24
2.3	Righting Moment Created During Tilting of TLP. (Subrata, 2005)	25
2.4	Normalized Displacement of Structure Against Tuning Ratio (β in this graph) graph for various head loss coefficient (ξ in this graph). (Matteo, et al., 2014)	29
2.5	Optimum Blocking Ratio against Mass Ratio. (Tanmoy and Subrata, et al., 2014)	30
2.6	The Effect of Length Ratio on the Performance Indices of TLCD on Various Mass Ratio. (Min, et al., 2005)	32
2.7	Variation of Performance Indices with respect to Tuning Ratio on Various Mass Ratio. (Min, et al., 2005)	33
2.8	Normalized Structure Displacement against Tuning Ratio for Various Mass Ratio. (Matteo, et al., 2014)	34

3.1	Sample of TLCD to be Built. (Wu, et al., 2005)	38
3.2	Sample of TLCD Parts Drawing For Manufacture	41
3.3	Vertical Bandsaw	42
3.4	Sample Perspex That Has Been Cut	43
3.5	Perspex Being Sticked Together With Book as Force	43
3.6	Cross Sectional Design of Aluminium Profile	44
3.7	Identical Left Hand Side and Right Hand Side of TLCD	45
3.8	Milling Machine	46
3.9	Platform With TLCD Installed	47
3.10	IMC Dynamic Signal Analyser and Kistler Type K Shear Accelerometer	48
3.11	Full Experimental Setup	48
3.12	Accelerometer to Channel Orientation	49
3.13	Wave Generation Method	49
4.1	Platform's Height	52
4.2	Height of Liquid Displaced	52
4.3	CG Calculated From SolidWorks	54
4.4	AutoCAD Front View Drawing For Calculation	54
4.5	Platform Tilted by 10° about CG	56
4.6	Righting Arm and Metacentric Height When Platform Tilted by 10° about CG	57
4.7	Graph of Metacentric Height against Angle Tilted	58
4.8	Graph of Righting Arm against Angle Tilted	59
4.9	Filtered Acceleration Response for 4 mm Diameter Orifice Plate	62

4.10	Displacement Response for 4 mm Diameter Orifice Plate	63
4.11	Vibration Motion of the Platform Using 4 mm Diameter Orifice	63
4.12	Displacement Response for 8 mm Diameter Orifice Plate	64
4.13	Vibration Motion of the Platform Using 8 mm Diameter Orifice	64
4.14	Power Spectrum Analysis for Channel 1 of Different Configuration	66
4.15	Power Spectrum Analysis for Channel 2 of Different Configuration	66
4.16	Performance in Mitigating Vibration against the Coefficient of Head Loss	67
4.17	Power Spectrum for Different Water Level at Channel 1	70
4.18	Power Spectrum for Different Water Level at Channel 2	71
4.19	Modelled Platform with TLCD installed	72
4.20	Technical Drawing of Platform	72
4.21	Stress Analysis by Simulation	73
4.22	Displacement Analysis by Simulation	73

LIST OF SYMBOLS / ABBREVIATIONS

F_B	Buoyant force, N
h_D	Height of liquid displaced, m
ρ	Density, kg/m ³
V_D	Volume of fluid displaced, m ³
g	Gravitational acceleration, m/s ²
B_D	Horizontal column length, m
$B_{D,New}$	Horizontal column length of another new TLCD, m
L_D	Vertical column length, m
$L_{D,New}$	Vertical column length of another new TLCD, m
L	Total length of liquid of the TLCD, m
L_{New}	Total length of liquid of another new TLCD, m
A	Cross sectional area of TLCD, m ²
A_D	Cross sectional area of liquid displaced, m ²
A_{New}	Cross sectional area of another new TLCD, m ²
D	Diameter of orifice plate, m
∇	Increment or decrement in length, m
m	Mass of the object, kg
m_{B_D}	Mass of liquid in the horizontal column, kg
m_{TLCD}	Mass of total liquid in the TLCD, kg
ω_D	Natural frequency of TLCD, rad/s
ω_w	Frequency of wave generated, rad/s
$W_{TLCD+Platform}$	Weight of TLCD and platform, N
$F_{Loading}$	Total loading on the platform, N
GM	metacentric height, m
RA	Righting arm, m
$CG_{new,y}$	CG of the platform and TLCD together with the weight, m

CG_y	y coordinate of the <i>CG</i> of the object, m
CB	Centre of Buoyancy
CG	Centre of Gravity
M	metacentre
ψ	blocking ratio
η	head loss coefficient
α	length ratio
μ	mass ratio
β	tuning ratio
<i>Actual</i>	Experimental result of a variable
<i>Theoretical</i>	Calculated result of a variable
TLCD	Tuned Liquid Column Damper
LCVA	Liquid Column Vibration Absorber
DTLCD	Double Tuned Liquid Column Damper
HTLCD	Hybrid Tuned Liquid Column Damper
PTLCD	Pressurized Tuned Liquid Column Damper
TLCBD	Tuned Liquid Column Ball Damper

LIST OF APPENDICES

APPENDIX	TITLE	PAGE
A	Result for Graphical Method of <i>GM</i> and <i>RA</i> for Different Tilting Angle at an increment of 10°	79
B	Accelerometer Response for Different Orifice Plate Diameter at Water Level of 15 cm	87
C	Accelerometer Response for 10 cm Orifice Plate Diameter at Different Water Level	94
D	Accelerometer Response for Platform without TLCD	97

CHAPTER 1

INTRODUCTION

1.1 Background

The offshore field has been growing rapidly due to the rising need of new energy source and minerals, consequently the exploration and development in the field of offshore oil and gas has been stimulated aggressively. Indirectly, this has given rise to many concepts and structure for application in the deep oceans for harvesting energy and minerals. (Subrata, 2005)

This includes the development of offshore structures design. Offshore structure is defined as structure which does not have fixed access to the dry land and may even be required to stay in position disregarding of the weather condition. There are two types of offshore structure which is the common one which is fixed to the seabed or the floating structures which may be anchored to the seabed by using either a rope or cable or dynamically positioned by other device such as thrusters which allows the floating structure to drift freely. (Subrata, 2005)

The offshore structure that will be discussed in this report in the latter part will be restricted to only floating platform due to the fact that the objective of the developed platform is for mounting solar panel but not for harvesting minerals from the seabed.

1.2 Types of Floating Platform

Even though there are many types of offshore structure, but for floating platform there is only 3 type which is the Semi-FPS (Floating Production Facility), Conventional Tension Leg Platform (TLP), Mini-TLP. All these 3 types of floating platform suits for different deep water system as shown in Figure 1.1 (Subrata, 2005)

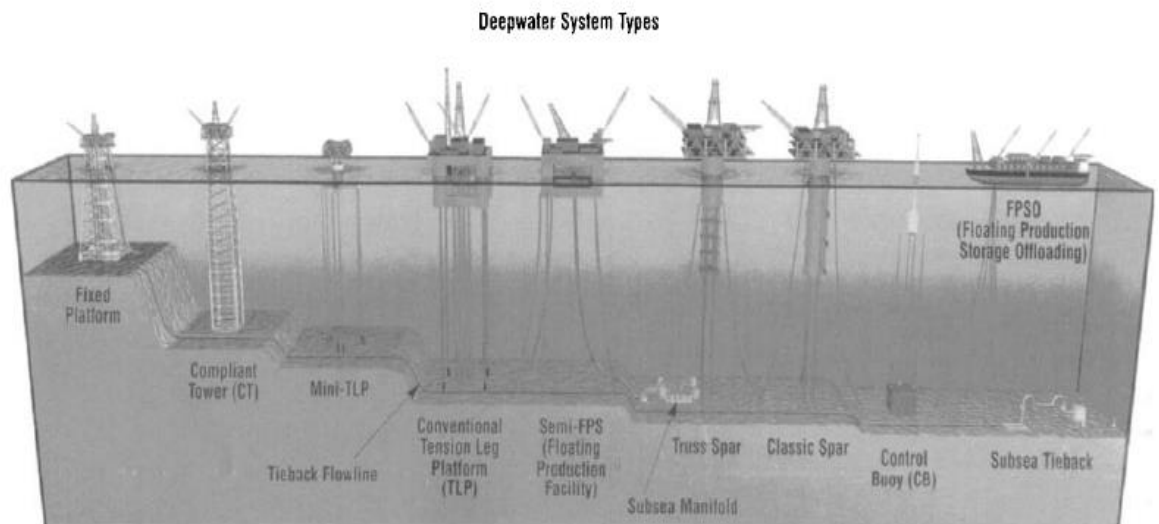


Figure 1.1: Types of Offshore Structure (Subrata, 2005)

A Semi FPS is a neutrally buoyant floating production unit which allows 6 degree of freedom. It is generally used to produce and harvest the oil and gas cost-effectively. On the other hand, Conventional TLP is a compliant platform which are vertically tethered to the seabed. For this type of TLP, the platform is designed with excess buoyant force and this excessive buoyant force is tethered by using cable or rope which are called tendon to allow only swaying and surging motion of the platform. For Mini TLP, as the name implied, is a miniature version of Conventional TLP. (Subrata, 2005)

1.3 Tuned Liquid Column Damper (TLCD)

The idea of utilising liquid in a U-tube to create damping effect for reducing structural vibration by merely allowing it to pass through a small orifice opening in the U-tube was first introduced by Sakai F. in the year of 1989. This device is termed as Tuned Liquid Column Damper as shown in Figure 1.2.(Sakai, 1989)

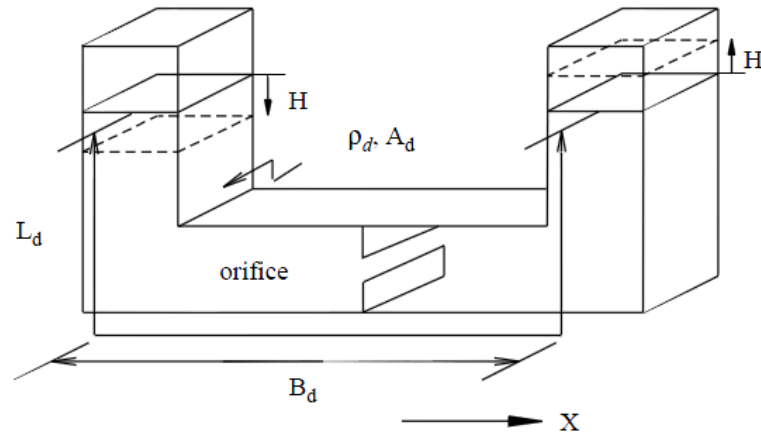


Figure 1.2: Illustration of TLCD (Lee, Wong and Lee, 2005)

This idea has then be used, further developed extensively and even several modification has been made to the original TLCD. The classification of TLCD available is shown at Figure 1.3.

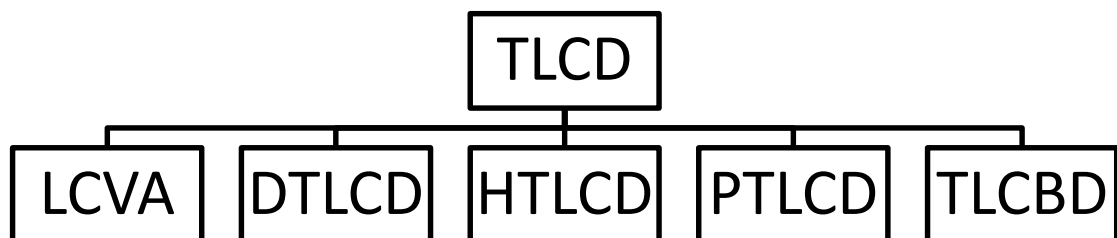


Figure 1.3: Family of TLCD. (Venkateswara, 2013)

The term LCVA stands for Liquid Column Vibration Absorber. The difference between LCVA and TLCD is that a LVCA has a different cross-section in the

horizontal and vertical column while TLCD has a same cross-section in the horizontal and vertical column. Double Tuned Liquid Column Damper, DTLCD , Hybrid Tuned Liquid Column Damper, as well as Pressurized Tuned Liquid Column Damper, PTLCD is not popular due to the complexity in building it and predicting their damping behaviour. (Wu, Shih and Lin, 2005) On the other hand, Tuned Liquid Column Ball Damper, TLCBD is the use of a rolling ball instead of an orifice to induce a head loss in the fluid flow of the TLCD. (Tanmoy and Subrata, 2014)

1.4 Problem Statement

The floating platform designed was meant to act as a platform for a place to hold or support the solar panel for harvesting solar energy. Hence, the first problem that has arise would be to design a platform with sufficient buoyant force to ensure that the platform is able to afloat in the ocean while providing the tendon with sufficient tension force.

In addition, it is well known that in order to have a floating structure to maintain stable afloat without tipping over, it would require a metacentre, M of higher than the centre of gravity of the floating object in order to produce a positive metacentric height, GM . Once the metacentric height is negative, the floating structure would be unstable and tip over. An illustration is shown in Figure 1.4 using a ship as an example.

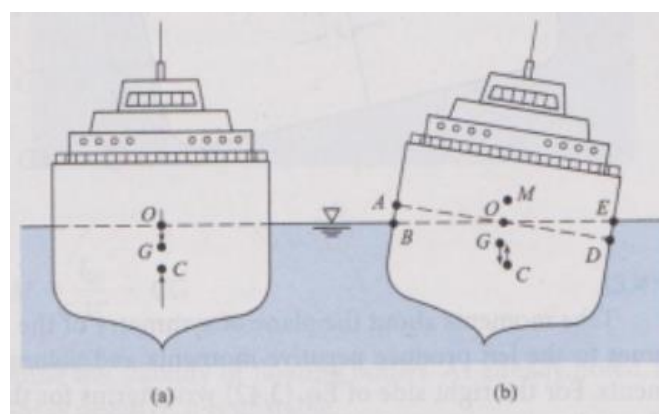


Figure 1.4: Illustration of Metacentre. (Donald, et al., 2013)

From Figure 1.4, it is clearly seen that once the ship has tilted, the centre of buoyancy, CB will change its location. The point of intersection of the buoyant force's line of action with the symmetric line passing through the centre of gravity, G is called the metacentre.

Since the metacentric height varies as the tilting angle of the floating structure varies, it has been a biggest challenge in obtaining the critical angle whereby the floating structure will failed by tipping over and this appear to be a significant problem to be solved.

Even though, we know that which at what critical angle will the floating structure fails, we still need a device to suppress the vibration of the floating platform so that it would not easily be tilted to the critical angle. Among so many damper such as Tuned Mass Damper, Tuned Liquid Column Damper, Controllable Tuned Liquid Damper and etc, TLCD is the easiest to be used and implemented. (Min, et al., 2005)

The parameter TLCD has been investigated and tested extensively in the main land by various researcher such as Balendra (1995) , Wu (2005) and Min (2005). However, there appears to be another big problem in which all these studies on TLCD were performed for structure on the main land but not for floating structure. Hence, the problem to be solved would be to test and validate whether TLCD in a floating structure responding to wave loading will react the same way as if the structure is a building in a main land subjected to the same loading.

Furthermore, the characteristic of wave has proven to be another big problem that has to be solved. Even though one could simplify the wave pattern by modelling the wave as regular wave, this may result in inaccuracy in response compared to the actual application of the floating platform.

1.5 Aims and Objectives

As to be restated once again, the aim of this project is to implement a Tuned Liquid Column Damper into the design of a small floating platform.

Since all the problem which may arise has been identified in the subsection 1.4 “Problem Statement”, the objective of this project can be stated clearly and concisely with reference to the problem statement. In short, the objective of that has be achieved is:

- i. To determine the buoyancy force, metacentre and the critical angle of tilting of the floating platform.
- ii. To determine the general effect of head loss coefficient on the TLCD installed on a floating platform.
- iii. To determine the composite effect of mass ratio and tuning ratio on the TLCD installed on a floating platform and which ratio has a more dominant effect on TLCD.

The first object corresponded to the first problem identified in the subsection “problem statement” whereby for a floating platform it is critical to find out the buoyant force require and the metacentre of the floating platform. Even with this data, it would prove quite useless for practical uses, hence these data is further processed into the critical angle in which the floating platform will tilt over.

For the next 3 objectives, it is to validate the effect of the fundamental parameters in TLCD installed on a floating against the effect which has been investigated by previous researcher such as Balendra (1995) , Wu (2005) and Min (2005) on main land structure.

The last problem is not listed as an objective and hence was not studied because wave itself is a broad field which meant to be investigated standalone in another project but not to be mingled up with this project concerning the floating platform and the device to suppress the vibration of the platform which is the TLCD.

CHAPTER 2

LITERATURE REVIEW

2.1 Floating Platform

Tension Leg Platform, TLP consist of column and pontoon, like any other floating structure. The uniqueness of this TLP is the mooring system or sometime called the tether which essentially mean the vertical tendon. A simple illustration of TLP is shown in Figure 2.1. (Subrata, 2005)

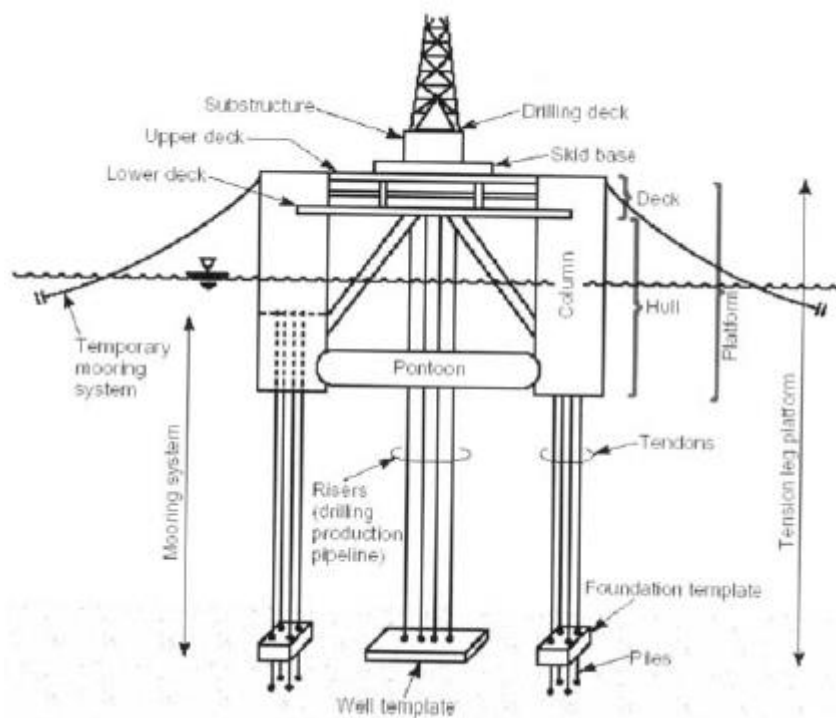


Figure 2.1: Illustration of TLP (Subrata, 2005)

The main function of the tether is to restrain the heave motion, hence in order to achieve this functionality the tendon has to be pretension (normally constitute of 25% to 45% of the total buoyant force). In addition, the presence of tether also makes the TLP to be less worry on the hydrostatic and stability issue. The mechanics of tendon is shown in Figure 2.2. (Subrata, 2005)

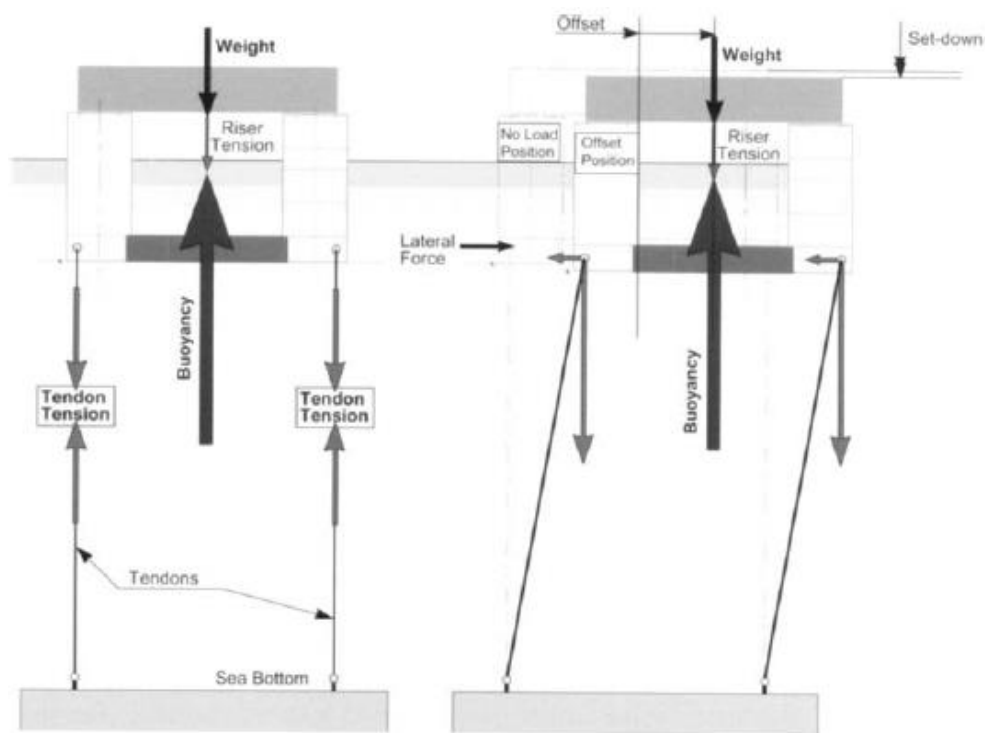


Figure 2.2: Mechanics of Tendon (Subrata, 2005)

It is also found that the key analytic area for the performance of a TLP is as follow:

- i. Weight and CG's
- ii. Wind Force
- iii. Current Force
- iv. Global Performance Analysis
 - a. Motions
 - b. Drift Force
 - c. Tendon Tensions
- v. Global Strength

This is where the key area that has to be focus in the preliminary stage of TLP designing. (Subrata, 2005)

From the Handbook of Offshore Engineering written by Subrata (2005), we can see that the metacentre is not a concern for the TLP. This is because the tension force from the tendon will tends to create a righting moment when it is tilted at certain angle as shown in Figure 2.3.

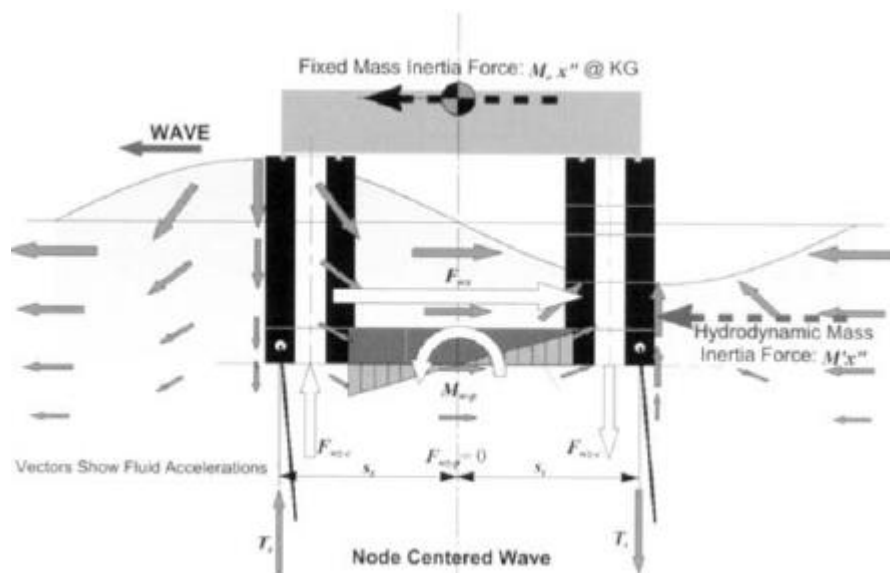


Figure 2.3: Righting Moment Created During Tilting of TLP. (Subrata, 2005)

On the other hand, the wind load is considered due to the fact that Subrata (2005) assumes the platform for the use of harvesting minerals such as hydrocarbon which require tall structure to be built on top of the platform. Hence in our case, the platform is used to mount solar panel which is of relatively low height, hence the wind load can be neglected.

In a nut shell, in our case the key area that is needed to be focus on is Weight and CG's, Current Force, Global Performance Analysis and Global Strength.

2.2 Archimedes' Principle

The Archimedes' Principle is perhaps one of the best known principle for its usefulness in determining the buoyant force of a fully immersed body as well as a floating body.

Buoyant force is defined as an upward (with respect to the gravity force) force acting on a body that is either totally or partially submerged in a fluid. The Archimedes' Principle defines that the buoyant force acting on a body is equal to the weight of the fluid displaced by the body.(Donald, et al., 2013) Hence, mathematically it can be shown as:

$$F_B = \rho V_D g \quad (2.1)$$

where:

F_B = buoyant force, N

ρ = density, kg/m³

V_D = volume of fluid displaced, m³

g = gravitational acceleration, m/s²

This principle is further extend to the stability of immersed body and floating body. When it comes to the stability, we need to introduce the centre of buoyancy, C which is the centre of gravity, CG of the displaced fluid. For an immersed body, if the centre of buoyancy is above the centre of gravity, any slight tipping on the immersed body will result in the right couple which is sometimes called righting moment. This moment will then tries to re-stabilize the body making it stable. If the centre of gravity, CG is above the centre of buoyancy, CB then instead of producing a righting moment, an overturning moment is produced instead which would overturn the immersed body. (Donald, et al., 2013)

For a floating body, it would be a bit difficult to determine the stability as the centre of buoyancy assumes different location when the floating body is tilted or takes another position. This is may be seen in Figure 1.4 whereby as the ship is tilted to one side, the centre of buoyancy also moves to that side. Hence, for a floating body, we can no longer use the position of centre of gravity and centre of buoyancy to determine

the stability, and another parameter called metacentric height is introduced. (Donald, et al., 2013)

$$GM = \frac{I_0}{V_D} - CG + CB \quad (2.2)$$

where

GM = metacentric height, m

I_0 = second moment of inertia at the waterline, m⁴

CG = centre of gravity, m

CB = centre of buoyancy, m

By utilizing the GM value, we can easily determine the stability of a floating body, a positive value indicate stable while a negative value indicate unstable. As a conclusion, in order to determine whether the floating platform designed is stable, we will need to determine the metacentric height of the platform. However, equation 2.2 is derived based on the small angle assumption, hence it only guarantee the stability of the platform for an angle of tilting of below 15 °. In order to determine the GM value for other tilting angle, graphical method is used instead with the aid of software called AutoCAD.

2.3 Head Loss Coefficient, of TLCD

Head loss coefficient, as it's name implies is the coefficient that correlates to the head loss of liquid flowing in the TLCD. Hence the value of head loss coefficient is the due to the inner resistance and cross sectional area of the liquid column. (Min, et al., 2005)

However, the inner resistance in the liquid may sometimes be too negligent and the dominating factor which contributes to the head loss is the orifice. Thus, head loss coefficient is significantly affected by the blocking ratio, ψ of the orifice. (Wu, et al., 2005) This is shown in the table 2.1 whereby 4 different TLCD is experimented with different blocking ratio and their corresponding head loss coefficient value

shows that for the different configuration of TLCD, unless the blocking ratio is varied or else the head loss coefficient will not varies much.

Table 2.1: Head Loss Coefficient of TLCD With Varied Blocking Ratio. (Wu, et al., 2005)

	Configured group			
	I	II	III	IV
Natural frequency ω_d (rad/s) (Error w.r.t. predicted)	0.4923 $\times 2\pi$ (1.8%)	0.4727 $\times 2\pi$ (1.7%)	0.4595 $\times 2\pi$ (1.3%)	0.4516 $\times 2\pi$ (1.3%)
Head loss coefficient				
Blocking ratio $\psi = 20\%$	3.96	3.55	3.40	3.40
Blocking ratio $\psi = 40\%$	6.10	5.80	5.70	5.55
Blocking ratio $\psi = 60\%$	12.80	12.40	12.50	12.00
Blocking ratio $\psi = 80\%$	54.50	54.00	59.00	56.00

Besides this, the test by Wu, et al. (2005) also shows that value of head loss coefficient of a TLCD is independent of the mass ratio, μ as well as the length ratio, α of the TLCD as the 4 different TLCD used in Table 2.1 has different mass ratio and length ratio. At the end, Wu, et al. (2005) has formulated a formula to estimate the head loss coefficient value of a TLCD provided the blocking ratio of the orifice which is :

$$\eta = (-0.6\psi + 2.1\psi^{0.1})^{1.6} \times (1 - \psi)^{-2} \quad (2.3)$$

where

η = head loss coefficient

ψ = blocking ratio

So much for the determining the head loss coefficient, nevertheless our main concern is the effect of the head loss coefficient on the performance of TLCD. Apparently, there is an optimum head loss coefficient, it is neither the higher the better nor the lower the better. This is shown in the Matteo, et al. (2014) result in Figure 2.4.

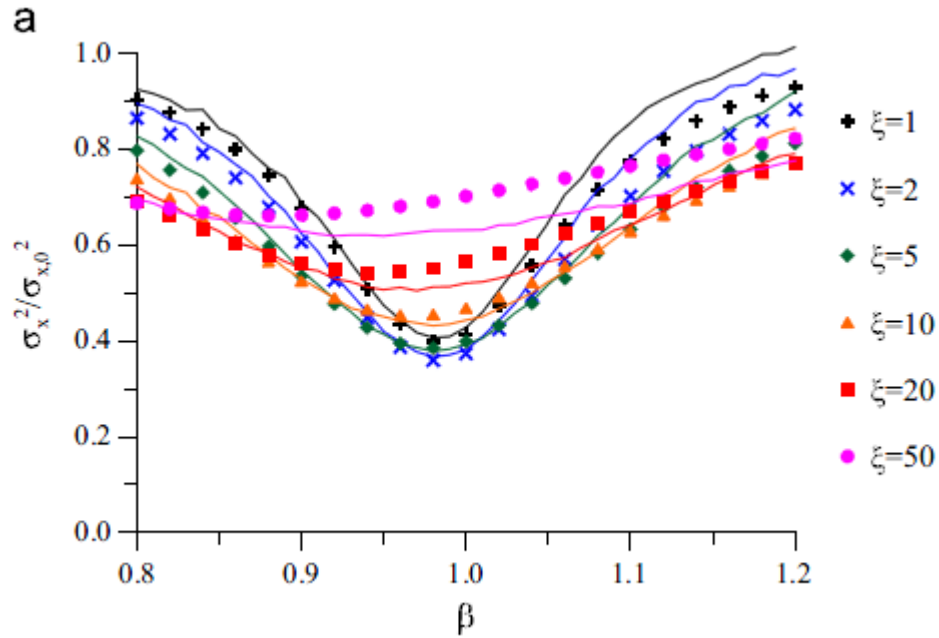


Figure 2.4: Normalized Displacement of Structure Against Tuning Ratio (β in this graph) graph for various head loss coefficient (ξ in this graph). (Matteo, et al., 2014)

From the result obtained by Matteo, et al. (2014) we can see that the optimum head loss coefficient depends on the tuning ratio of the TLCD. As the tuning ratio of the TLCD varies the effect of the head loss coefficient is different. The one remark to be taken is that Matteo, et al. (2014) did not consider the effect of mass ratio on the optimum value of the head loss coefficient. This makes Figure 2.4 to be quite meaningless apart from letting us know that the tuning ratio will affect the optimal head loss coefficient.

The effect of mass ratio on the optimum head loss coefficient can be obtained by common sense that is a higher mass ratio would essentially means the liquid inside the TLCD is carrying a high amount of energy and thus a higher head loss to dampen the fluid flow while a low mass ratio would mean the liquid inside the TLCD to be carrying low amount of energy, hence if high head loss is to be applied, the fluid inside the TLCD would be bring to a stop in short period resulting in no damping effect. This is agreed by Min, et al. (2005) whereby he stated that the optimal value of head loss increases as the mass ratio increases or in another way round a TLCD with a higher

mass ratio will have a higher optimum head loss coefficient. Min, et al. (2005) further stated that the performance of TLCD will deteriorate in spite of large mass ratio value when the head loss coefficient is low. This trend is then backed up by the optimum parameter of TLCD developed by Shum (2009) as shown in Table 2.2. This is also agreed by experiment down by Tanmoy and Subrata (2014) shown in Figure 2.5.

Table 2.2: Optimum Parameter of TLCD for Various Mass Ratio(μ in this table) and Liquid Length Ratio(α in this table). (Shum, 2005)

μ	α	λ	ξ_1	ξ_2	β_1	β_2
0.005	0.7	0.99629	0.03006	0.03041	0.97993	1.01478
0.010	0.7	0.99262	0.04230	0.04300	0.97019	1.01928
0.020	0.7	0.98538	0.05933	0.06072	0.95513	1.02397
0.050	0.7	0.96445	0.09183	0.09522	0.92136	1.02755
0.005	0.8	0.99592	0.03432	0.03478	0.97739	1.01723
0.010	0.8	0.99188	0.04829	0.04920	0.96658	1.02270

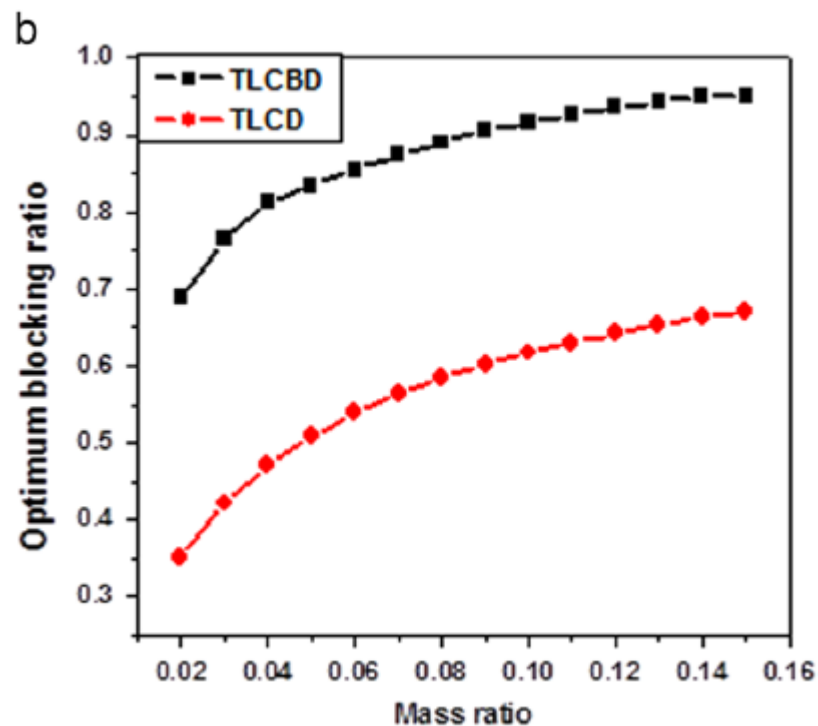


Figure 2.5: Optimum Blocking Ratio against Mass Ratio. (Tanmoy and Subrata, et al., 2014)

2.4 Length Ratio, α of TLCD

Length Ratio of TLCD is defined as the horizontal length of the TLCD to the total length of the TLCD. However this is only true provided that the TLCD has uniform cross sectional area that is the vertical column and horizontal column of the TLCD has the same cross sectional area. (Wu, et al., 2005)

By referring to Figure 1.2, the length ratio, α can be expressed as:

$$\alpha = \frac{B_D}{B_D + 2L_D} \quad (2.4)$$

where

B_D = horizontal column length, m

L_D = vertical column length, m

If the cross sectional area of the vertical and horizontal column is different, then the length can be redefined as the mass of liquid in the horizontal column to the total mass of liquid in the TLCD. (Matteo, et al., 2014)

$$\alpha = \frac{m_{B_D}}{m_{TLCD}} \quad (2.5)$$

where

m_{B_D} = mass of liquid in the horizontal column, kg

m_{TLCD} = mass of total liquid in the TLCD, kg

Generally, a larger length ratio will result in a better performance of the TLCD, but if the length ratio exceeds a certain threshold value than it may destroy the basic characteristic of the TLCD. (Min, et al., 2005)

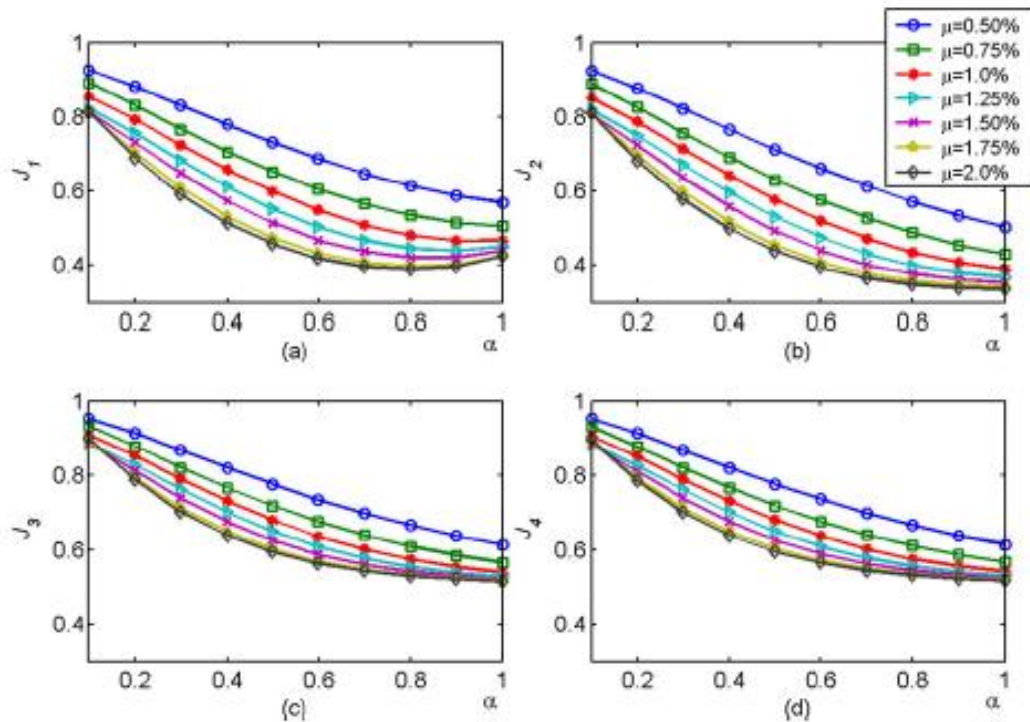


Figure 2.6: The Effect of Length Ratio on the Performance Indices of TLCD on Various Mass Ratio. (Min, et al., 2005)

Since the length ratio is often restricted by the design environment like space available, hence there is no an optimum value but up to the designer to decide the value which is usually suggested to be 0.7. (Wu, et al., 2005)

2.5 Tuning Ratio, β of TLCD

The tuning ratio is defined as the ratio natural frequency of the TLCD to the natural frequency of the structure. The natural frequency of the structure, generally refers to the principal mode if the structure possesses multiple mode of vibration. (Min, et al., 2005).

One of the advantage of TLCD in the tuning ratio is that the natural frequency of the TLCD can be controlled precisely by simply varying the total length of the liquid. The formula for the natural frequency of TLCD is:

$$\omega_D = \sqrt{\frac{2g}{L}} \quad (2.6)$$

where

ω_D = natural frequency of TLCD, rad/s

L = total length of liquid in the TLCD, m

Even though this is theoretical formula, Wu, et al. (2005) has tested the practicability of this formula. The result is that the natural frequency of TLCD predicted by using equation 2.6 varies by less than 2% from the actual value. (Wu, et al., 2005)

The effect of tuning ratio on the performance of TLCD is like the head loss coefficient. There exist an optimum value of tuning ratio, too high or too low will only render the TLCD useless. The theoretical optimum value of tuning ratio is 1 however, in actual life, the optimum value of tuning ratio only approaches 1 when the mass ratio decreases while at other times, the optimum tuning ratio is less than 1. (Min, et al., 2005)

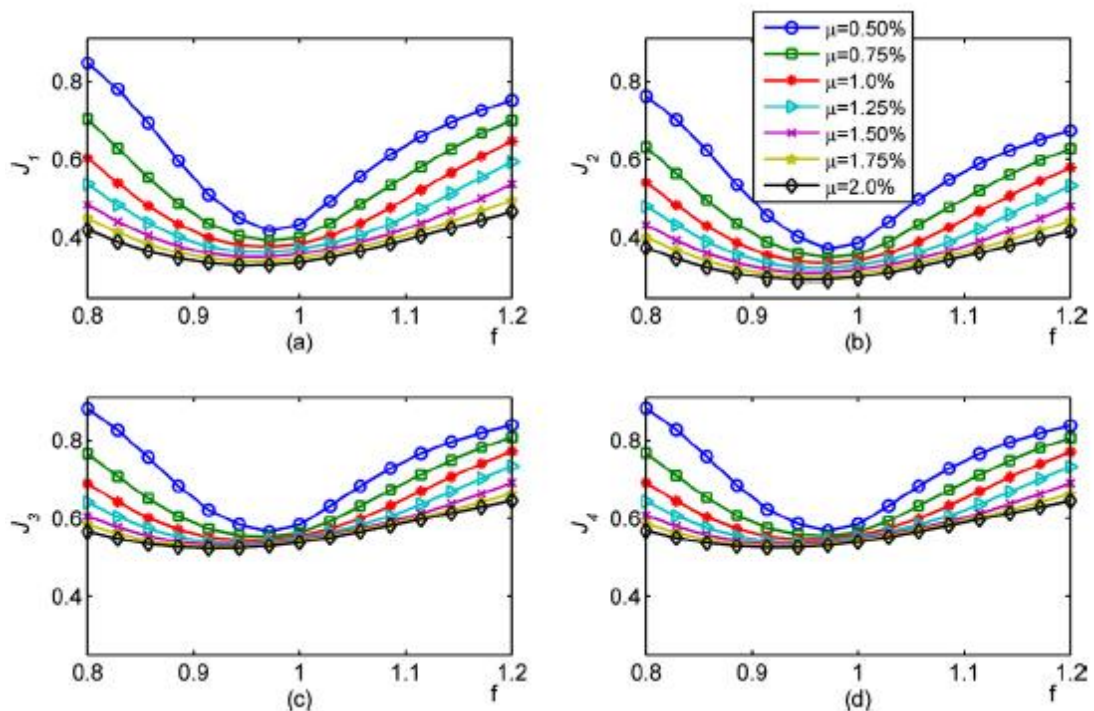


Figure 2.7: Variation of Performance Indices with respect to Tuning Ratio on Various Mass Ratio. (Min, et al., 2005)

Besides this, the same trend has been witness from both Figure 2.7 and Table 2.2 whereby when the mass ratio is getting smaller, the optimum tuning ratio approaches 1. This may be due to the fact that by installing the TLCD onto the structure, it introduces a new degree of freedom and weight to it, resulting in some deviation of the natural frequency of the structure from what we have calculated.

2.6 Mass Ratio, μ of TLCD

The mass ratio, μ is defined as the ratio of the mass of the TLCD to the mass of the structure. In general, the effect of mass ratio on the performance of TLCD is very straight forward, which is the higher the better. (Min, et al., 2005)

This is also supported by Matteo, et al., (2014) whereby in this result, the normalized structure displacement is getting lesser as the mass ratio increases. This is show in Figure 2.7

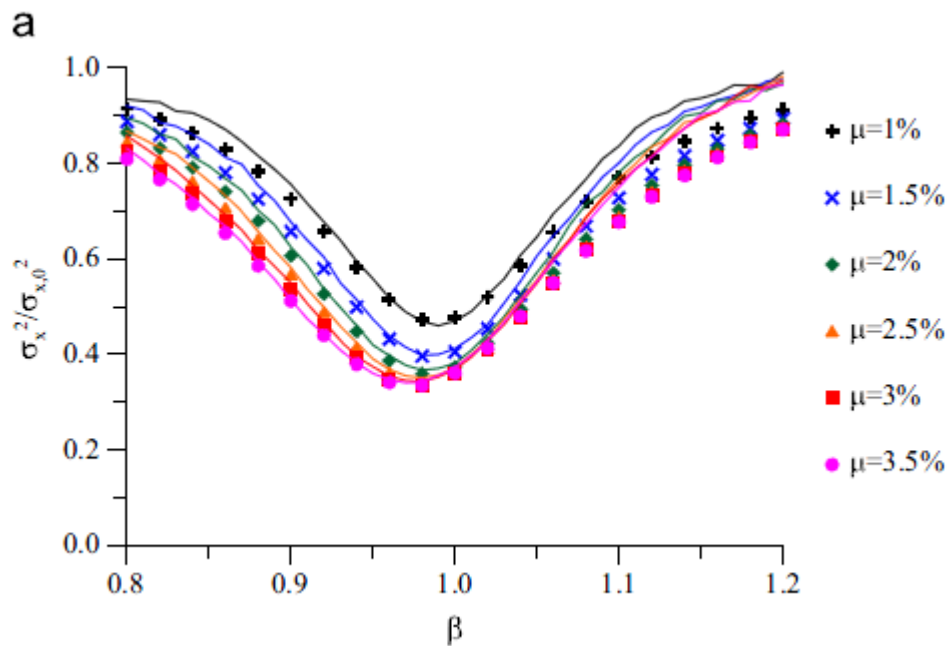


Figure 2.8: Normalized Structure Displacement against Tuning Ratio for Various Mass Ratio. (Matteo, et al., 2014)

Mass ratio is similar a bit similar to the length ratio, there is no optimum value of it, it is up to the designer to decide the mass ratio he required depending on the designing environment. An overrated mass ratio would be impractical as it is hard to achieve, nevertheless too small will also results in the inefficiency of the TLCD. Hence, usually the mass ratio is limited below 5%. (Tanmoy and Subrata, 2014) This is also one of the advantage of using TLCD, that is the low mass ratio required compared to Tuned Mass Damper which require a lot higher of mass ratio. (Tanmoy and Subrata 2014)

In addition, from the Figure 2.7, we can see that the control performance improvement of the TLCD gradually decrease and becomes negligible when the mass ratio, μ increases beyond 1.5%. Min, et al. (2005) also comes to the same conclusion that the improvement becomes negligible when $\mu > 1.5\%$.

CHAPTER 3

METHODOLOGY

3.1 Platform Design Stage

The floating platform to be designed is a 1.5 m by 1.5 m wide platform for the mounting of solar panel while the total weight of the housing and the solar panel is estimated to be 150 kg. However, due to the fact that this project is a low budget fund with only RM500, a smaller prototype of 450 mm by 500 mm wide platform is made instead, that is the size is scaled down by approximately 3 times. On the other hand the total weight of the housing and the solar panel is scaled down to 5 kg instead of 50 kg due to the fact that in our project the main purpose is to test the functionality and feasibility of the TLCD instead of the rigidity and strength of the platform.

In this floating platform, the only thing that we will adopt in the Mini-TLP is the mooring system. However, since the function of mooring system to prevent heave, the presence of the mooring system is simulated by using a wave with lateral force only. The reason being for no pontoon and hull will be designed in our floating platform but only the deck which is a square container is that the intention of the platform is for mounting solar panel which require very less buoyant force and hence pontoon is not needed while the stability of the platform is preserved by utilizing the TLCD and hence the hull is not needed as well. Thus, what to be cared in the designed platform is to allocate a place for the housing of TLCD only.

In order to for the platform to float, the buoyancy force must be greater than the 150 kg weight plus the weight of the platform and TLCD itself. In order to calculate that:

$$F_B = W_{TLCD+Platform} + F_{Load} \quad (3.1)$$

where

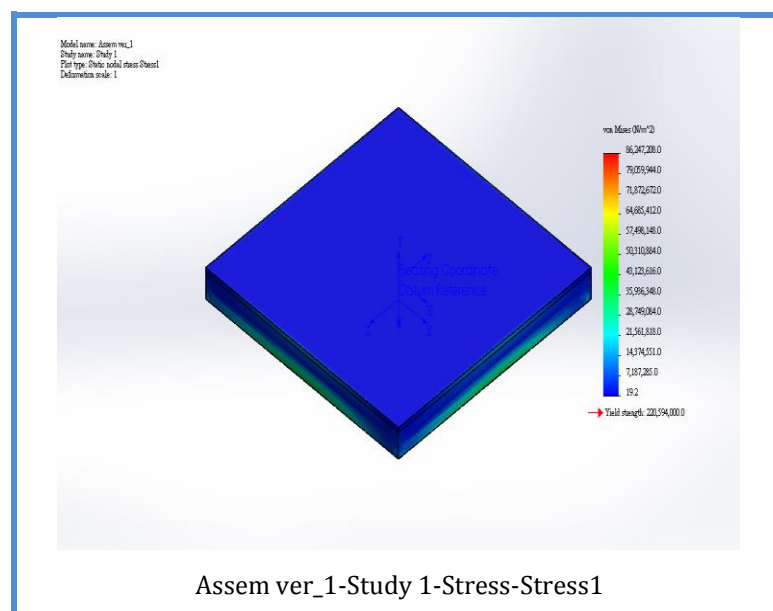
$W_{TLCD+Platform}$ = weight of the TLCD and the platform, N

F_{Load} = loading force, N

By utilizing equation 3.1, the desired height of the floating platform can be calculated. Once the height is calculated, the centre of gravity and the required second moment of inertia of the platform is obtained by using a software which is SolidWorks. These data is needed for the calculation of metacentric height in equation 2.2 to ensure the platform is stable neutrally and the critical angle to which the platform can tilt.

In addition, in order to ensure the platform is able to sustain the global strength, a simulation is done using SolidWorks to simulate the hydrostatic force and the loading force acting on the platform as shown in Figure 3.1. Due to this, the whole platform and TLCD will be modelled by using SolidWorks as well. The exact calculation and simulation will be discussed in Chapter 4 which is the Result and Discussion Part.

Table 3.1: Example of the Simulation Done on the Platform



3.2 TLCD Design Stage

Since, the various parameter of TLCD has to be tested, multiple TLCD suits for each different parameter study is designed as it is impossible to perform all the variation of parameter in a single TLCD.

The TLCD designed will be of constant parameter except the parameter that has to be study. Generally, the TLCD designing will be start by choosing a suitable mass ratio and length ratio due to the design constraint such as the space available, then the optimum value of tuning ratio and head loss coefficient will be determined by using the optimum parameter table developed by Shum (2009) which will be shown in the appendix. The optimum head loss coefficient is then achieved by using suitable blocking ratio orifice plate. The head loss coefficient value of each orifice plate is calculated using equation 2.3. On the other hand, the optimum tuning ratio is achieved by adjusting the total length of liquid in the TLCD.

Finally, the last step is to check whether the liquid surface displacement in the TLCD will exceed the vertical column length to prevent the worst case which is the spilling of liquid out of the TLCD. This is performed by utilizing the method proposed by Wu, Chang and Lin. (2009)

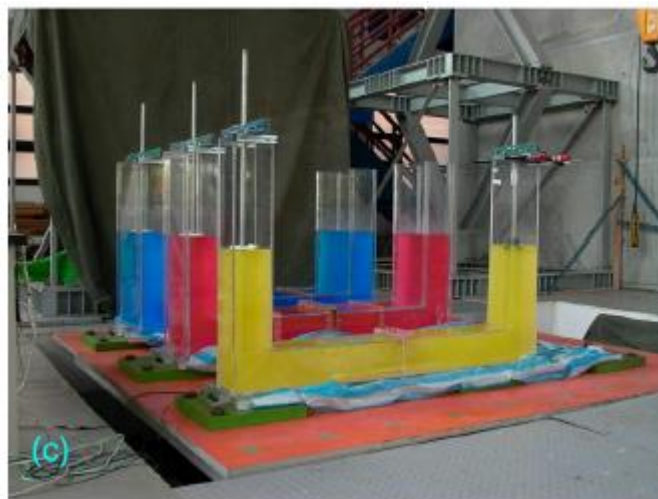


Figure 3.1: Sample of TLCD to be Built. (Wu, et al., 2005)

3.2.1 Head Loss Coefficient Study

By following the general concept of designing except that the optimum value of head loss coefficient is not used. Instead, different orifice plate with different blocking ratio is used. By referring to equation 2.3, the head loss coefficient for each orifice plate is calculated and the response of the floating platform is obtained by using an accelerometer.

From here, we can conclude that only one TLCD is required to study the Head Loss Coefficient

3.2.2 Tuning Ratio and Mass Ratio Study

For tuning ratio study, it is a bit similar to length ratio study. The only difference is that in order to maintain the length ratio and mass ratio while varying the tuning ratio, the dimension of the new TLCD is calculated in a different way. Thus a few TLCD with different dimension is needed to maintain other parameter while varying tuning ratio.

On the other hand, for mass ratio study, it is first started off by following the general principle which is first, by deciding the mass ratio and length ratio to obtain the optimum tuning ratio and head loss coefficient from the optimum parameter table in appendix. From there onwards, the mass ratio is varied while maintaining the other optimum parameter by varying the cross-sectional dimension of TLCD. Hence, again multiple TLCD is needed to study the mass ratio parameter.

From here, it can be concluded that in order to study the effect of tuning ratio and mass ratio alone a mass number of TLCD with different dimension is needed. However, due to the budget constraint in buying the material for TLCD, as well as the time constraint in producing these vast amount of TLCD (at least 8 if it would to follow the original approach), hence an alternative approach is used instead.

In this new approach, the effect of tuning ratio and mass ratio is grouped as one parameter and is then studied all together the composite effect of tuning ratio and mass ratio. This is done by varying the total length of liquid in TLCD which can be achieved by simply reducing or increasing the amount of water inside the TLCD using a straw. From equation 2.6, by reducing the total length of liquid in TLCD, the natural frequency of the TLCD is increased, hence equivalent in increasing the tuning ratio.

At the same time, when the total length of liquid in the TLCD is reduced, the mass ratio of TLCD will reduced as the reduced in total length of liquid in TLCD is equivalent in reducing the mass of TLCD as the amount of liquid in it is lessen. Thus, as the total length of liquid of TLCD is reduced, it is equal to increasing tuning ratio and reducing the mass ratio.

3.3 Manufacturing and Material Selection Approach

In this project, there is two main parts that has to be manufactured which is the platform that is used for the mounting of the solar panel and the TLCD which is used to mitigates the vibration of the platform. However, due to rigidity concern of the platform, reinforcement bone frame at the top of the platform is made to prevent the platform from bending and buckling in shape.

When preparing to manufacture the parts, a parts drawing produced by using SolidWorks is printed out before any actual manufacturing process is carried to prevent minor mistake in the dimension of the parts being manufactured. In addition this extra steps also provides a systematic ways to manufacture the parts without fear of duplication and wrong doing. A sample of parts drawing produced by using SolidWorks is shown in Figure 3.2.

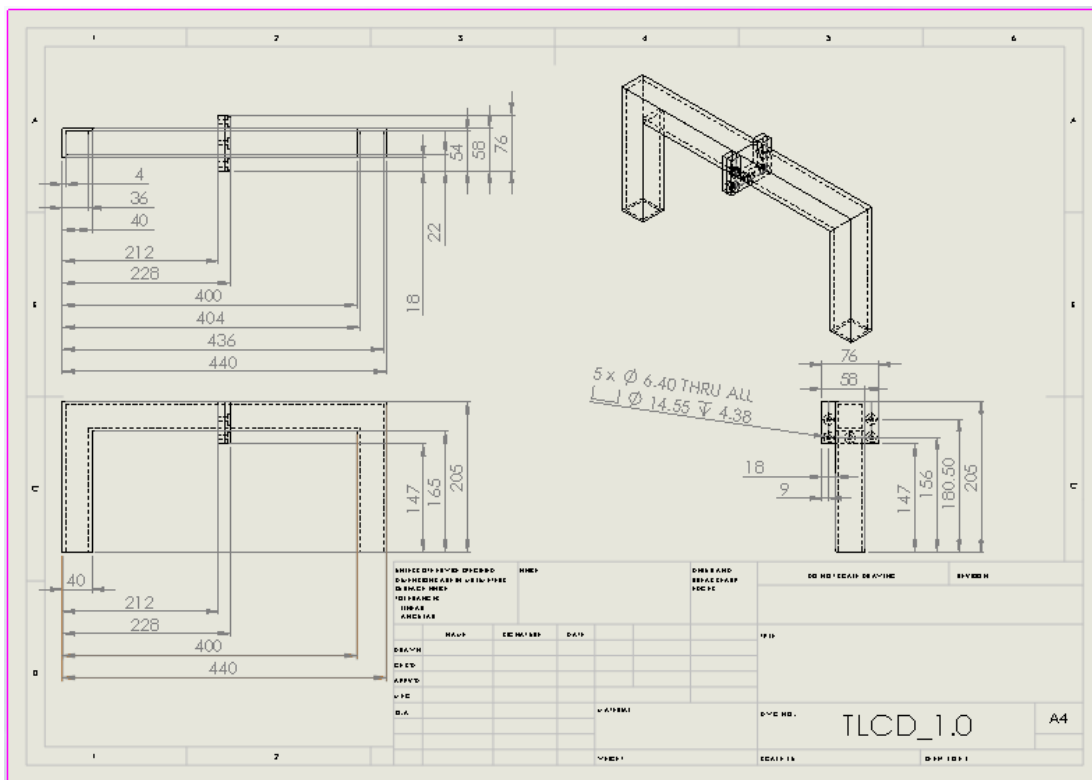


Figure 3.2: Sample of TLCD Parts Drawing For Manufacture

3.3.1 Platform Manufacturing

For the platform that is to be manufactured, the material used is perspex. This is because compared to material used in the conventional industrial for making a floating platform which is mild steel, perspex is much easier to work with as it does not require the skill of welding. Even with the skill of welding, it does not guarantee the welded platform will be “water tight” as the welded portion of the platform maybe porous especially at the edges resulting in water sipping into the platform, which is why in the offshore industrial, all the welding worker must be certified by corresponding organization to prove that they are skilled professional technician in welding that is capable of welding parts which are meant to be water proof.

With the difficulty in utilizing mild steel, perspex is chosen as the material of the platform. The next issue will then be determining the thickness of the perspex sheet that is being used for manufacturing the platform. From the advice of mechanical

technician, perspex sheet of thickness lesser than 4 mm is very flexible, hence perspex sheet of 4 mm thickness is chosen. After which, a simulation on the stress performance of the platform using perspex of 4 mm thickness is done to double confirm the stress performance of the platform under load. The result will be discuss in chapter 4.

First of all, the exact size of perspex that has to be cut is drawn onto the perspex sheet using either a marker pen or a pencil. Then the exact dimension of perspex wanted is cut off from the whole perspex sheet by using a machine call Vertical Bandsaw as shown in Figure 3.3 while the sample perspex sheet cut is shown in Figure 3.4.



Figure 3.3: Vertical Bandsaw



Figure 3.4: Sample Perspex That Has Been Cut

With all the perspex sheet necessary to build the platform being cut out, all these sheet is joined together to form the platform by using the chloroform. Chloroform is the solvent for perspex, hence by applying it onto one of the perspex surface it can temporarily dissolve the perspex allowing two surface to be joined together by simply pressing the two surface of perspex together. After the chloroform vaporizes, the perspex returns back to solid state and the part is joined together through the two surface as shown in Figure 3.5. Simply put, the chloroform works like a glue that is specially only for perspex.



Figure 3.5: Perspex Being Sticked Together With Book as Force

3.3.2 Bone Frame Reinforcement Manufacturing

For the bone frame of the platform, it is wanted to be rigid in nature to withstand load as well as act as support when two piece of perspex is joined together as shown in Figure 3.5. Thus, aluminium which is light and rigid is chosen as the material for this bone frame reinforcement.

Instead of using aluminium bar, aluminium profile is used. This is because solid aluminium bar is too heavy and the high rigidity of this solid aluminium bar is not a necessary to our platform. Hence choosing solid aluminium bar would only means over design for our platform. However, the hollow aluminium bar is too fragile, a simple process of drilling 8 mm hole might bend the surface of the hollow aluminium bar. Thus, the aluminium profile which is sometimes known as “conveyor aluminium” is chosen. It has the optimum property that platform needed which is light and sufficiently rigid. The rigidity of this aluminium profile comes from the cross sectional design of the aluminium profile as shown in Figure 3.6, which makes it lighter than solid aluminium bar yet possesses higher rigidity than hollow aluminium bar.

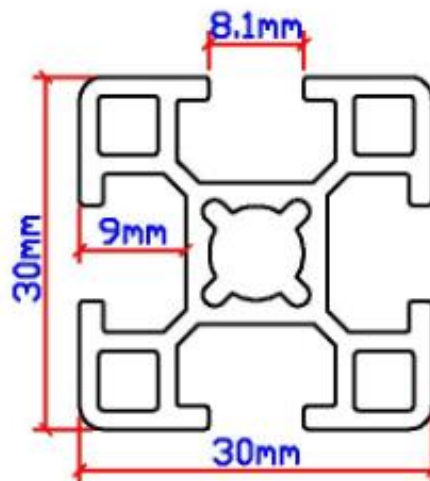


Figure 3.6: Cross Sectional Design of Aluminium Profile

3.3.3 TLCD Manufacturing

For the TLCD manufacturing, it is divided into multiple smaller parts. All of these part is manufactured using perspex sheet of 4 mm due to the flexibility of perspex in machining out the precise shape of TLCD. By referring to Figure 3.2 which is the part drawing of TLCD as a whole, it is divided into 3 part for the ease of manufacturing that is the orifice plate which is inside of the TLCD, the left hand side of TLCD and the right hand side of TLCD. The TLCD is split into left hand side and right hand side part because it can be seen from Figure 3.2 that the TLCD is symmetric about the centre (left hand side is identical to right hand side), hence by splitting it into two parts makes the manufacturing process more easier as we would only need to duplicate another set of the left hand side of TLCD instead of directly producing the U shape TLCD as shown in Figure 3.7.

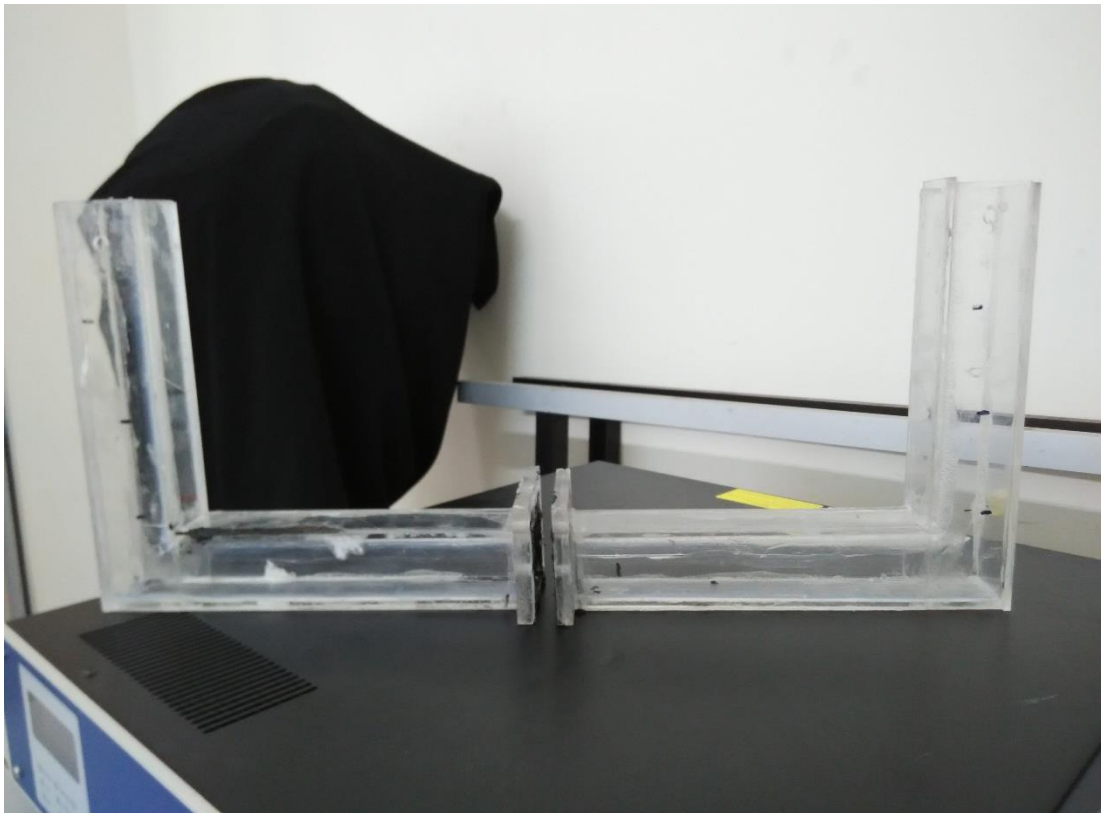


Figure 3.7: Identical Left Hand Side and Right Hand Side of TLCD

By using the Vertical Bandsaw machine as shown in Figure 3.3, the TLCD is cut into pieces of rectangular shape perspex sheet which is then joined together through

the use of chloroform. However, since the TLCD require a certain degree of precision, another machine call milling machine as shown in Figure 3.8 is used to mill the perspex sheet to the exact dimension as well as producing a smooth surface.



Figure 3.8: Milling Machine

For the orifice plate manufacturing, it involves cutting out a small piece of perspex sheet after which a hole is drilled on top of it, representing the vena contracta channel. Since a gasket is used to ensure the “water proof” in inserting the orifice plate onto the TLCD, hence the orifice plate does not require a high degree of precision.

3.4 Experimental Setup

In this project, the main objective is to develop a floating platform which utilizes TLCD to mitigate vibration originate from the ocean waves. Thus the main experimental setup will be the floating platform with the TLCD installed as shown in Figure 3.9. The technical drawing with specification of the platform and TLCD will be included in the appendix as reference.



Figure 3.9: Platform With TLCD Installed

Besides the platform with the TLCD installed, a data logger with analyser function as well as accelerometer sensor is needed as well. The data logger used is IMC Cronos-PL2 while the accelerometer used is Kistler Type K-shear as shown in Figure 3.10. In order to mount the accelerometer to the platform, a small amount of wax is applied to the surface of the platform which is in contact with the accelerometer. The wax used in this project is petroleum wax which sticks the accelerometer onto the platform firmly and securely but with the disadvantage of leaving a stain behind when the accelerometer is dismounted from the platform. After mounting the accelerometer to the platform, a data cable is used to connect each accelerometer to the data analyser

while the data analyser is connected a laptop using a network cable where the data logged during the experiment can be in real time recorded inside the laptop as shown in Figure 3.11.



Figure 3.10: IMC Dynamic Signal Analyser and Kistler Type K Shear Accelerometer

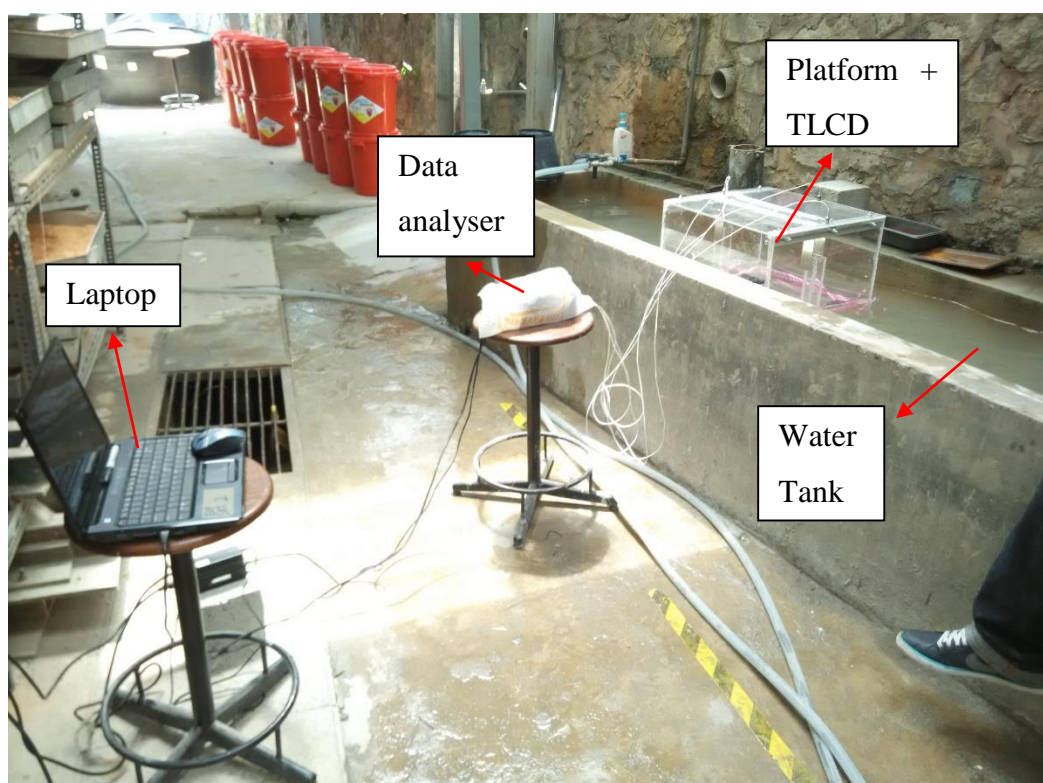


Figure 3.11: Full Experimental Setup

The 4 accelerometer which is mounted on the platform as shown in Figure 3.11 is connected to the 4 channel of the data analyser in an orientation as shown in Figure 3.12. Channel 3 and Channel 4 is for the sole purpose of determining whether the wave generated is one directional or not, hence only response of channel 1 and channel 2 will be analysed.

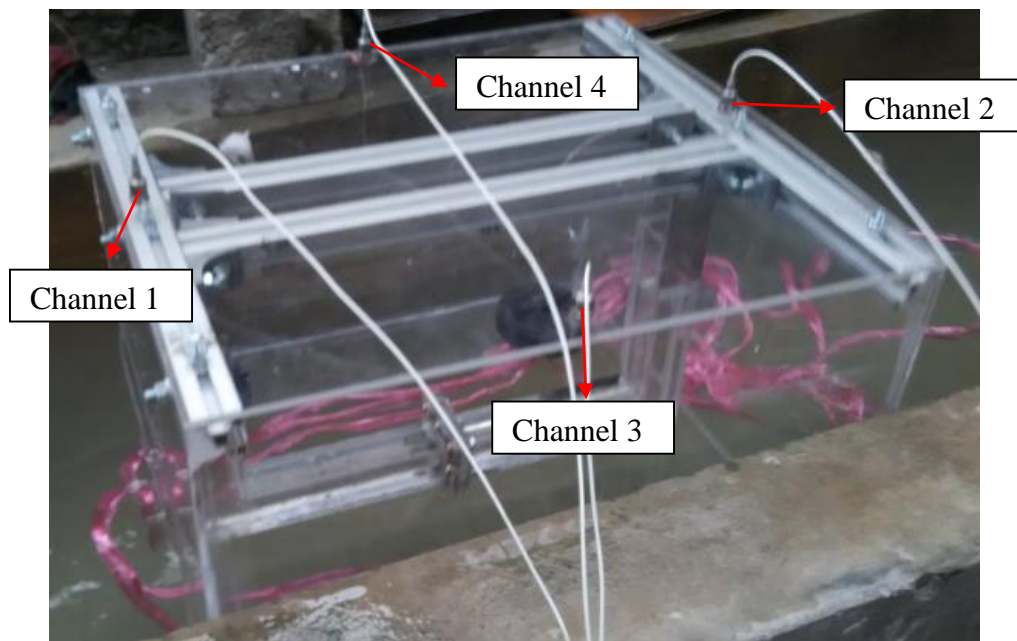


Figure 3.12: Accelerometer to Channel Orientation

On the other hand, the wave generation is done manually by hand, using a metal plate to pushes the water front and back at a frequency of 1 Hz as shown in Figure 3.12 to produce a one directional wave.

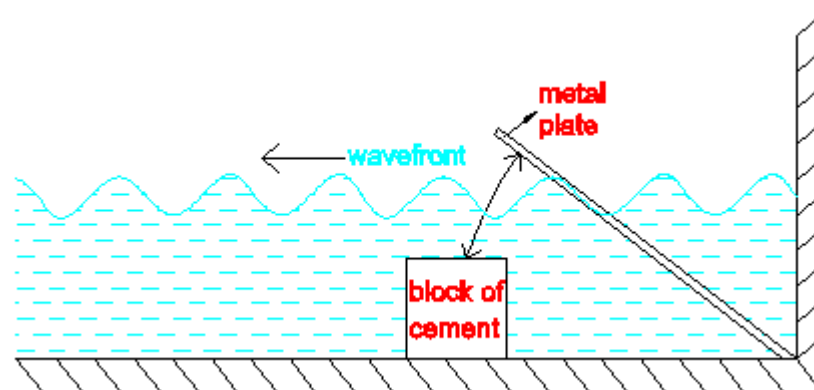


Figure 3.13: Wave Generation Method

In order for the experiment to be carried out, the wave produced has to be in one direction, hence the output of accelerometer of channel 3 and 4 is monitored in real time to determine whether or not the wave is in one directional. If the output of accelerometer of channel 3 and 4 is relatively high, it indicates that the waves is not in one direction towards the other end. Thus once the output of accelerometer of channel 3 and 4 is high, the experiment has to be redo again. In conventional method, the wave generation should be done by a mechanism installed in a wave tank. However due to the cost constraint, a wave tank is not used, instead a water tank with a manual wave generation as illustrated in Figure 3.13 is used instead.

With all these, the experiment can be carried out by first measuring the height of liquid displaced as well as the actual critical angle at which the platform will capsize and record it down. After which, the wave generation is started at approximately constant frequency of 1 Hz and constant amplitude in which later on the acceleration data of the platform is recorded for 30 s for the orifice plate of 4 mm diameter, 6 mm diameter, 8 mm diameter, and 10 mm diameter to test the effect of head loss coefficient. Throughout this testing, the TLCD is filled with water to a level of 15 cm. For each of the orifice plate, the experiment is carried out 5 times, in order to average out result.

For the testing of composite effect of mass ratio and tuning ratio, the TLCD installed with orifice plate of 10 mm diameter is used. However the water level at which TLCD is filled is changed to 5 cm and 10 cm respectively. At each water level, the acceleration data is recorded for 30 s and the test is repeated 5 times to average the result.

CHAPTER 4

RESULTS, CALCULATION AND DISCUSSION

4.1 Theoretical Buoyancy Calculation and Comparison to Experimental Result

The buoyant force and metacentre is an important aspect in determining whether the platform will float steadily or easily tilted over by waves. The load is 4 kg while the mass of TLCD and platform is obtained from SolidWorks as shown in Figure 4.4 while the buoyant force required is calculated by using equation 3.1. From there, the minimum height of platform required is determined as shown below:

$$\begin{aligned}F_B &= W_{TLCD+Platform} + F_{Load} \\F_B &= 62.14 \text{ N} + 40 \text{ N} \\V_D \rho g &= 102.14 \text{ N} \\A_D h_D \rho g &= 102.14 \text{ N} \\h_D &= \frac{102.14 \text{ N}}{(0.45 \text{ m} \times 0.5 \text{ m})(1000 \text{ kg/m}^3)(9.81 \text{ m/s}^2)} \\h_D &= 0.04627 \text{ m}\end{aligned}$$

Where

A_D = Cross sectional area of liquid displaced, m^2

h_D = Height of liquid displaced, m

This shows that the minimum requirement height of platform needed is 4.627 cm. In our platform the height is 31.4 cm as shown in Figure 4.1 which is more than sufficient for it to afloat.

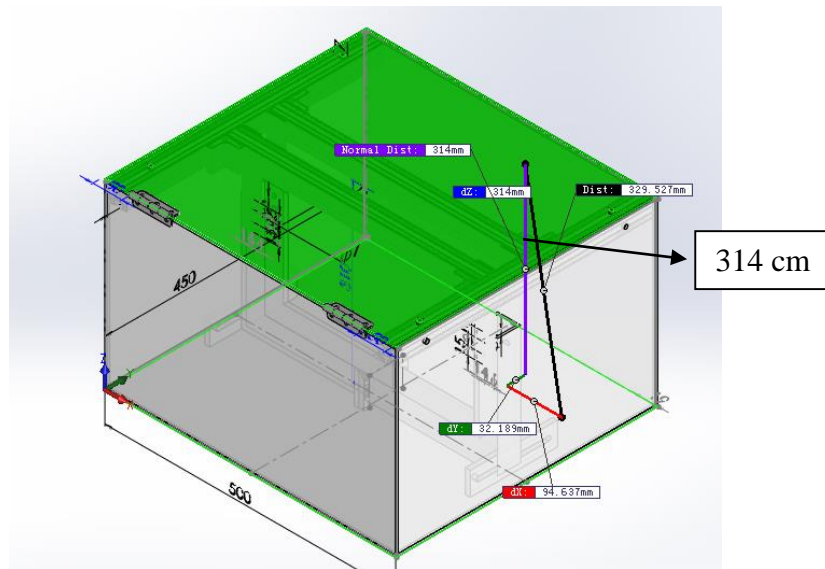


Figure 4.1: Platform's Height

This is also proven by the actual testing of the platform that only approximately 5 cm of platform is submerged in the water as shown in Figure 4.2. The slight difference from the calculated value might be due to the manufacturing error. In fact the whole platform which is supposed to be 500 x 450 mm turns out to be 501 x 451 mm while the TLCD which supposed to be 440 mm turns out to be 412 mm. This slight difference in manufacturing causes the increase in the total weight of the platform and the TLCD, resulting in this slight deviation. Furthermore, the unit weight which is used as load in the testing is not exactly 4 kg, it is slightly more than 4 kg, which indirectly contributes to this error as well.

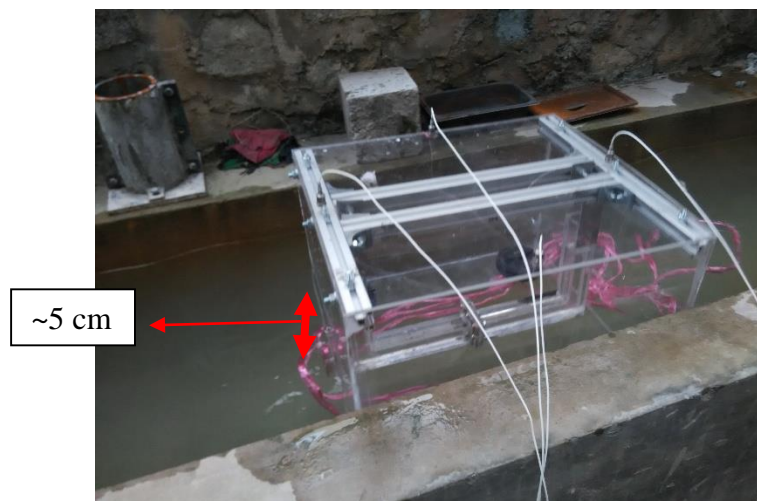


Figure 4.2: Height of Liquid Displaced

In order to determine the actual buoyant force exerting on this platform, a different definition of buoyant force is used, which is buoyant force is equal to the weight of liquid displaced (in this case is water), mathematically it is expressed by equation 2.1.

$$F_B = \rho V_D g$$

$$F_B = (1000 \text{ kg/m}^3) (0.45 \text{ m} \times 0.5 \text{ m} \times 0.05 \text{ m})(9.81 \text{ m/s}^2)$$

$$F_B = 110.3625 \text{ N}$$

$$\begin{aligned} \text{Percentage of deviation} &= \frac{|Actual - Theoretical|}{Theoretical} \times 100 \% \quad (4.1) \\ \text{Percentage of deviation} &= \frac{|110.3625 - 102.14|}{102.14} \times 100 \% \\ \text{Percentage of deviation} &= 8.05 \% \end{aligned}$$

Where

Actual = Experimental result of a variable

Theoretical = Calculated result of a variable

The percentage of deviation of the actual buoyant force from the calculated buoyant force is 8.05 % which is less than 10 %. This shows that the even with a poor manufacturing skill, the actual buoyant force acting on the body would hardly deviates from the theoretical value for more than 10 %. The reason being for this deviation is the same as the reason being for the deviation in the height of liquid displaced as discussed in the previous paragraph and hence will not be repeated.

4.2 Metacentric Height Calculation and Evaluation

The metacentric height is essential in determining the stability of the system. It is also a preliminary study of the stability of an object which is floating. It is calculated by using equation 2.2. However before using equation 2.2, basic parameter such as the CG of the platform including the load has to be determined. By referring to Figure 4.4,

the CG is calculated. The CG of the platform without the weight is calculated by using the software SolidWorks as shown in Figure 4.3.

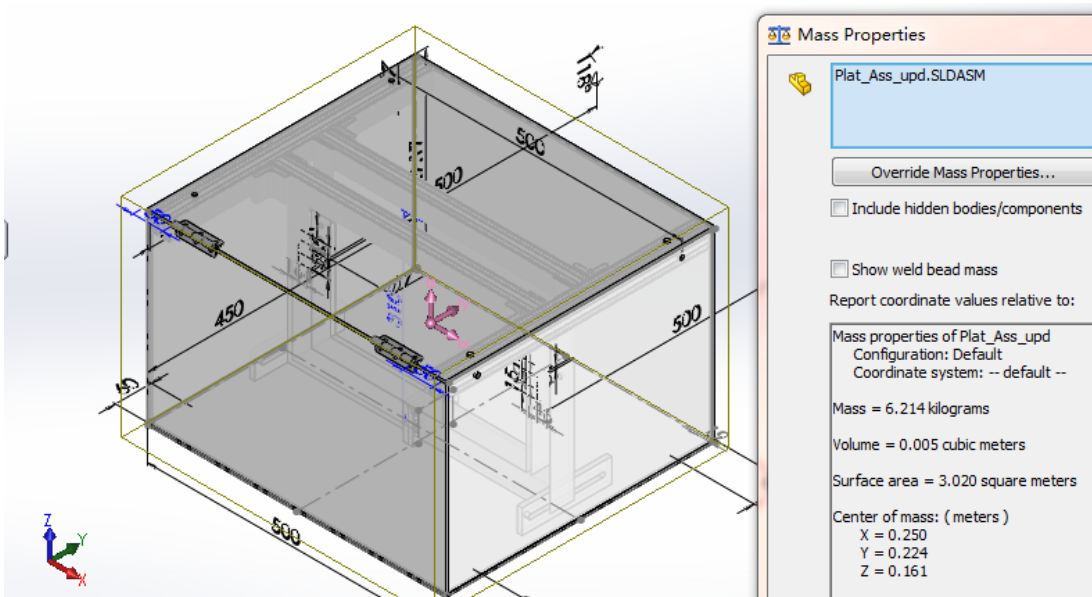


Figure 4.3: CG Calculated From SolidWorks

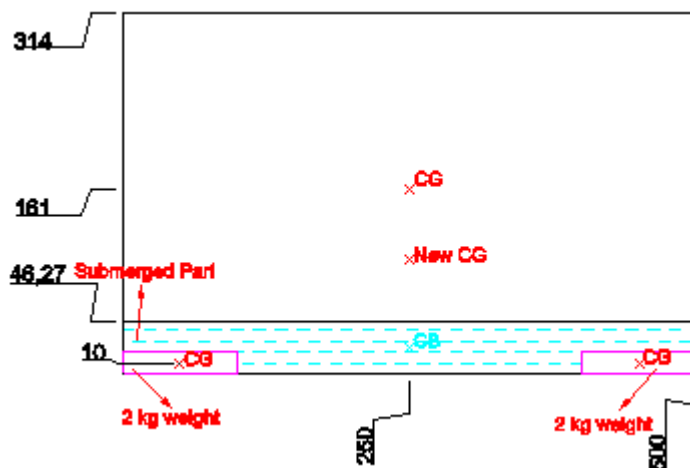


Figure 4.4: AutoCAD Front View Drawing For Calculation

$$CG_{new,y} = \frac{\sum mCG_y}{m} \tag{4.2}$$

$$CG_{new,y} = \frac{(6 \text{ kg} \times 161 \text{ mm}) + 2 (2 \text{ kg} \times 10 \text{ mm})}{6 \text{ kg} + 2 \times 2 \text{ kg}}$$

$$CG_{new,y} = 100.6 \text{ mm} = 0.1006 \text{ m}$$

Where

$CG_{new,y}$ = CG of the platform and TLCD together with the weight, m

CG_y = y coordinate of the CG of the object, m

m = Mass of the object, kg

Since the platform together with the weight is symmetric about the centre line, the x coordinate of the new CG is the same as the x coordinate of the CG of the platform and the weight as shown in Figure 4.4. Thus the new coordinates for the CG of the whole platform together with weight and TLCD is (0.25 m, 0.1006 m).

The next basic parameter to be determined before the metacentric height can be calculated is the volume of liquid displaced by using equation 2.1 while the centre of buoyancy is calculated by dividing the height of liquid displaced by 2.

$$V_D = \frac{F_B + W_{TLCD+Platform}}{\rho g}$$

$$V_D = \frac{102.14 \text{ N}}{1000 \text{ kg/m}^3 \times 9.81 \text{ m/s}^2}$$

$$V_D = 0.01041 \text{ m}^3$$

$$CB = \frac{h_D}{2} \quad (4.3)$$

$$CB = \frac{0.04627 \text{ m}}{2}$$

$$CB = 0.023135 \text{ m}$$

With all these value calculated, the metacentric height can be calculated by using equation 2.2.

$$GM = \frac{I_0}{V_D} - CG + CB$$

$$GM = \frac{\frac{1}{12}(0.45 \text{ m})(0.5 \text{ m})^3}{0.01041 \text{ m}^3} - 0.1006 \text{ m} + 0.023135 \text{ m}$$

$$GM = 0.3728 \text{ m}$$

The value of metacentric height is positive indicating that the metacentre is above the *CG* of the platform, hence the platform is in stable state. However, this positive metacentric height is calculated at zero angle tilting state, hence it will only guarantee the stability of the platform within the range of 0° to 15° . For safety reason, the metacentric height should be recalculated again for tilting angle greater than 15° to determine whether or not the platform will capsize.

4.2.1 Metacentric Height and Righting Arm at Different Tilting Angle

Since it is very tedious to determine the centre of buoyancy which keeps moving around as the platform is tilting about the *CG* as shown in Figure 4.5. Thus, the centre of buoyancy is located by utilizing graphical method as proposed in chapter 3 methodology. This graphical method is done with the aid of a software called AutoCAD. By selecting the region at which the water is displaced, the AutoCAD software can compute the centroid of the volume of water displaced. Since in this case the centre of gravity coincide with the centroid due to same density and same width of volume of water displaced, the centre of buoyancy is equivalent to the centroid.

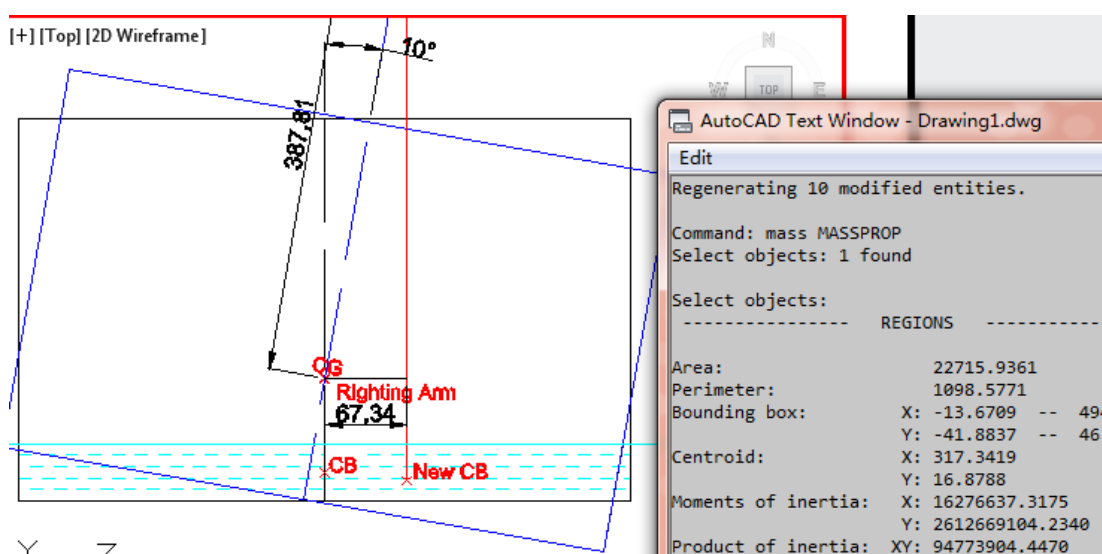


Figure 4.5: Platform Tilted by 10° about *CG*

The degree to which the righting moment will tilt the platform back to the original position is depending on the righting arm to which the centre of buoyancy and the weight act as a couple force to rotate the platform back to the original position. The righting arm of each tilting angle is obtained by graphical method as shown in Figure 4.6.

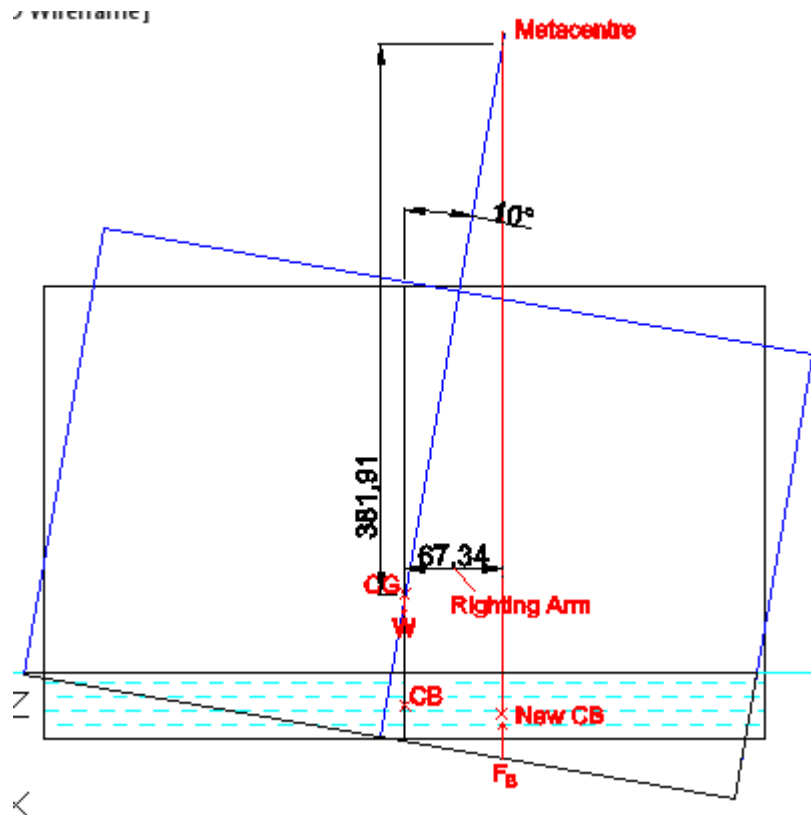


Figure 4.6: Righting Arm and Metacentric Height When Platform Tilted by 10° about CG

All of the Metacentric Height and Righting Arm for different tilting angle at the increment of 10° is tabulated in Table 4.1. The result of the graphical method for the metacentric height and righting arm listed in Table 4.1 is attached in appendix A

Table 4.1: Metacentric Height and Righting Arm Distribution on Different Tilting Angle

Angle Tilted ($^\circ$)	GM (m)	Righting Arm (m)
0	0.0000	0.0000
10	0.3819	0.0673

20	0.2765	0.1006
30	0.1827	0.1055
40	0.1255	0.1053
50	0.0901	0.1074
60	0.0602	0.1042
70	0.0334	0.0917
80	0.0132	0.0751
90	0.0000	0.0564
100	-0.0065	0.0370
110	-0.0065	0.0180
120	-0.0004	0.0006
130	0.0111	-0.0132
140	0.0237	-0.0199

From the Table 4.1, a graph of metacentric height against angle tilted and a graph of righting moment against the angle tilted are plotted to evaluate the stability of the platform designed as well as to determine whether or not the platform will return to its original position or is being capsized.

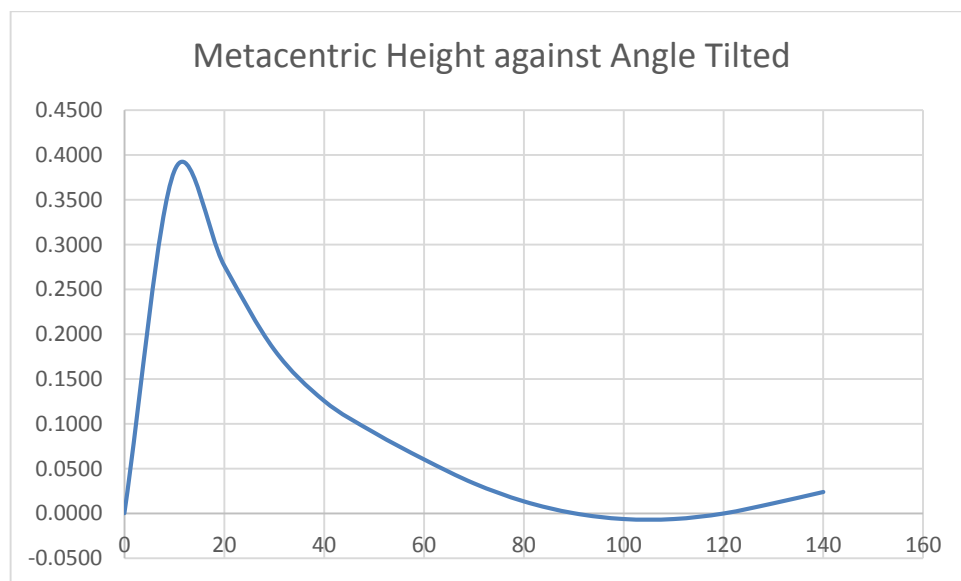


Figure 4.7: Graph of Metacentric Height against Angle Tilted

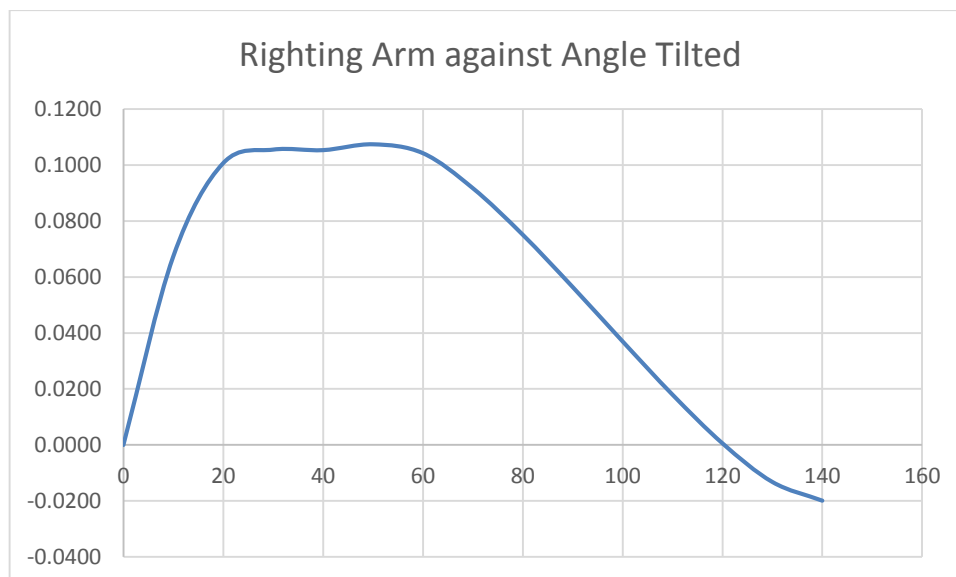


Figure 4.8: Graph of Righting Arm against Angle Tilted

From Figure 4.6, the righting arm is defined as positive when the resulting righting moment (the couple moment produced by F_B and total weight of the platform acting about the righting arm). Thus, when the righting arm is negative value, it shows that the platform is capsized in which in this case is at clockwise 120° tilting by referring to Figure 4.7. In addition, Figure 4.7 also provides a mean to measure how fast the platform will return to its original position. If the value of righting arm is large, it means that the righting moment acting on the platform to return it to the original position is large.

For Figure 4.7, it shows the stability of the platform by means that if the platform would be left at that position would it be still stable. It is noticed from Figure 4.7 that at about clockwise 100° of tilting, the metacentric height becomes negative. This shows that at this stage, even if the platform is to left undisturbed at this stage, it will also oscillate indefinitely. From a second point of view is that, the righting moment has dropped to critical value in which it no longer can maintain the platform stability, but the platform is yet to be capsized.

From these theoretical value, it shows that the platform is well designed as it is able to withstand a tilting of 120° before being capsized. However, in actual case, the platform started to capsize at approximately 110° due to the fact that the top lid of the

platform is not water proof, hence the water starts to sips in when the platform is tilted to 90 ° clockwise. The water enters the platform at a slow rate, which is why the platform capsizes first before sinking.

The percentage of deviation of the critical angle is calculated by using equation 4.1.

$$\text{Percentage of deviation} = \frac{|\text{Actual} - \text{Theoretical}|}{\text{Theoretical}} \times 100 \%$$

$$\text{Percentage of deviation} = \frac{|110^\circ - 120^\circ|}{120^\circ} \times 100 \%$$

$$\text{Percentage of deviation} = 8.33 \%$$

There is a total of 8.33% of deviation in the actual critical angle and the calculated critical angle. This deviation is mainly due to the inadequate manufacturing skills. The platform designed was meant to be water proof at the top lid as well, but it ended up that there is a small gap whereby the water can sips in. This can be overcome by applying gasket maker on the surface where the top lid is contact with the body of the platform. Apart from that, the slight deviation in the geometry of the manufactured platform also contributes to this error. If there is an error in the geometry of the platform, the *CG* of the platform will deviates from the calculated value. This deviation will have a huge impact on the critical angle calculated due to the fact that the tilting angle is done by rotating the platform about the *CG*.

4.3 Effect of Head Loss Coefficient

The head loss coefficient is the key parameter in the TLCD design. Thus it is essential to determine the whether the general effect of head loss coefficient is the same as it is applied on building to counter translational vibration.

The effect of head loss coefficient is tested by using orifice plate of different diameter. Hence, the first step would be to obtain the head loss coefficient of each of

the orifice plate by using equation 2.3. In order to use equation 2.3, the diameter of each orifice plate has to be converted into blocking ratio which is the ratio of the cross-sectional area flow being blocked to the total cross-sectional area of flow by using equation 4.4.

For 4 mm diameter orifice plate:

$$\psi = \frac{A_D - \frac{\pi}{4}D^2}{A_D} \quad (4.4)$$

$$\psi = \frac{(0.036 \text{ m} \times 0.036 \text{ m}) - \frac{\pi}{4}(\frac{4}{1000})^2}{(0.036 \text{ m} \times 0.036 \text{ m})}$$

$$\psi = 0.9903$$

Where

A_D = Cross-sectional area of liquid displaced, m²

D = Diameter of orifice plate, m

$$\eta = (-0.6\psi + 2.1\psi^{0.1})^{1.6} \times (1 - \psi)^{-2}$$

$$\eta = (-0.6 \times 0.9903 + 2.1 \times 0.9903^{0.1})^{1.6} \times (1 - 0.9903)^{-2}$$

$$\eta = 20430.6$$

The blocking ratio and head loss coefficient for different diameter of orifice plate is calculated in the same manner as for 4 mm diameter orifice plate by using a software call Excel. The result is then tabulated in Table 4.2.

Table 4.2: Blocking Ratio and Head Loss Coefficient for Different Diameter Orifice Plate

Diameter of Orifice Plate (mm)	Blocking Ratio, ψ	Head Loss Coefficient, η
4	0.990304	20430.63
6	0.978183	4055.84
8	0.961215	1292.18
10	0.939398	533.92

The response from the accelerometer is in acceleration, it has to be converted into displacement by integrating twice the acceleration response. The first integration converts the acceleration response into velocity response while the second integration converts the velocity response into displacement response. However, the accelerometer used is very sensitive to noise which is the same as other conventional accelerometer due to the effect of the gravitational acceleration acting on the accelerometer as well as the low frequency direct current content of the sensor. Hence, a high pass filter is needed to filter off these noises to obtain the correct displacement response.

By using the software call IMC FAMOS, a Butterworth High Pass filter is used to filter the acceleration response at the second order and cut off frequency of 1 Hz. The Butterworth High Pass filter is set to a cut off frequency of 1 Hz due to the fact that the response which we wanted is the wave generated at a constant frequency of 1 Hz while the noise which is unwanted is of low frequency that are less than 1 Hz. The acceleration response of the platform with the use of 4 mm diameter orifice plate is as shown in Figure 4.9. Each colour in Figure 4.9 represents a channel that is stated in Figure 3.12, and all the peak value of each channel is labelled.

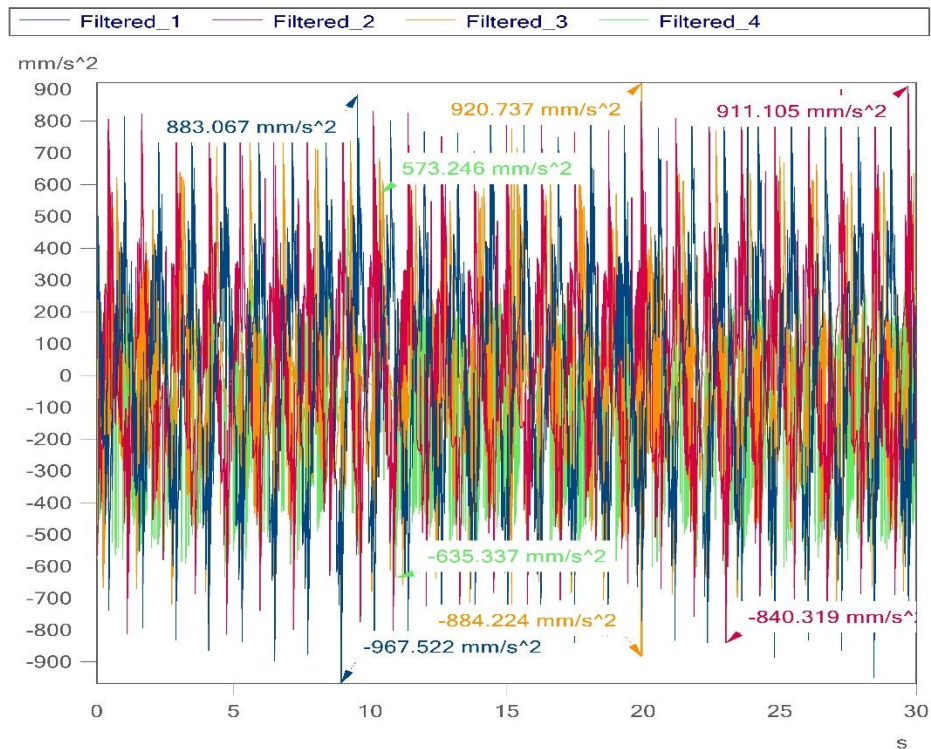


Figure 4.9: Filtered Acceleration Response for 4 mm Diameter Orifice Plate

In most cases, the acceleration response is hard to analyse and hence it is integrated twice into displacement response as shown in Figure 4.10.

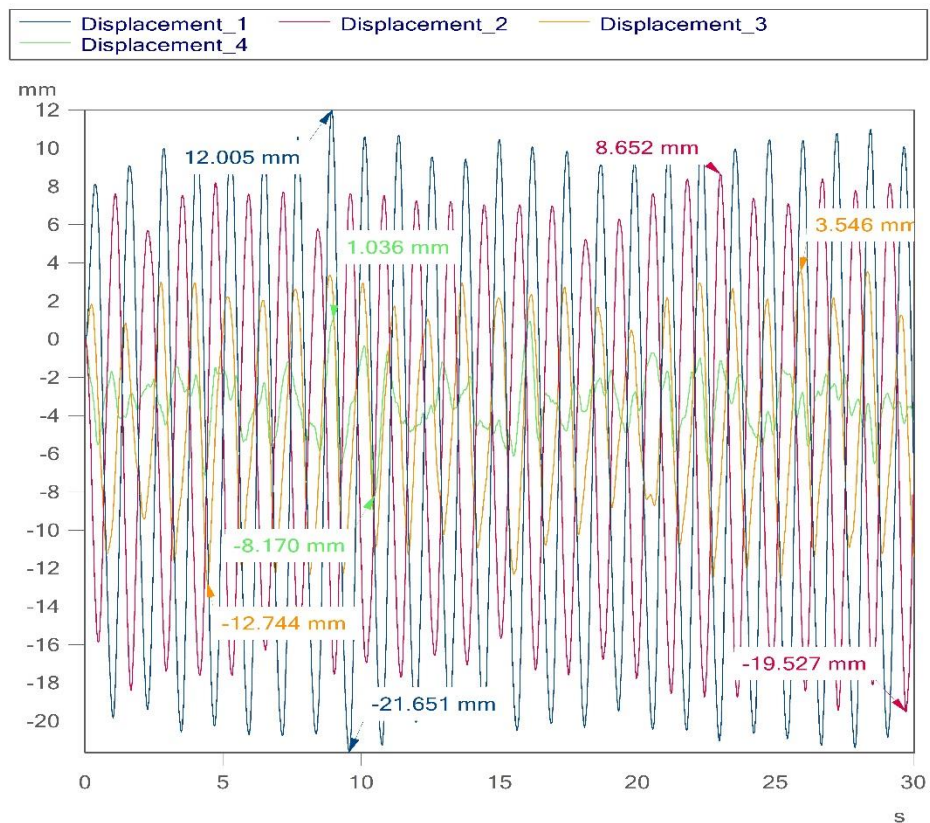


Figure 4.10: Displacement Response for 4 mm Diameter Orifice Plate

It is notice that the displacement of channel 1 and channel 2 is out of phase by one cycle which is when channel 1 is positively peaked, channel 2 is negatively peak which is the same pattern of displacement response when the TLCD isn't installed in the platform. From this inference, the vibration motion of the platform is the same as the sine wave generated as shown in Figure 4.11.

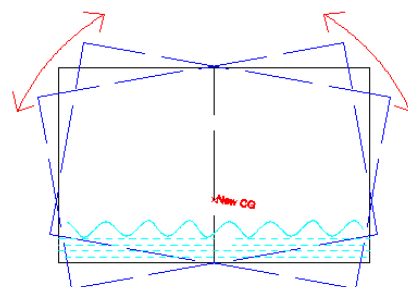


Figure 4.11: Vibration Motion of the Platform Using 4 mm Diameter Orifice

However, this vibration motion changes when the orifice plate of 6 mm and 8 mm diameter is used. This shows that the fundamental mode of vibration is altered. Since the general vibration motion of 6 mm and 8 mm diameter orifice plate is the same, only 8 mm diameter orifice plate response is shown. All the response that isn't shown in this chapter will be attached in the appendix as a reference.

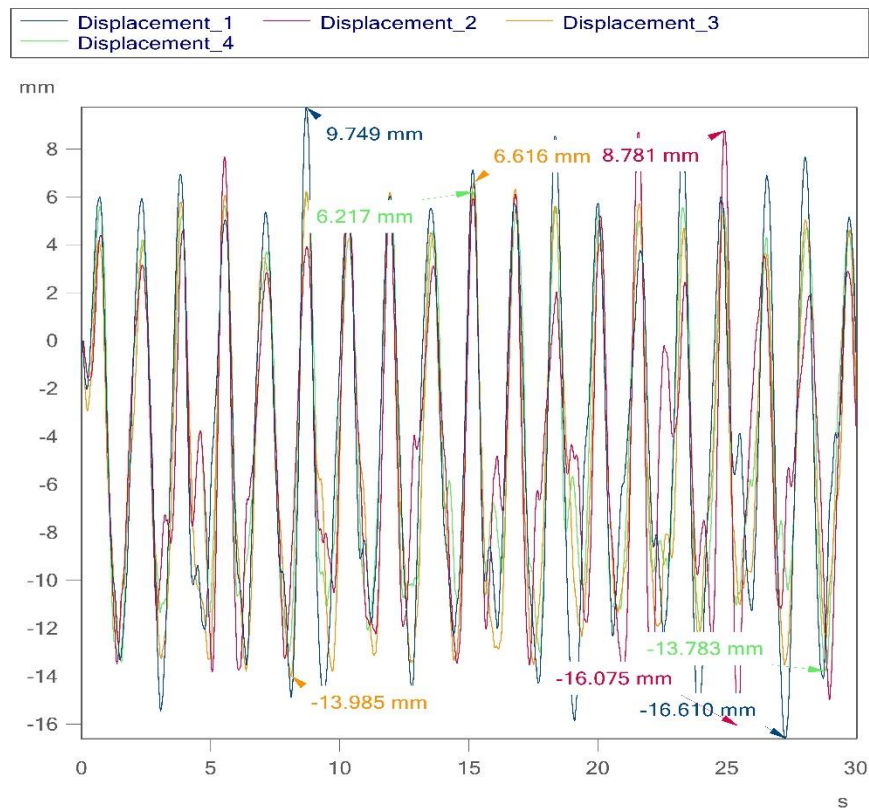


Figure 4.12: Displacement Response for 8 mm Diameter Orifice Plate

This pattern of displacement response as shown in Figure 4.12 essentially means that the vibration motion is in up and down motion as shown in Figure 4.13.

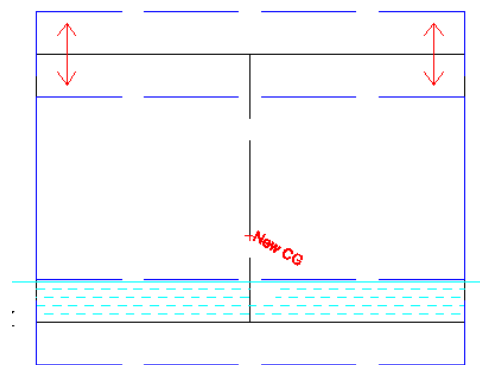


Figure 4.13: Vibration Motion of the Platform Using 8 mm Diameter Orifice

For 10 mm diameter orifice plate, the pattern of the vibration motion is the same as that of 4 mm diameter orifice plate. This shows that the fundamental mode of vibration has returned back to the wave generated mode, indicating the in effectiveness in reducing vibration of this frequency. The maximum absolute displacement of channel 1 and channel 2 for each orifice diameter is tabulated in Table 4.3.

Table 4.3: Maximum Absolute Displacement Amplitude of Channel 1 and Channel 2 for Each Orifice Plate Diameter

TLCD Configuration	Channel 1 (mm)	Channel 2 (mm)
Without TLCD	23.550	23.589
TLCD with 4 mm Orifice Plate	21.651	19.527
TLCD with 6 mm Orifice Plate	17.172	21.216
TLCD with 8 mm Orifice Plate	16.610	16.075
TLCD with 10 mm Orifice Plate	17.841	18.952

However, the maximum absolute displacement amplitude hardly describe the behaviour of the vibration motion as it may be peak at this value once a while only or could be frequently peak at this value. Hence, in order to determine the performance of each of the TLCD configuration towards the wave generated, a power spectrum analysis is need. The power spectrum analysis is done individually for channel 1 as shown in Figure 4.14 and then for channel 2 as shown in Figure 4.15. From the Power Spectrum analysis, it is shown that the fundamental mode of vibration without the TLCD installed is near 1Hz as predicted. The power spectrum also proves that the use of 4 mm and 10 mm diameter orifice plate results in the same fundamental mode of vibration as inferred from the displacement response graph.

For 6 mm and 8 mm diameter orifice plate, it successful in supressing the fundamental mode of vibration but at the cost of amplifying the vibration at 1.3 Hz and 0.7 Hz, creating harmonics of 2 mode. If the vibration at this two harmonics is small, it would seems as a good way to mitigate the vibration of 1 Hz.

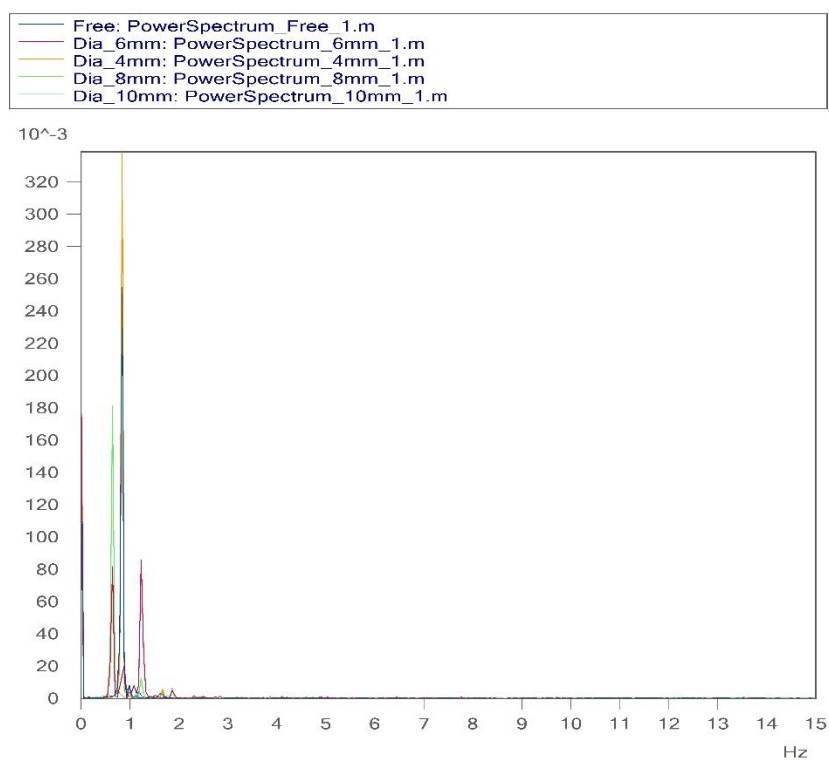


Figure 4.14: Power Spectrum Analysis for Channel 1 of Different Configuration

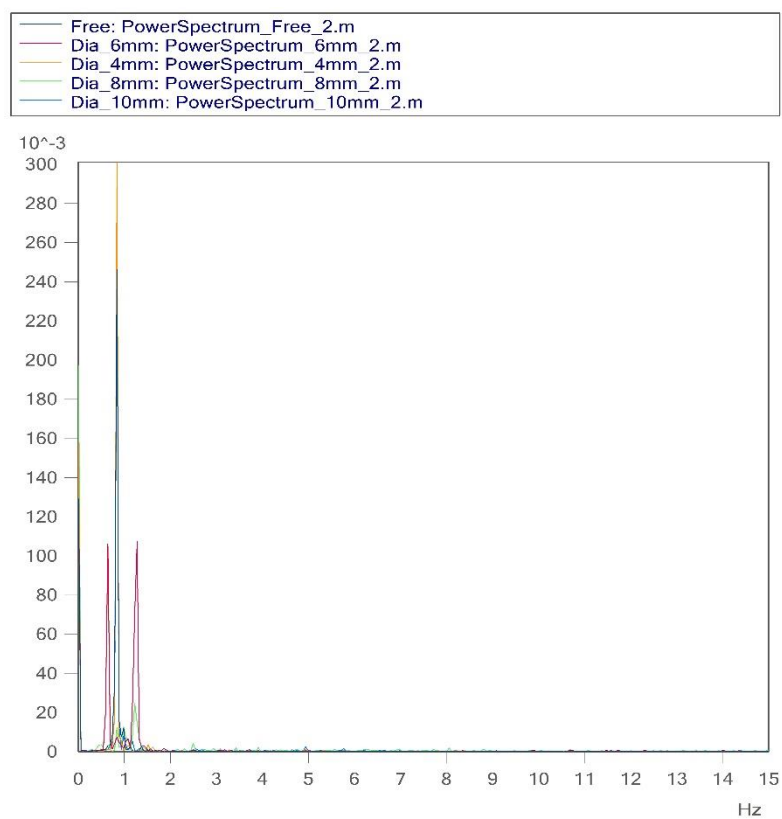


Figure 4.15: Power Spectrum Analysis for Channel 2 of Different Configuration

By plotting the reciprocal of summation of amplitude of the power spectrum of each configuration against the coefficient of head loss, the correlation between the performance in mitigating the vibration and the coefficient of head loss can be determined as shown in Figure 4.16. From Figure 4.16, the general effect of head loss of coefficient is determined, that is it initially increases to an optimum value in which this case is 4000, after which the performance of the TLCD in mitigating the vibration will starts to decline.

Table 4.4: Table of Reciprocal of Amplitude of Power Spectrum for each Orifice Plate

Diameter of Orifice Plate (mm)	Head Loss Coefficient, η	Summation of Amplitude	Reciprocal of Summation of Amplitude
4	20430.6294	340	0.0029
6	4055.8384	160	0.0063
8	1292.1756	180	0.0056
10	533.9185	250	0.0040

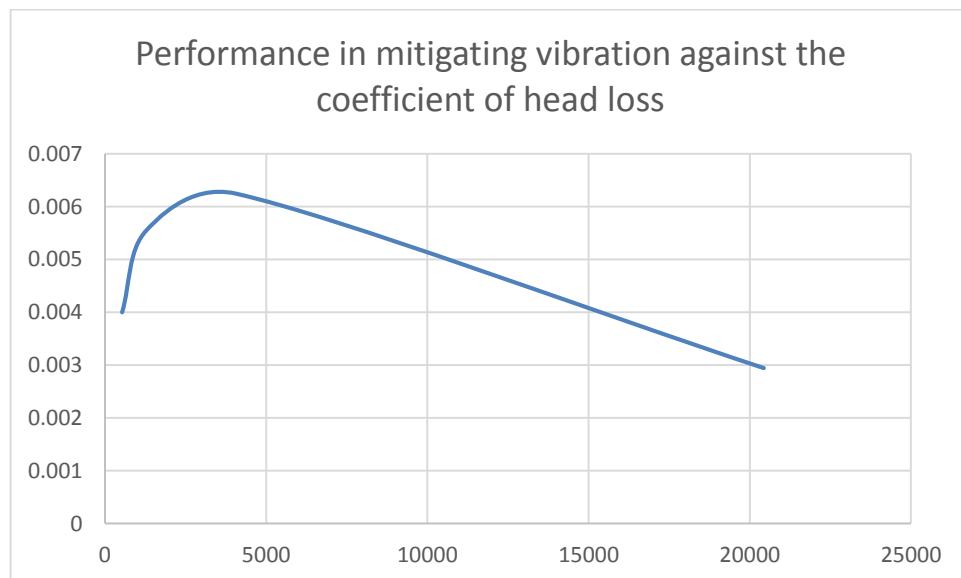


Figure 4.16: Performance in Mitigating Vibration against the Coefficient of Head Loss

4.4 Composite Effect of Mass Ratio and Tuning Ratio

The composite effect of mass ratio and tuning ratio is tested by reducing the water level of TLCD from 15 cm to 10 cm then to 5 cm. When it is lowered down, the mass ratio decreases but the tuning ratio increases. The mass ratio and tuning ratio is computed using the equation 4.5 and 2.6

$$\mu = \frac{m_{TLCD}}{W_{TLCD+Platform}/9.81} \quad (4.5)$$

Where

m_{TLCD} = Mass of total liquid in the TLCD, kg

For 15 cm height water level, effective height is only 13 cm as the calculation is performed based on the centre line, hence need to subtract off the 2 cm from the 15 cm. From equation 4.5, the mass ratio for 15 cm water level is computer.

$$\mu = \frac{(0.036 \text{ m} \times 0.036 \text{ m}) \times 1000 \text{ kg/m}^3 \times (0.4 \text{ m} + 2 \times 0.13 \text{ m})}{\left(\frac{102.14}{9.81}\right) \text{ kg}}$$

$$\mu = 0.082$$

By equation 2.6,

$$\omega_D = \sqrt{\frac{2g}{L}}$$

$$\omega_D = \sqrt{\frac{2 \times 9.81}{0.4 + 2 \times 0.13}}$$

$$\omega_D = 5.45 \text{ rad/s}$$

The tuning ratio is defined as the ratio of natural frequency of the TLCD to the natural frequency of the structure to prevent the earthquake from resonating with the structure. For wave vibration mitigation, it would be ratio of natural frequency of the TLCD the frequency of the wave generated. In our case is 1 Hz. Thus the tuning ratio for 15 cm

water level is calculated by using this new definition, mathematically expressed as equation 4.6.

$$\beta = \frac{\omega_D}{\omega_w} \quad (4.6)$$

Where

ω_w = Frequency of wave generated, rad/s

The frequency of wave generated is in Hz, however to utilize equation 4.6, it is needed to be converted into rad/s by multiplying with 2π as 1 Hz is equivalent to 2π rad/s. By using equation 4.6, the tuning ratio is calculated.

$$\beta = \frac{\omega_D}{\omega_w}$$

$$\beta = \frac{5.45}{2\pi \times 1}$$

$$\beta = 0.8678$$

The tuning ratio and mass ratio for different water level is calculated and tabulated in Table 4.3.

Table 4.5: Mass Ratio and Tuning Ratio for Different Water Level

Water Level (cm)	Mass Ratio, μ	Tuning Ratio, β
5	0.0573	1.0394
10	0.0697	0.9421
15	0.0822	0.8678

A higher mass ratio generally serves a better purpose in mitigating the vibration but a tuning ratio closer to 1 is better at suppressing the vibration. Hence in this study, which ratio has a more dominant effect will be determined, as the water level increases, one ratio will increase (mass ratio), the other ratio will decrease (tuning ratio) which allows us to compare the effect of the two ratio.

The power spectrum analysis of each of the water level for channel 1 is shown in Figure 4.17 while for channel 2 is shown in Figure 4.18. From Figure 4.17, it is shown that the effect of mass ratio is more dominant than that of tuning ratio. This can be seen that as the tuning ratio is closer to 1 that is for water level of 5 cm the amplitude of the response in power spectrum is much higher than that of 15 cm water level due to the fact that the mass ratio of the TLCD configuration with water level of 5 cm is too low.

On the other hand, for TLCD configuration of 10 cm water level, the tuning ratio of it is very close to that of 15 cm water level. Hence, the response still falls on the same frequency unlike water level 5 cm which shifted the fundamental mode of vibration to somewhere nearer to 1 Hz. However, the drop in mass ratio for TLCD configuration of 10 cm water level has causes the amplitude of the response to rises sharply to 0.29597 unlike the 15 cm water level which has only 0.25463 . This double confirm that the effect of mass ratio is more dominant over tuning ratio

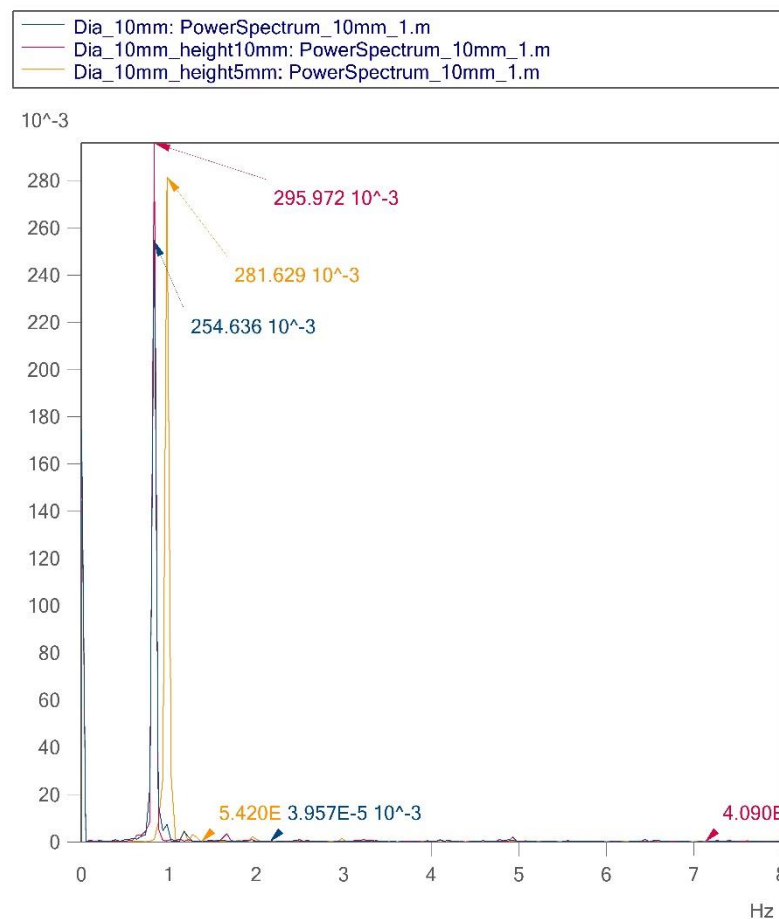


Figure 4.17: Power Spectrum for Different Water Level at Channel 1

The same pattern could be observed from power spectrum of channel 2 as well, with the exception that the amplitude of 5 cm water level is a little bit lower than that of 15 cm water level. This might be due to the misdistribution of weight and the positioning of channel 2 which might be slightly run off from the centre. At any rate, by averaging the amplitude response of channel 1 and channel 2, the amplitude of 5 cm water level is clearly higher than that of 15 cm water level.

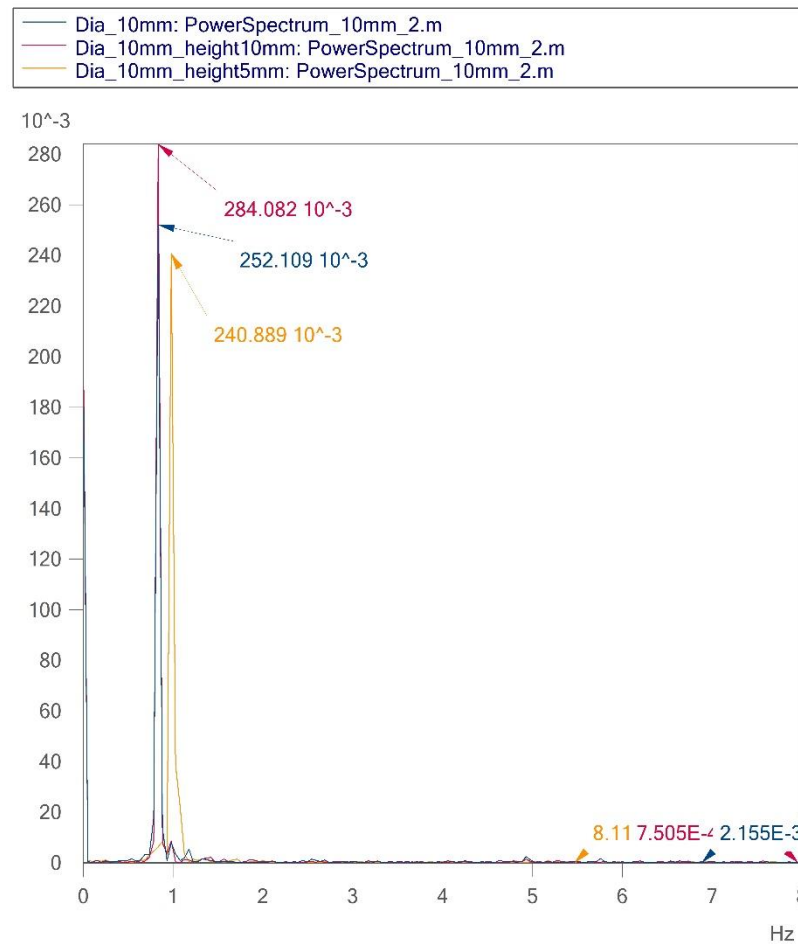


Figure 4.18: Power Spectrum for Different Water Level at Channel 2

4.5 Hydrostatic Force Simulation Result and Specification of Platform

In the early design, a hydrostatic force simulation is done on the platform to ensure that the platform is able to withstand the hydrostatic force from the surrounding without collapsing.

4.5.1 Technical Drawing of Platform and TLCD

Before performing the simulation, the platform and the TLCD has to be modelled out using SolidWorks. Figure 4.19 shows the modelled platform with the TLCD installed, while Figure 4.20 technical drawing with specification of the Platform with TLCD installed

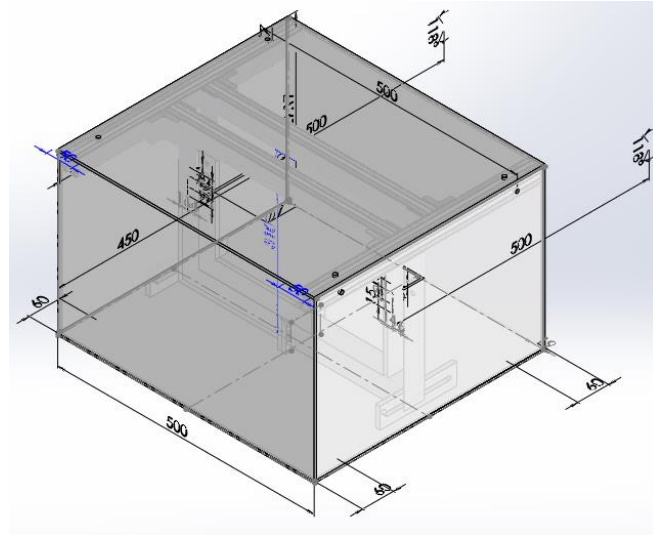


Figure 4.19: Modelled Platform with TLCD installed

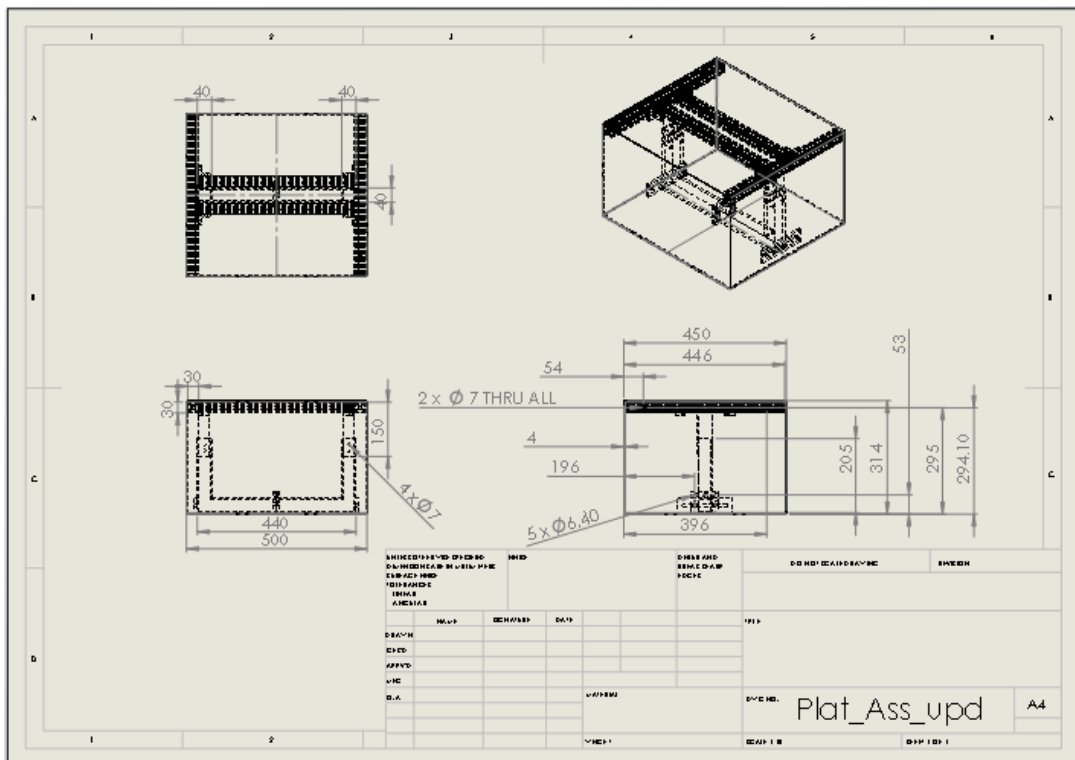


Figure 4.20: Technical Drawing of Platform

4.5.2 Simulation Result

The stress simulation shows that under 4 kg load and hydrostatic pressure from the water is not a problem to the platform designed. On the other hand, the displacement simulation shows that only the middle of the perspex sheet will experience bulking out by the most 0.0155 mm which is negligible in this case. This simulation double ascertain the rigidity of platform designed against the load that is going to be applied on it.

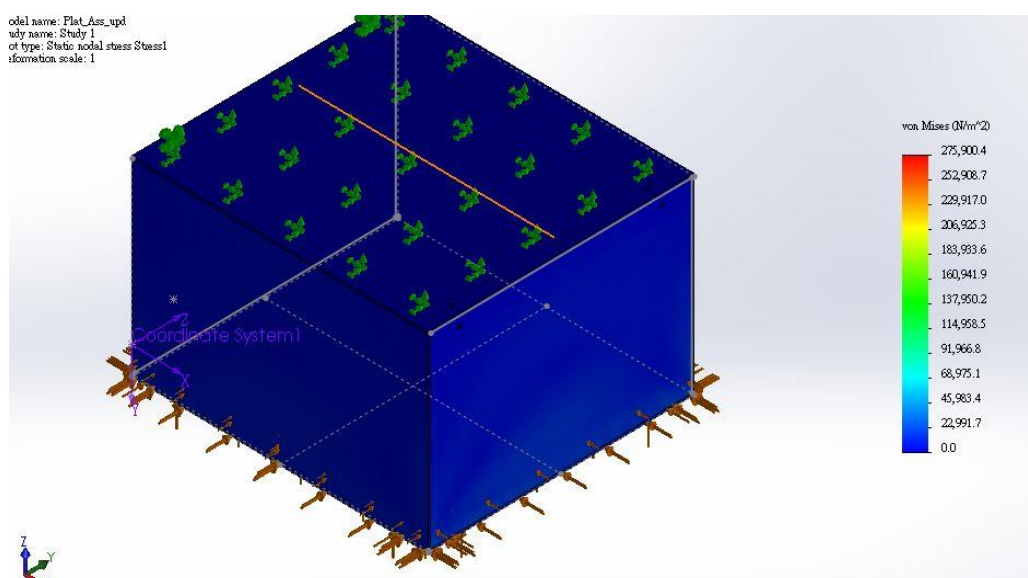


Figure 4.21: Stress Analysis by Simulation

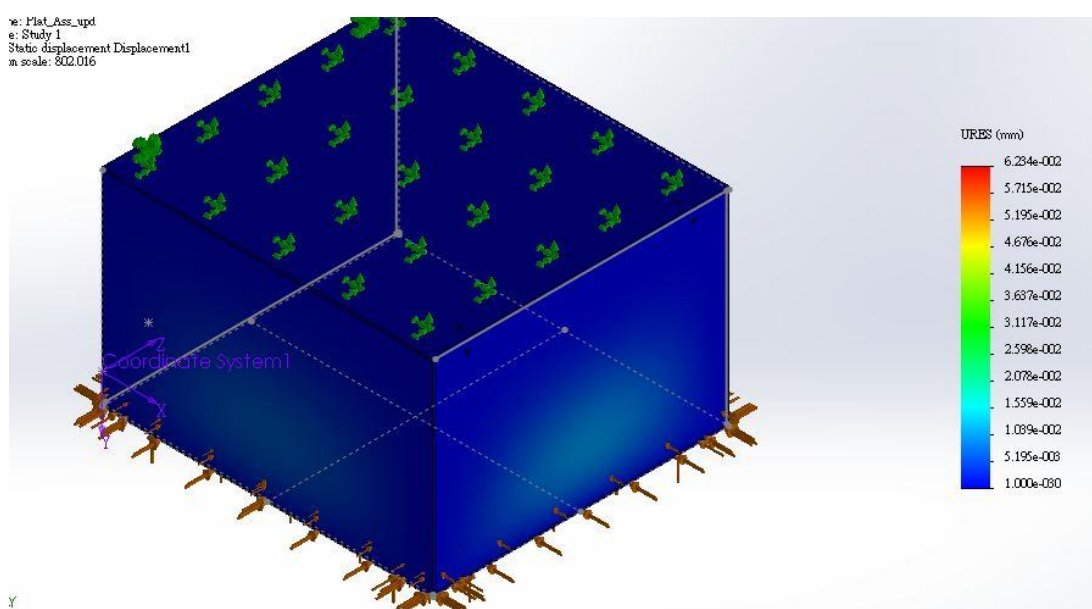


Figure 4.22: Displacement Analysis by Simulation

CHAPTER 5

CONCLUSION AND RECOMMENDATIONS

5.1 Problem Encountered and Future Recommendations

There are lots of problem encountered during the manufacturing stage. First of all, in order to join up two pieces of perspex nicely and water proof, the surface of contact between the two pieces of perspex must be extremely smooth. This is why the platform manufactured in the early stage is not water proof, the water keeps sipping into the platform via tiny leakage. This can be overcome by using milling machine as shown in Figure 3.8 to perform an additional steps of surface finishing on the surface of contact between the two pieces of perspex.

The next major problem encountered is that, the solvent which is the chloroform used to join up two pieces of perspex vaporizes too quickly. After applying on one of the surfaces, it has to be joined onto the other perspex within several seconds, or else the chloroform will vaporizes into air. If one inhale too much these chloroform vapour, he or she may get dizzy and eventually fainted. Thus, the process of joining together the perspex sheet into a platform has to be carried out in a room where there is sufficient air flow to blow away the chloroform vapour.

The recommendation for this problem is to have a few person to help apply the chloroform onto the surface of contact, while the other person quickly join up the two perspex sheet to prevent the chloroform from vaporizing. There is also another solution to this problem which is premixing the chloroform solution with perspex chips. This helps prolonged the duration at which the chloroform vaporises at the cost of

sacrificing the power of chloroform to dissolve the perspex surface that is wanted to be joined to another perspex sheet. Thus, a reasonable ratio between the chloroform and perspex chips is needed. From the author's experience, a ratio of 1.5 portion of chloroform to 1 portion of perspex chips works the best.

Even if steps is taken during the manufacturing stage to ensure the platform to be water proof, it would seems that the platform is still vulnerable to water sipping in especially for the case of TLCD. This is due to the presence of air bubble which traps in between the surface of contact between two pieces of perspex sheet. In order to completely water proof the whole thing, it is recommended to use silicon glue to seal off all the contact surfaces. In this project, a cheap silicon glue is used due to low in fund, it is recommended to use a better quality silicon glue to seal off the gap as the harden silicon glue used in this project becomes soft after long time exposure to water.

During the testing of TLCD, a manually produced waves has proposed a big problem to the experiment. This is because it is hard to produce a constant amplitude wave manually by human hands, and this may causes a deviation in the resulting acceleration amplitude collected by the accelerometer. It is recommended that a mechanism to actuate a constant amplitude and constant frequency wave to be manufactured for this testing purpose. In addition, during the actuation of wave by human hands, it is observed that it needs a high amount of torque to start off the wave, hence a conventional small motor might not fit this purpose. Even pneumatic system is not recommended to be used as actuator may ended up bending as it is used over a period of time. The highly recommended system to actuate the wave would be hydraulic system. If a motor is to be used, a high torque gear box would be needed and this high torque gear box is often very expensive, not inclusive of the price of medium duty motor yet.

5.2 Conclusion

For the first objective, it can be concluded that the buoyant force that the platform is experiencing is 102.14 N. This because the percentage of deviation is only 8.05 %.

This shows the calculation approach is sufficiently close enough to the actual value in a sense that we can assumed it to be the same. For the metacentric height calculation method shown in chapter 4, it helps to analyse the stability of a floating object but further detail analysis is needed which is the righting arm analysis if floating object designed is to be tilted for more than 15° .

By calculating the righting arm through the method shown in chapter 4.2.1, the graph of righting arm against angle tilted can be plotted. The angle at which is the righting arm becomes negative indicates that the floating object will capsize. The calculation shows that the platform should capsize when the angle tilted exceeds 120° but in actual the platform starts to capsize at approximately 110° resulting in a deviation of 8.33 % from the actual value. This is due to the poor water proof of the top lid of the platform. If the platform is water proof as planned, the angle at which it capsize should be way closer to 120° . Thus it is convincing enough to take the calculated critical angle of tilting as the actual value for future design of floating object.

On the other hand, the second objective which is the general effect of coefficient of head loss on the performance of TLCD installed on the platform is determined as when it is too low, the TLCD will have a low performance , however when it is too high the TLCD is merely a tank of water doing nothing. There is an optimum value for the coefficient of head loss, and in this case it is around 4000.

For the third objective, it is found out that the effect of mass ratio will be more dominant over the effect of tuning ratio. Hence when the design is under constraint, one should sacrifice the tuning ratio to preserve the mass ratio.

REFERENCES

- Donald, F.E., Barbara, C.W., Clayton, T.C., John, A.R., 2012. *Engineering Fluid Mechanics*. 10th edition. United States: John Wiley & Sons, Inc.
- Lee, H.H., Wong, S.H. and Lee, R.S., 2005. Response Mitigation on the Offshore Floating Platform System With Tuned Liquid Column Damper. *Ocean Engineering*, 33(8-9), pp. 1118-1142.
- Matteo, A.D., Iacono, F.L., Navarra, G., Pirrotta, A., 2014. Direct Evaluation of the Equivalent Linear Damping for the TLCDC systems in Random Vibration for Pre-design Purposes. *International Journal of Non-Linear Mechanics*, 63, pp. 19-30.
- Min, K.W., Kim, H.S., Lee, S.H., Kim, H.J., Ahn, S.K., 2005. Performance Evaluation of Tuned Liquid Column Dampers For Response Control of a 76-story Benchmark Building. *Engineering Structures*, 27(7), pp. 1101-1112.
- Sakai, F., Takeda, S., Tamaki, T., 1989. Tuned Liquid Column Damper – New Type Device For Suppression of Building Vibrations. In: Proceedings of the International Conference on Highrise Buildings. Nanjing, China, 25-27th March 1989
- Shum, K.M., 2009. Closed Form Optimal Solution of a Tuned Liquid Column Damper for Suppressing Harmonic Vibration of Structures. *Engineering Structures*, 31, pp. 84-92.
- Subrata, K., 2005. *Handbook of Offshore Engineering*. Plainfield, USA: Elsevier
- Tanmoy, C., Subrata, C., 2014. Vibration Mitigation of Structures Subjected to Random Wave Forces By Liquid Column Dampers. *Ocean Engineering*, 87, pp. 151-161.
- Venkateswara, R.K., 2013. *Experimental and Numerical Studies On Tuned Liquid Damper*. Master. National Institute of Technology Rourkela.
- Wu, J.C., Chang, C.H., Lin, Y.Y., 2009. Optimal Designs For Non-uniform Tuned Liquid Column Dampers In Horizontal Motion. *Journal of Sound and Vibration*, 326, pp. 104-102.

Wu, J.C., Shih, M.H. and Lin, Y.Y., 2005. Design Guidelines for Tuned Liquid Column Damper for Structures Responding to Wind. *Engineering Structures*, 27(13), pp. 1893-1905.

APPENDICES

APPENDIX A: Result for Graphical Method of GM and RA for Different Tilting
Angle at an increment of 10°

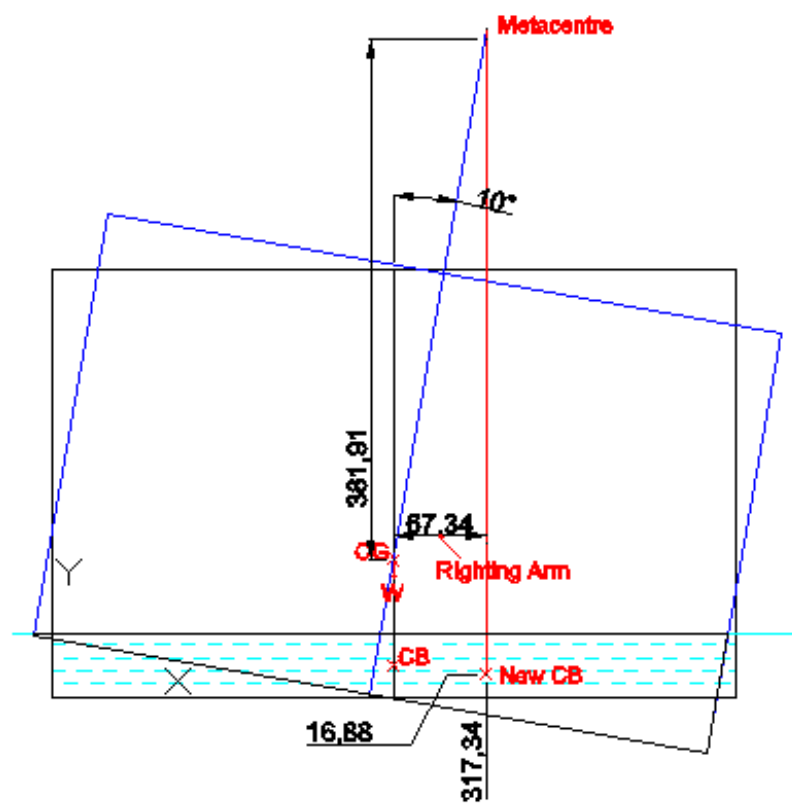


Figure A-1: GM and RA for 10° of Tilting

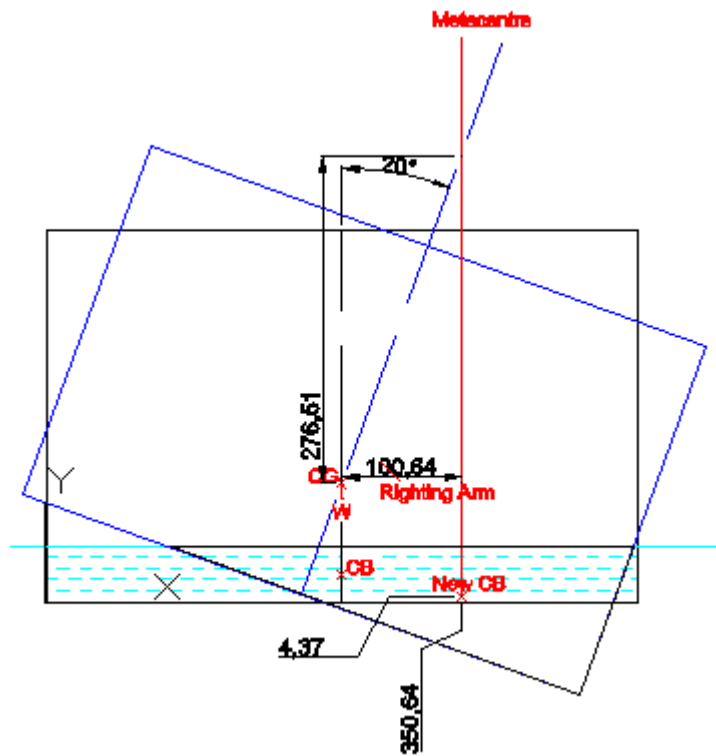


Figure A-2: *GM* and *RA* for 20° of Tilting

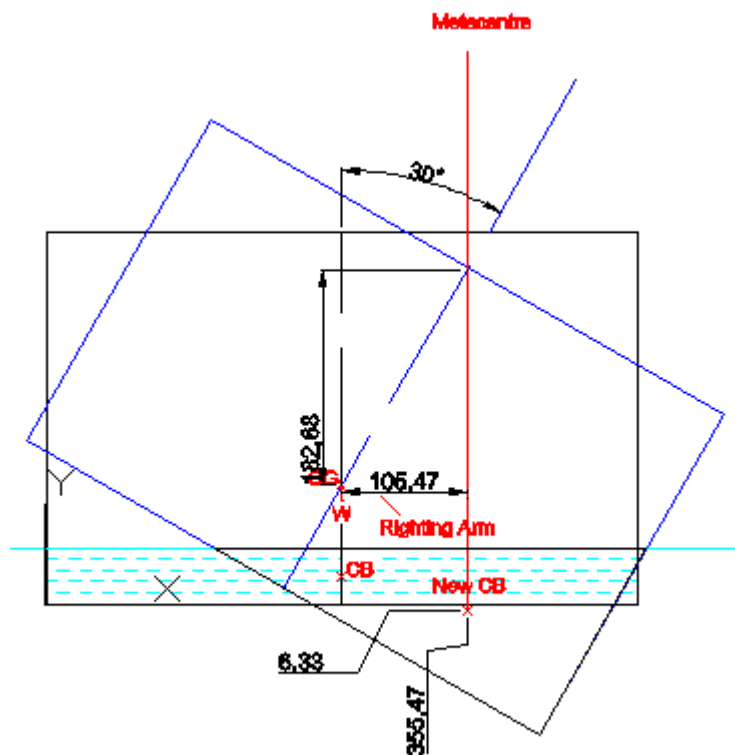


Figure A-3: *GM* and *RA* for 30° of Tilting

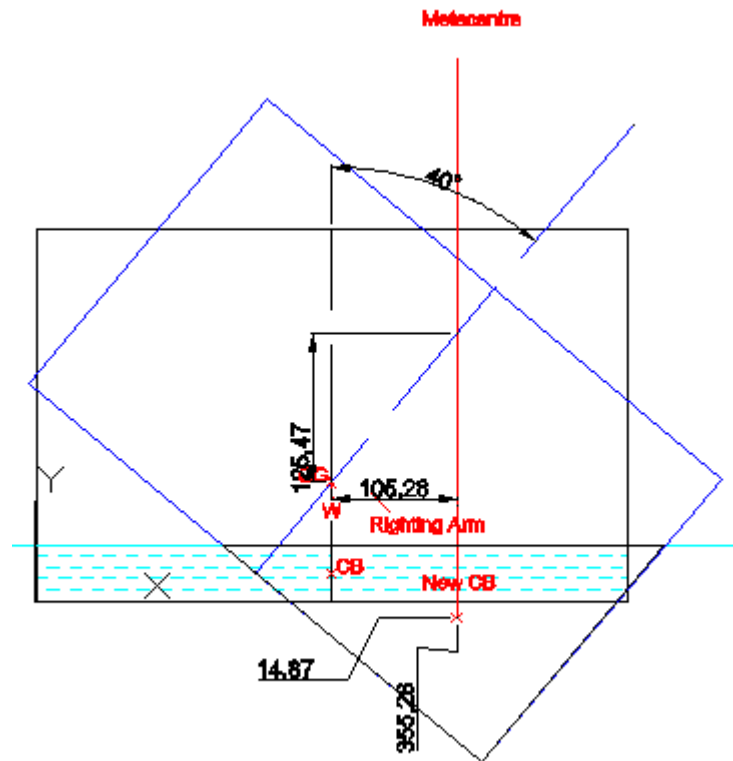


Figure A-4: *GM* and *RA* for 40° of Tilting

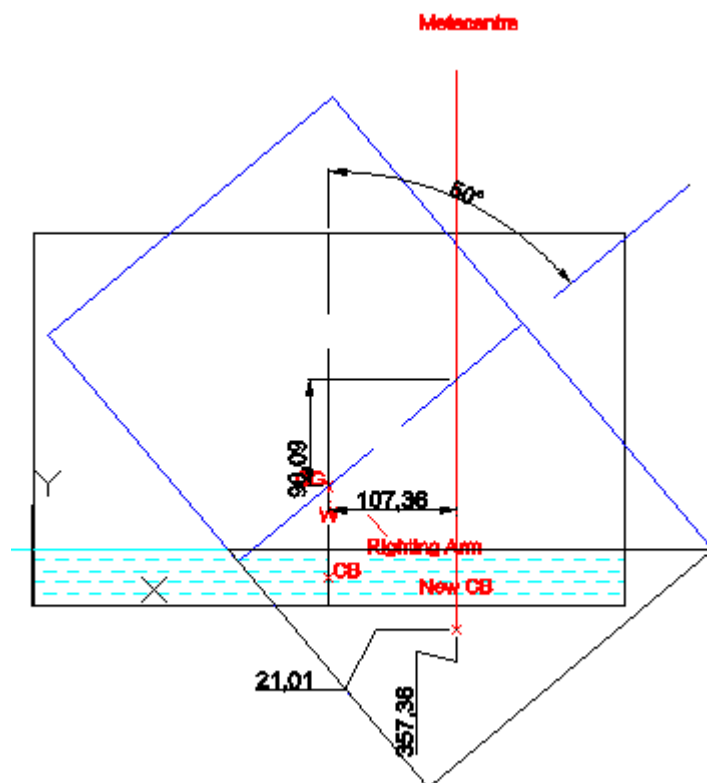


Figure A-5: *GM* and *RA* for 50° of Tilting

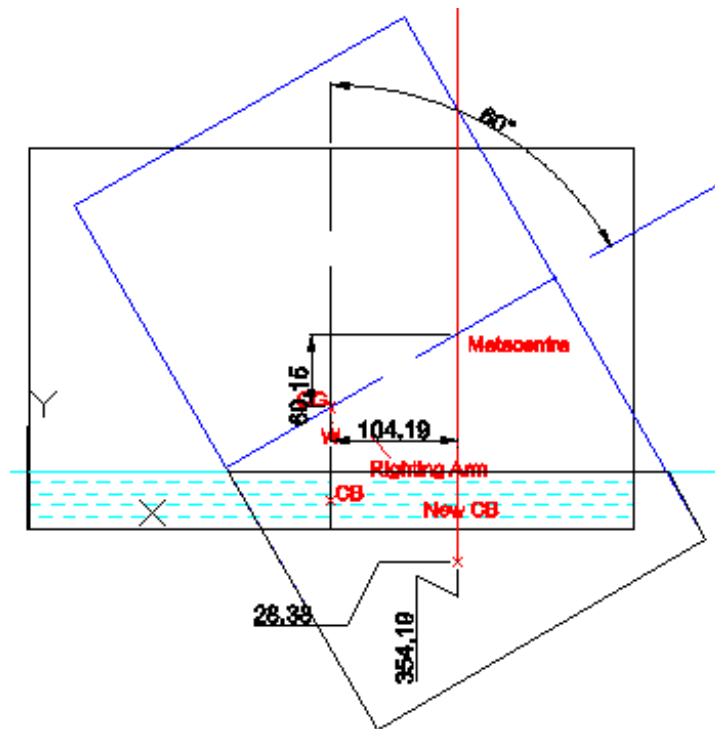


Figure A-6: *GM* and *RA* for 60° of Tilting

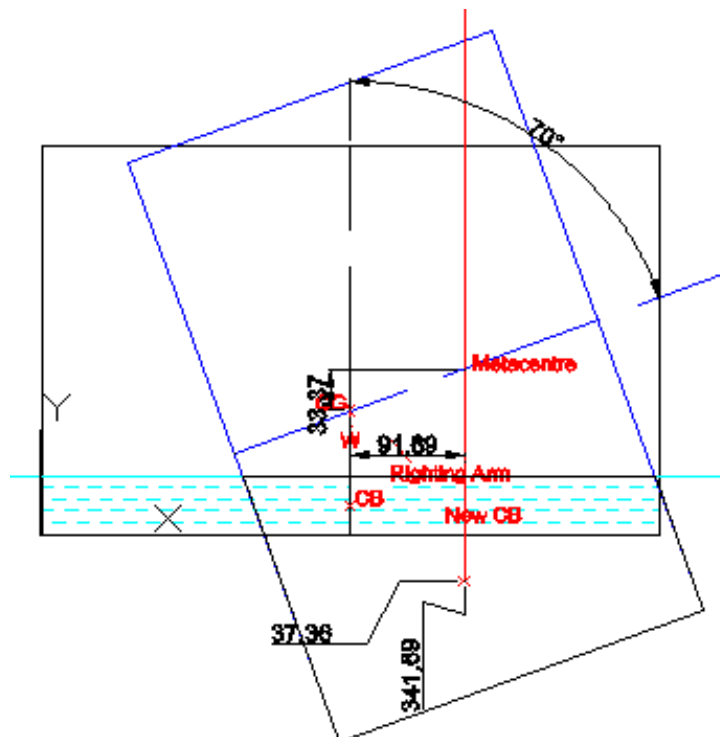


Figure A-7: *GM* and *RA* for 70° of Tilting

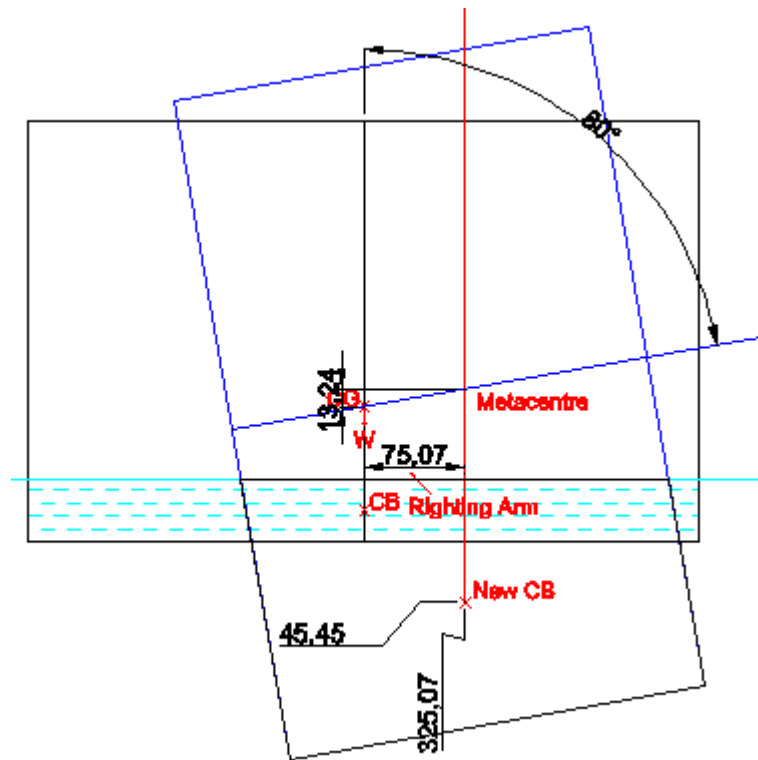


Figure A-8: *GM* and *RA* for 80° of Tilting

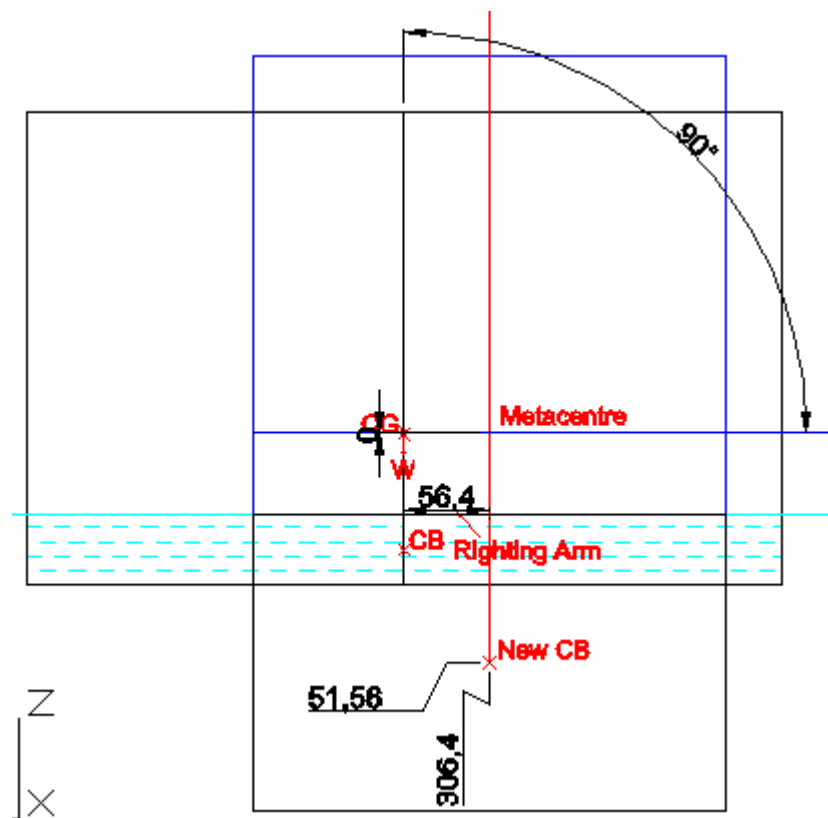


Figure A-9: *GM* and *RA* for 90° of Tilting

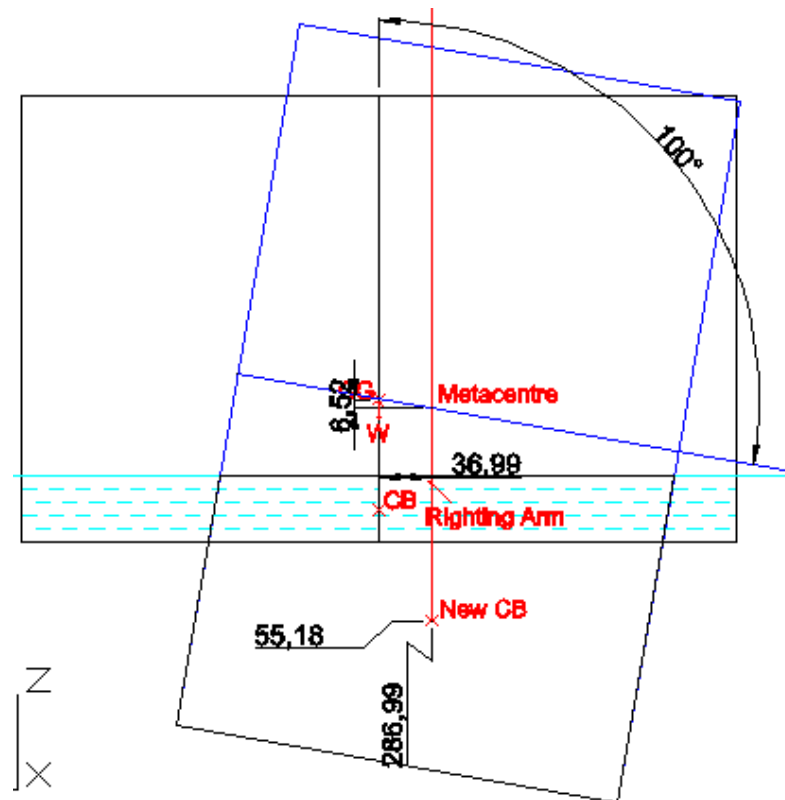


Figure A-10: *GM* and *RA* for 100 ° of Tilting

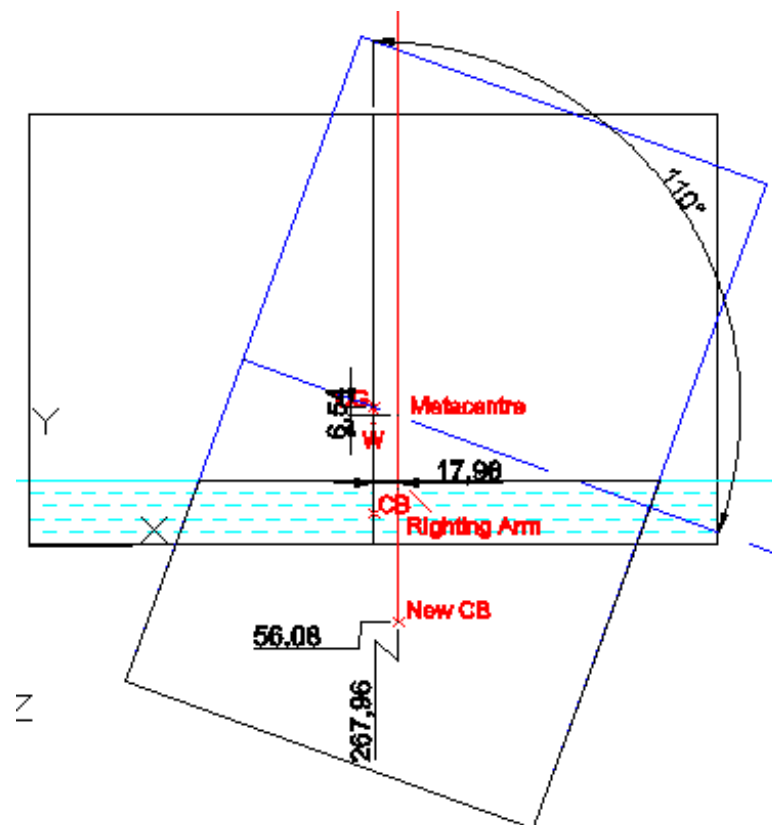


Figure A-11: *GM* and *RA* for 110 ° of Tilting

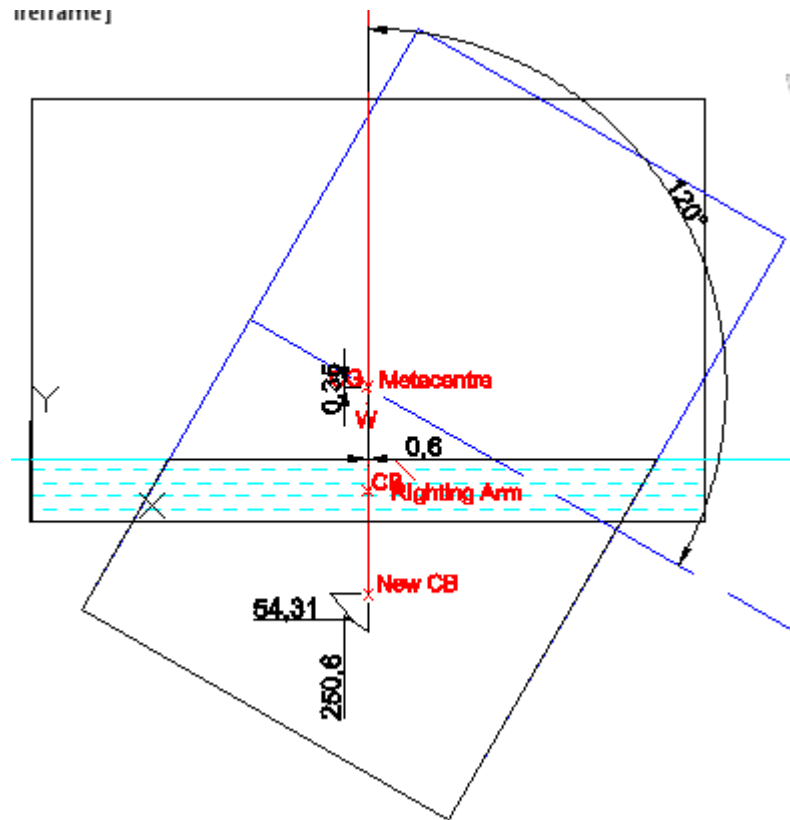


Figure A-12: *GM* and *RA* for 120° of Tilting

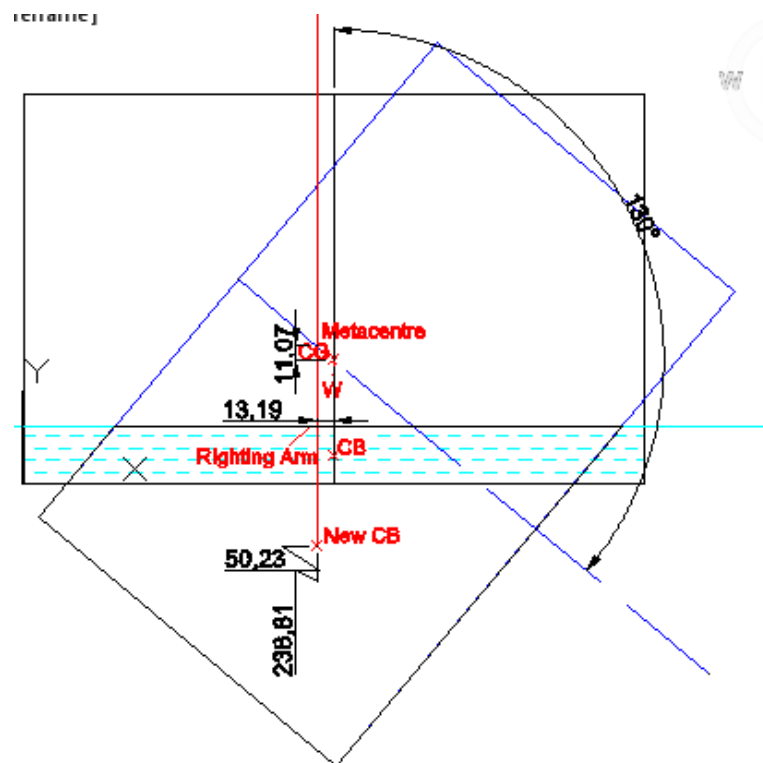


Figure A-13: *GM* and *RA* for 130° of Tilting

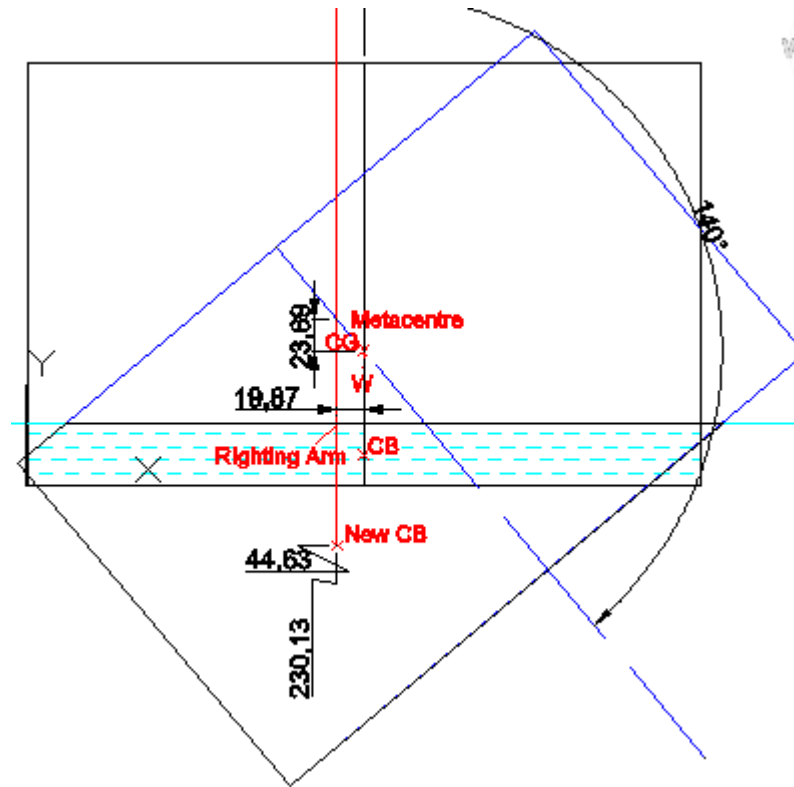


Figure A-14: *GM* and *RA* for 140° of Tilting

APPENDIX B: Accelerometer Response for Different Orifice Plate Diameter at
Water Level of 15 cm

*The 1, 2, 3 and 4 numbering at the back of the signal represents the number of the channel. That is Filtered Acceleration_1 represents Filtered Acceleration of Channel 1 and so forth.

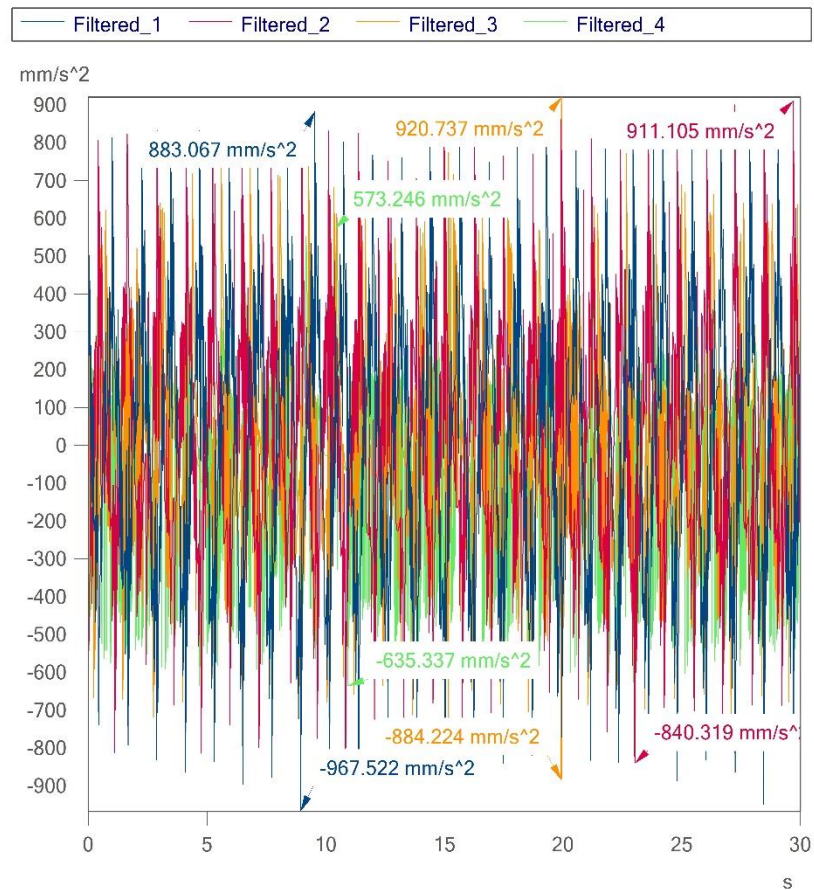


Figure A-15: Filtered Acceleration Response for 4 mm Diameter Orifice Plate

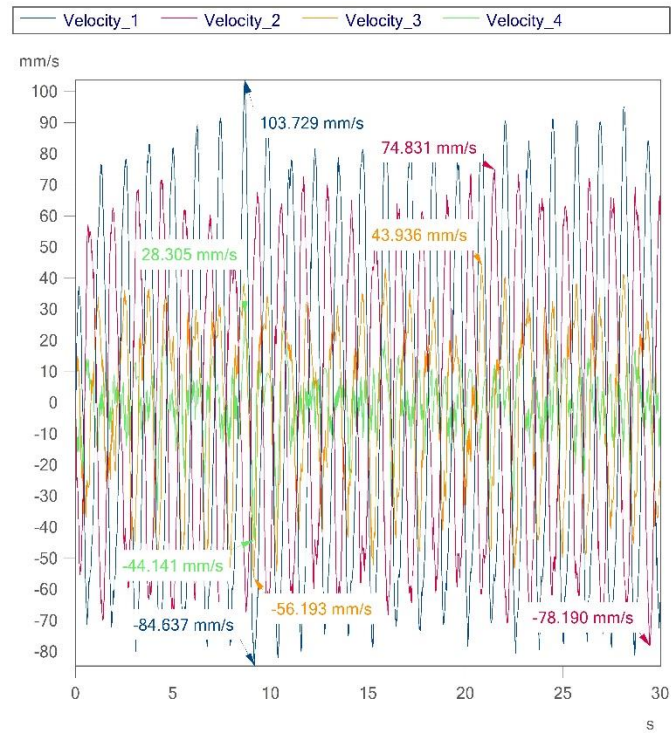


Figure A-16: Velocity Response for 4 mm Diameter Orifice Plate

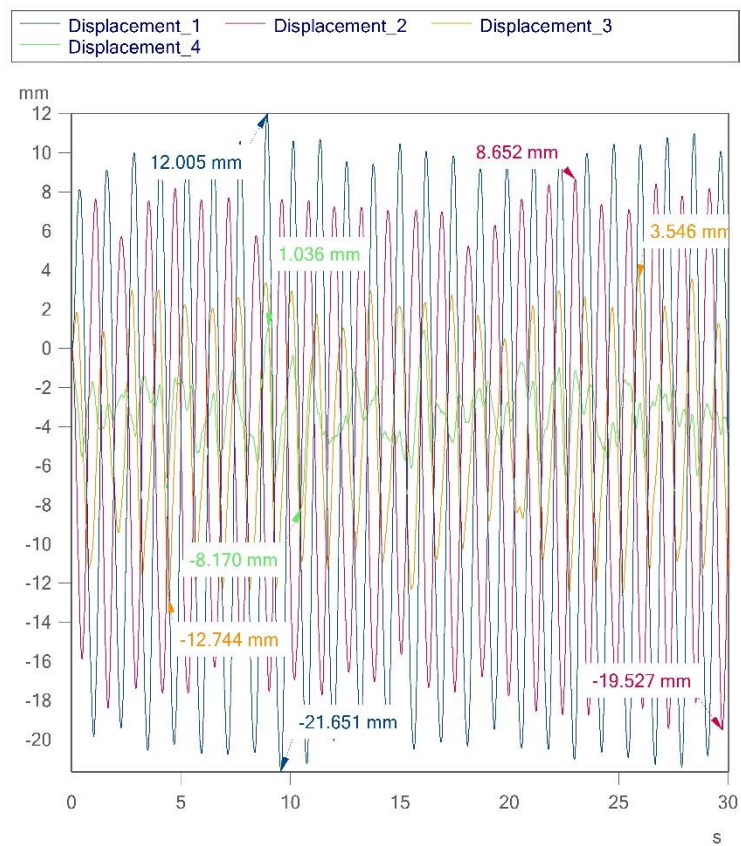


Figure A-17: Displacement Response for 4 mm Diameter Orifice Plate

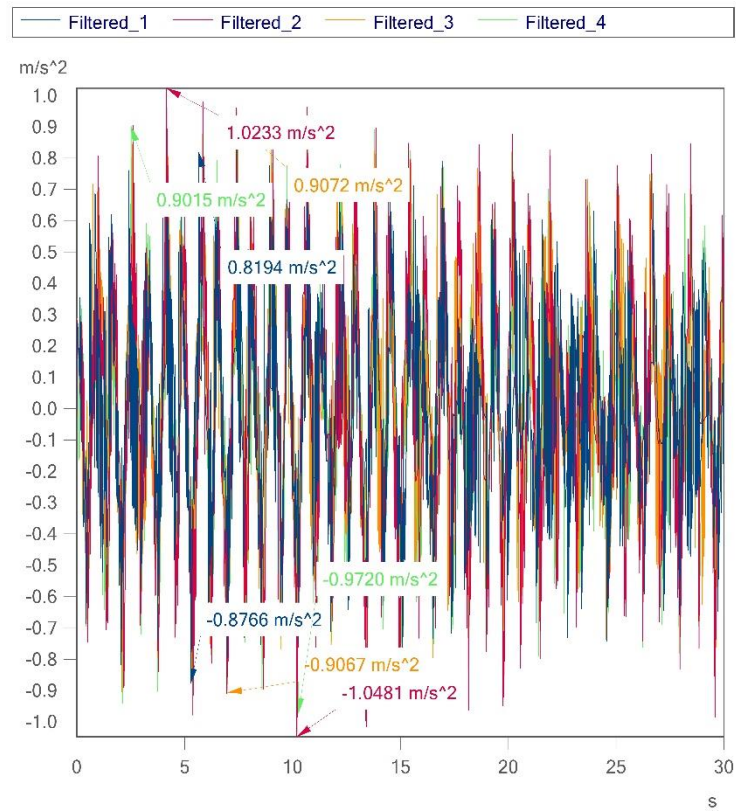


Figure A-18: Filtered Acceleration Response for 6 mm Diameter Orifice Plate

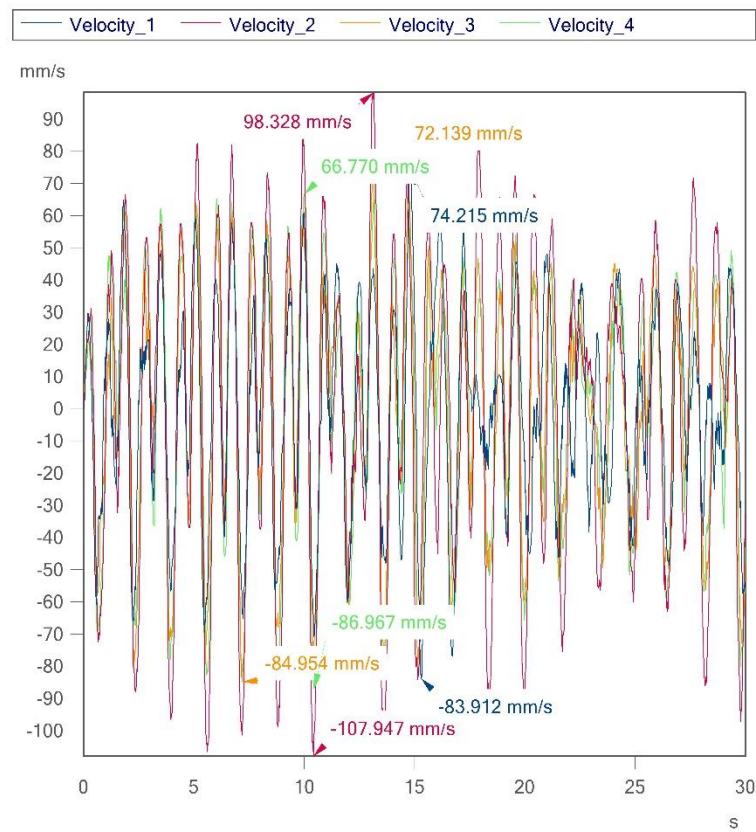


Figure A-19: Velocity Response for 6 mm Diameter Orifice Plate

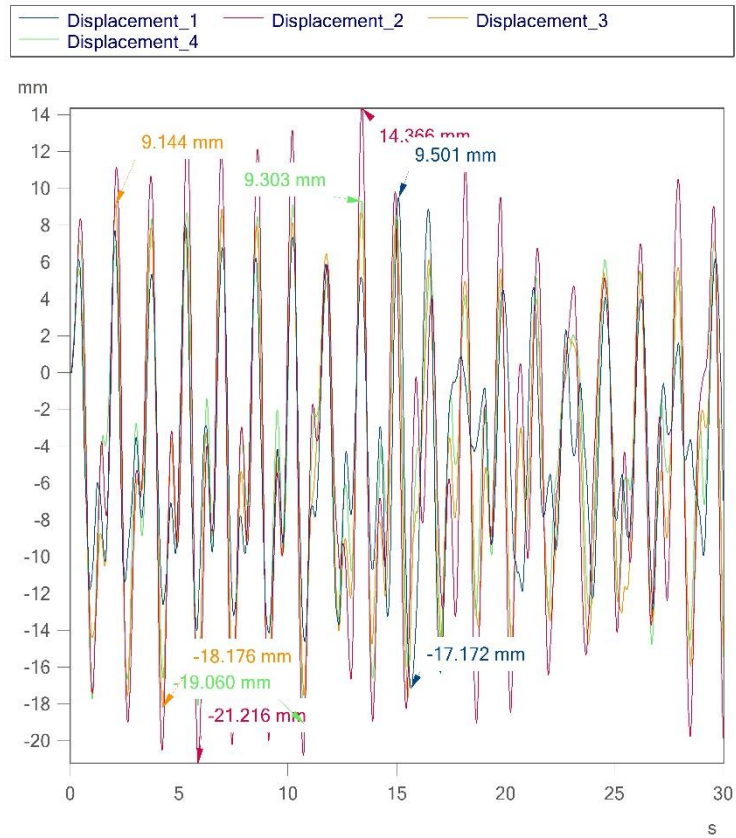


Figure A-20: Displacement Response for 6 mm Diameter Orifice Plate

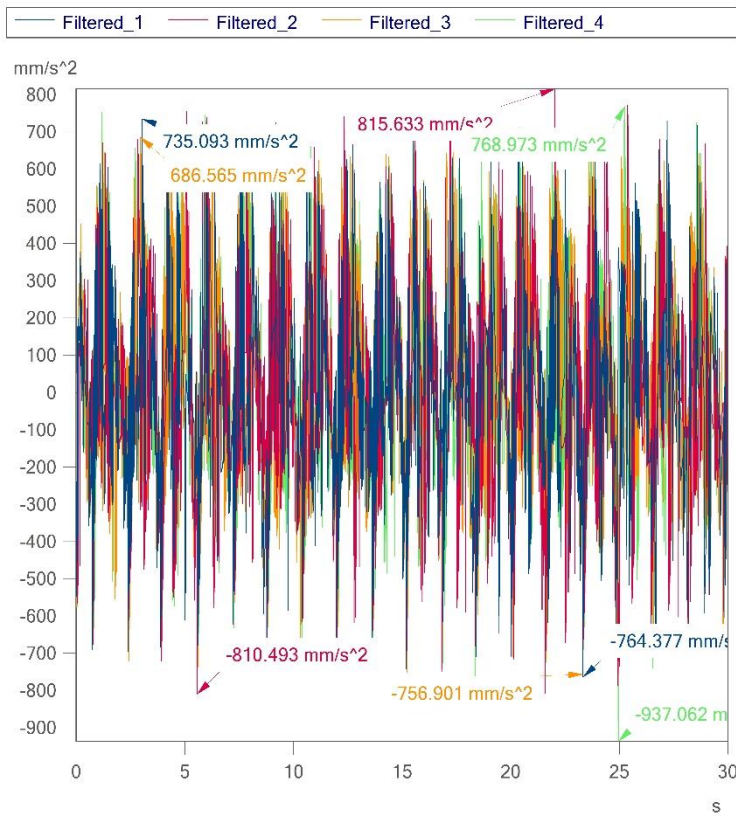


Figure A-21: Filtered Acceleration Response for 8 mm Diameter Orifice Plate

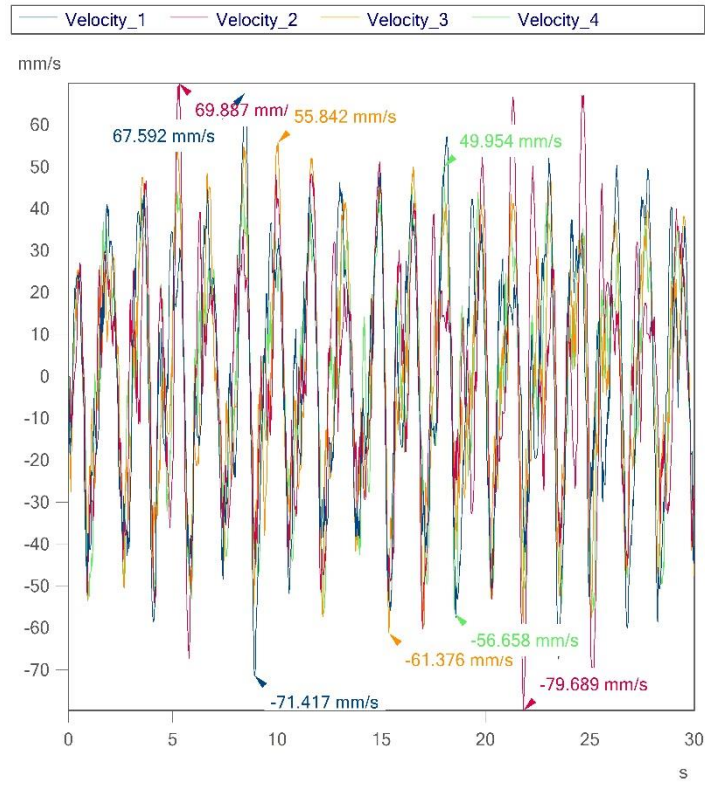


Figure A-22: Velocity Response for 8 mm Diameter Orifice Plate

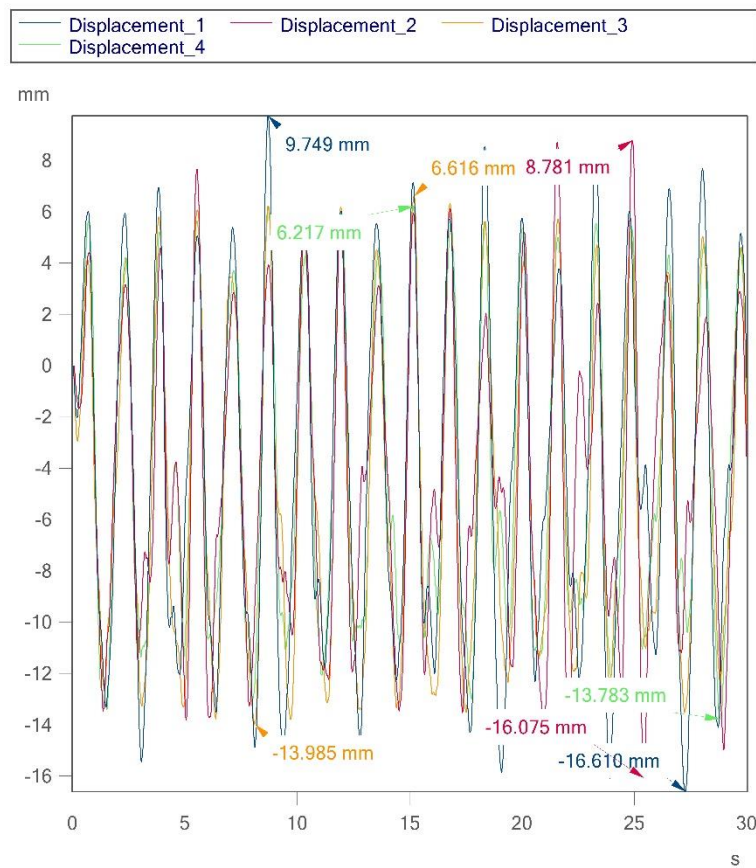


Figure A-23: Displacement Response for 8 mm Diameter Orifice Plate

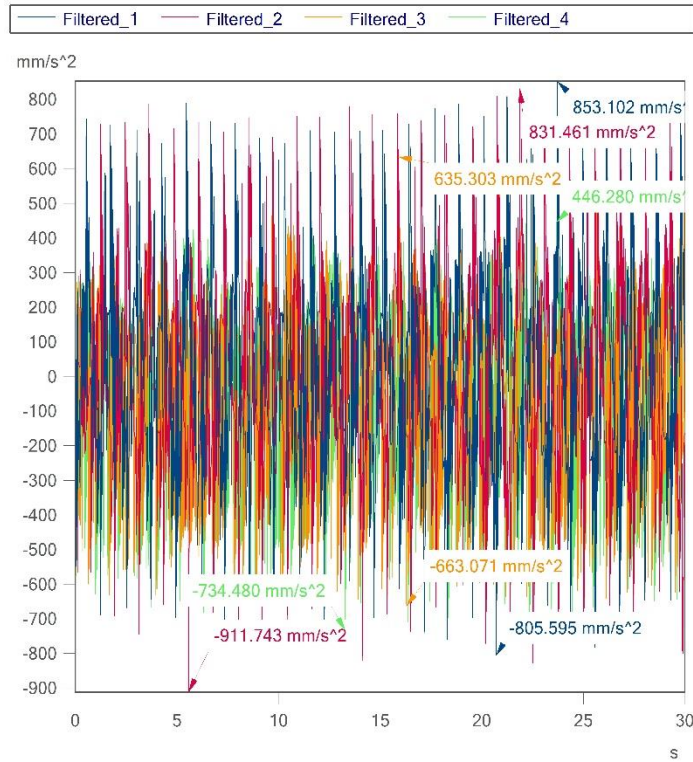


Figure A-24: Filtered Acceleration Response for 10 mm Diameter Orifice Plate

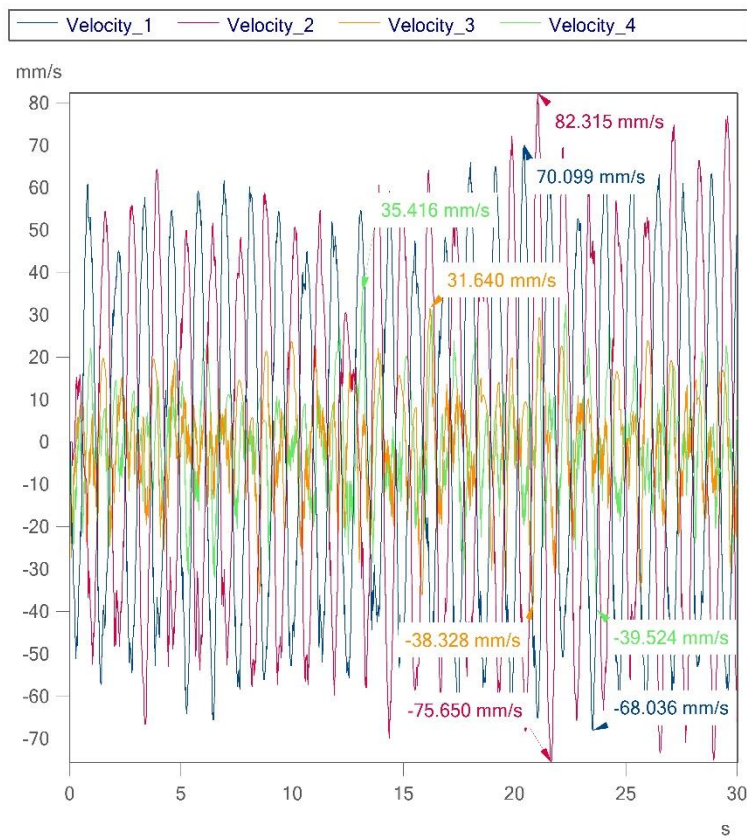


Figure A-25: Velocity Response for 10 mm Diameter Orifice Plate

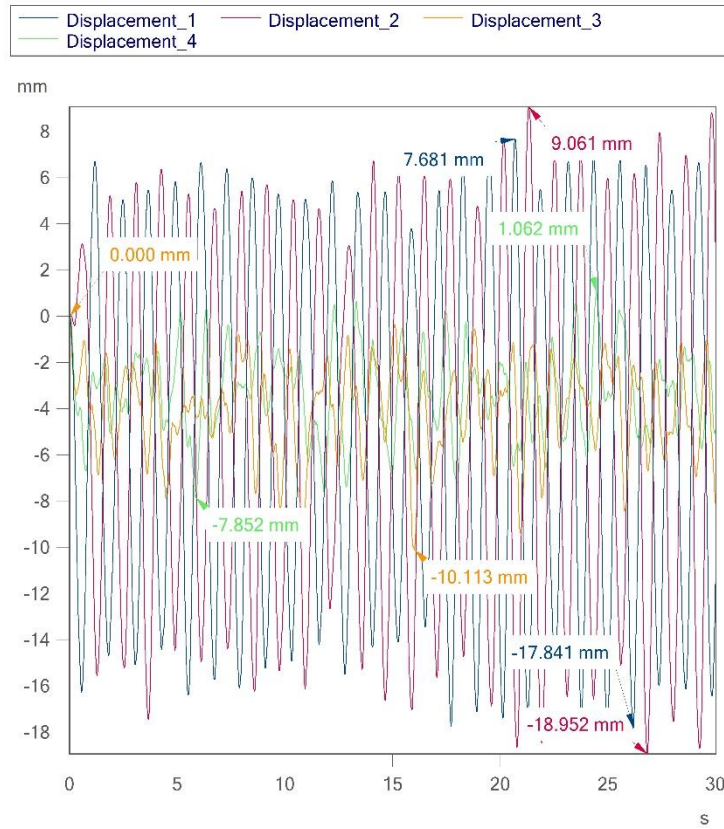


Figure A-26: Displacement Response for 10 mm Diameter Orifice Plate

APPENDIX C: Accelerometer Response for 10 cm Orifice Plate Diameter at Different Water Level

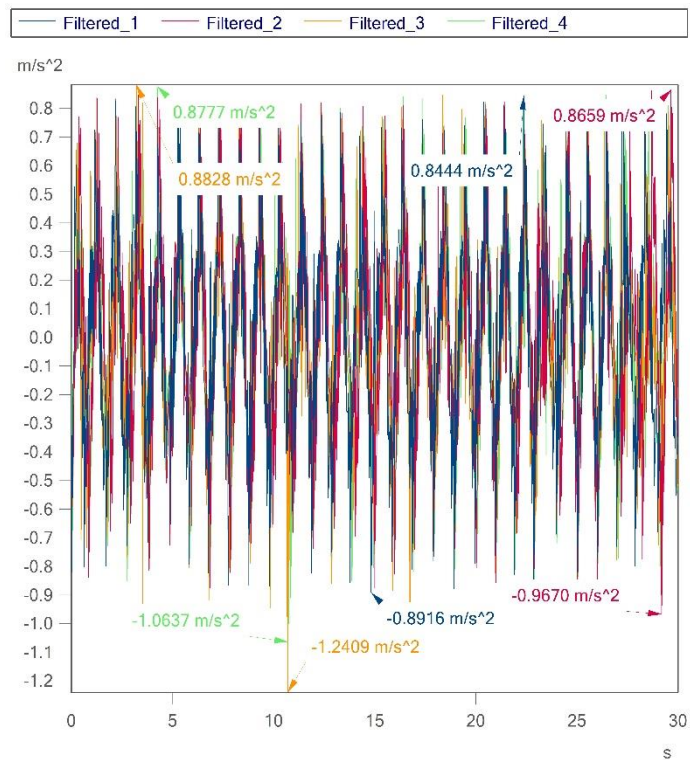


Figure A-27: Filtered Acceleration Response for Water Level of 5 cm

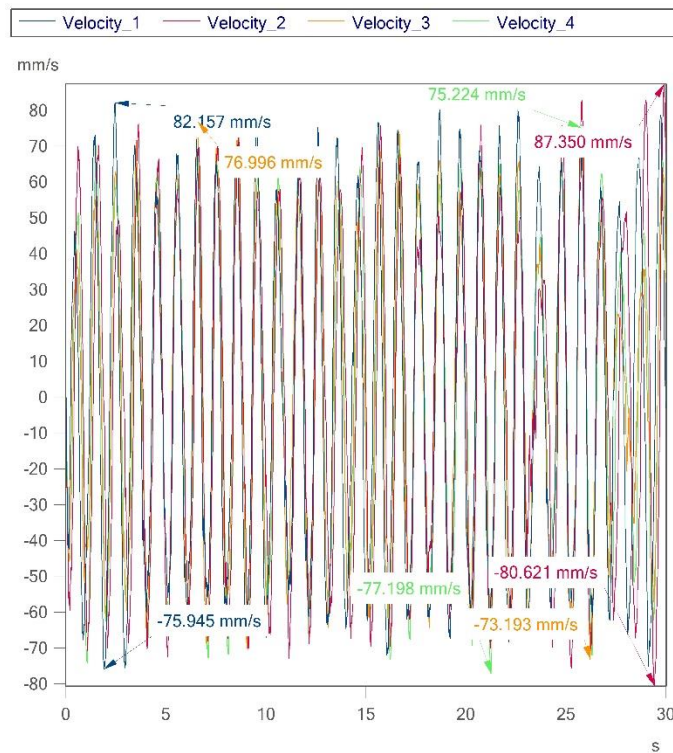


Figure A-28: Velocity Response for Water Level of 5 cm

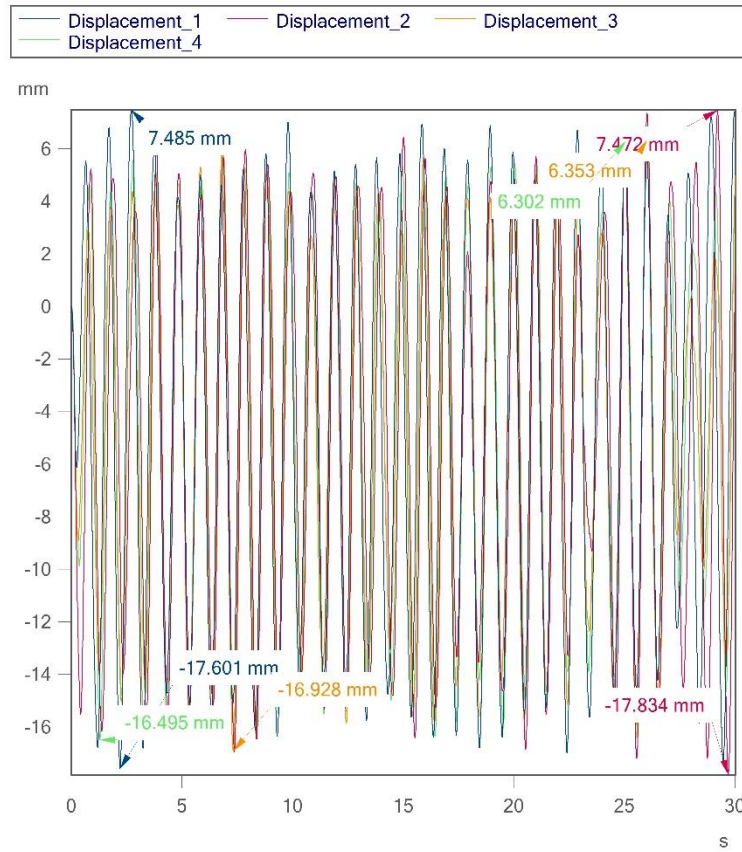


Figure A-29: Displacement Response for Water Level of 5 cm

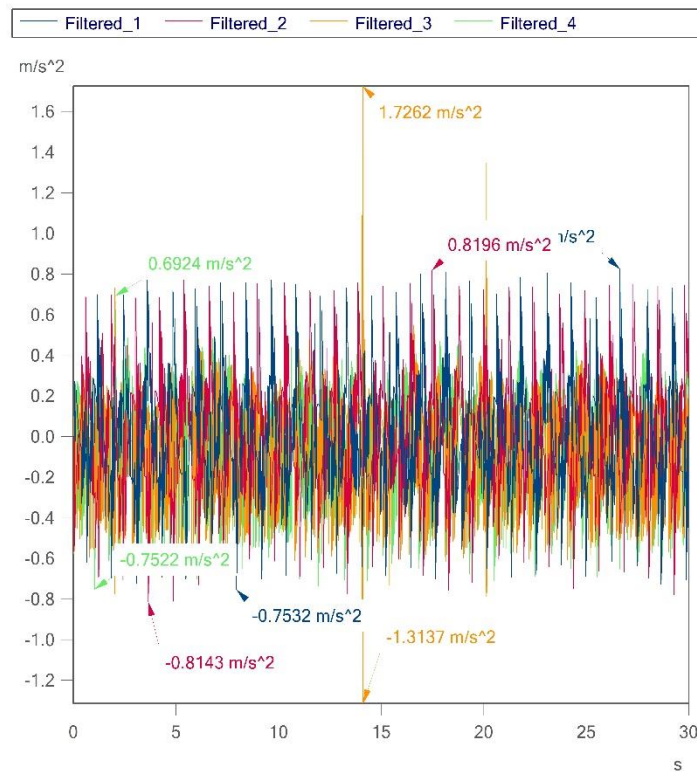


Figure A-30: Filtered Acceleration Response for Water Level of 10 cm

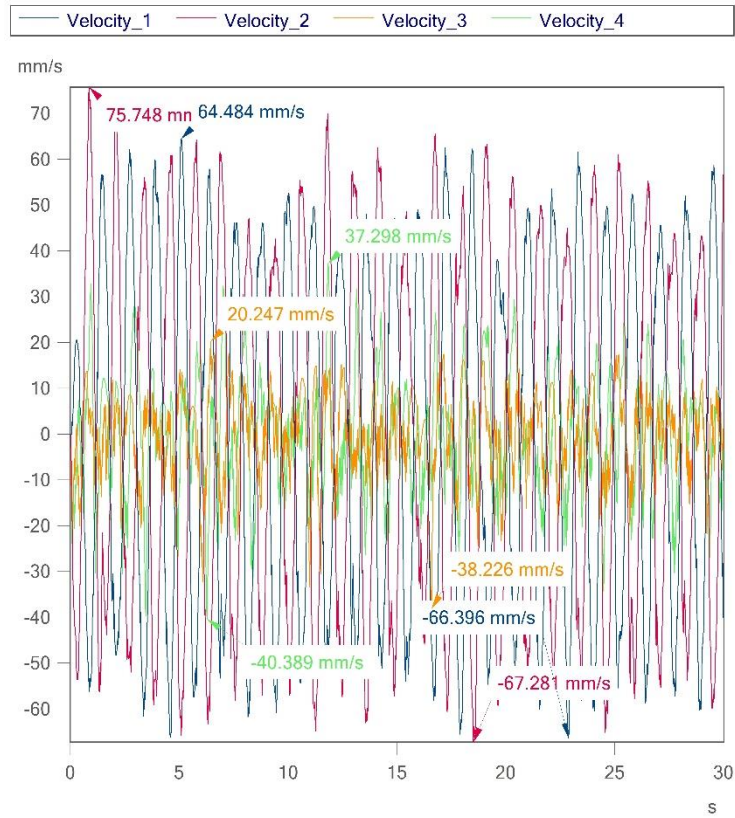


Figure A-31: Velocity Response for Water Level of 10 cm

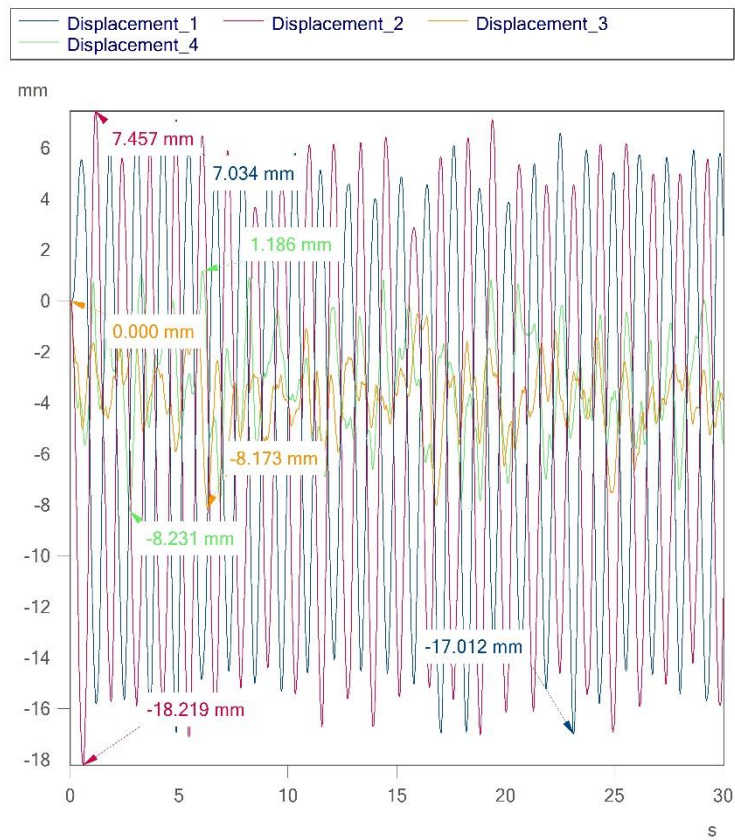


Figure A-32: Displacement Response for Water Level of 10 cm

APPENDIX D: Accelerometer Response for Platform without TLCD

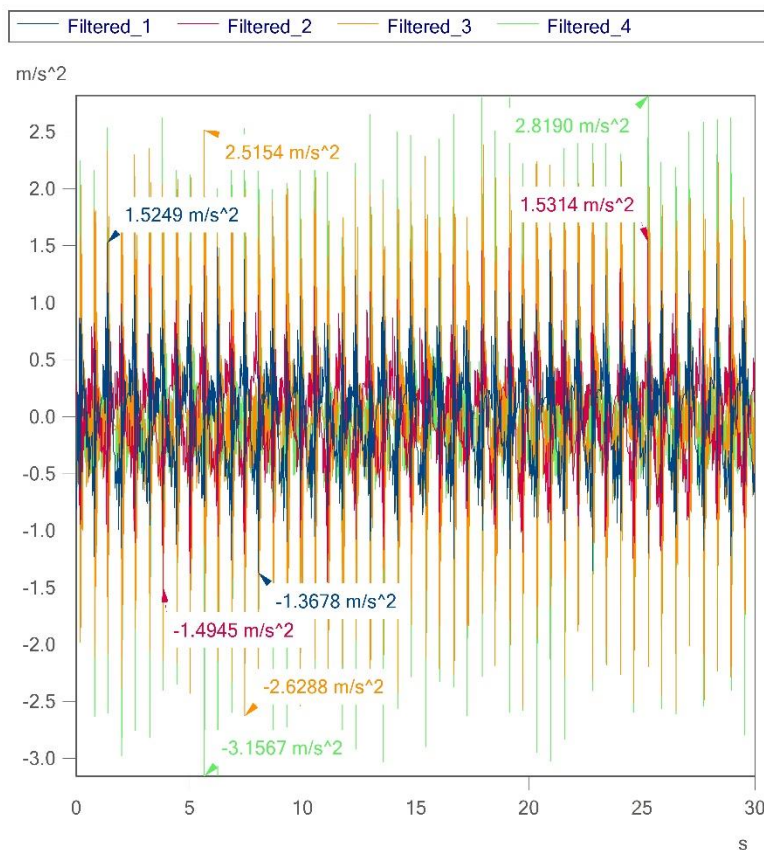


Figure A-33: Filtered Acceleration Response for Platform without TLCD

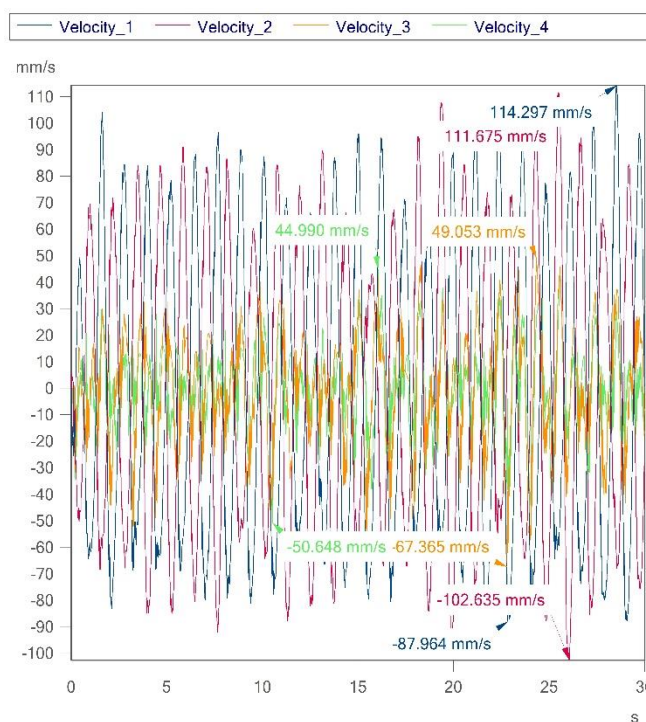


Figure A-34: Velocity Response for Platform without TLCD

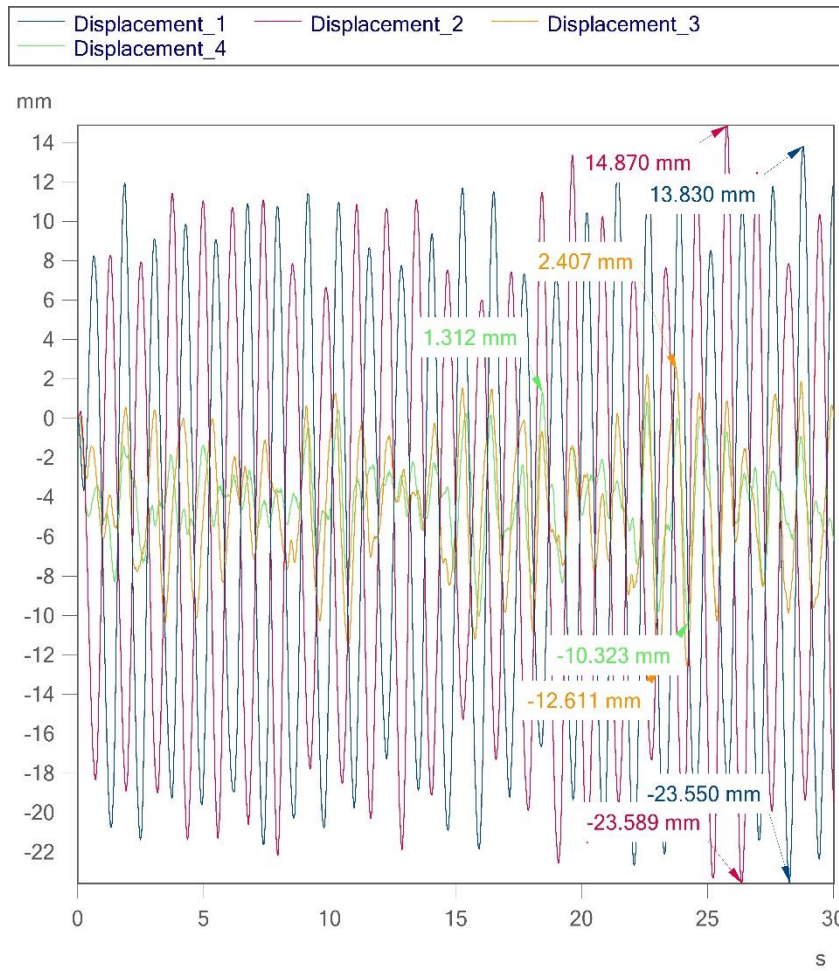


Figure A-35: Displacement Response for Platform without TLCD